NMR Metabonomics in an *in vitro* Model of HIV-1 latency

by

Thato Pearl Nonodi

Submitted in partial fulfillment of the requirements for the degree:

Magister Scientiae Biochemistry

In the Faculty of Natural and Agricultural Sciences

University of Pretoria

Pretoria

South Africa

09 December 2015

Submission declaration:

This page states:

I, Thato Nonodi, declare that the thesis/dissertation, which I hereby submit for the degree *Magister Scientiae* in the Department of Biochemistry, at the University of Pretoria, is my own work and has not previously been submitted by me for a degree at this or any other tertiary institution.

SIGNATURE:………………………………….

DATE……09 December 2015………………………………………

Plagiarism Declaration

UNIVERSITY OF PRETORIA

FACULTY OF NATURAL AND AGRICULTURAL SCIENCES

DEPARTMENT OF BIOCHEMISTRY

Full name: _____   Student number: _____

Title of the work: _____

Declaration

1. I understand what plagiarism entails and am aware of the University's policy in this regard.

2. I declare that this _____ (e.g. essay, report, project, assignment, dissertation, thesis etc) is my own, original work. Where someone else's work was used (whether from a printed source, the internet or any other source) due acknowledgement was given and reference was made according to departmental requirements.

3. I did not make use of another student's previous work and submit it as my own.

4. I did not allow and will not allow anyone to copy my work with the intention of presenting it as his or her own work.

Signature_____   Date _____

ii

Acknowledgements

I would like to acknowledge the following people and organisations for their contribution towards the success of this dissertation. I am very sincerely grateful.

- To my Supervisor Prof. D Meyer, I thank you for your supervision, guidance and patience throughout the course of carrying out this research and writing this dissertation

- To the funders, Technology Innovation Agency (TIA) and the National Research Foundation (NRF) thank you for providing the financial support needed to complete this dissertation

- To the staff, colleagues and friends, I appreciate the time I have spent with you and your words of comfort and encouragement I received from you

- To the Department of Chemistry (Dr. L Pilcher and Mr. E Palmer) and Prof. D Steffens from the Department of Statistics, the knowledge and assistance you have provided me was indeed invaluable for this research, thank you

- To my family, words cannot express my gratitude and the love I have for you. Thank you for your love, support and encouragement you have given me and still continue to give me. May the Almighty God bless you all always! Mazo sugar!!

- Most importantly, I would like to give thanks and praise to the Lord Jesus Christ for the constant hope and motivation. His love, He has placed in me. You are a mighty and wonderful God. Amen.

Output

- **Conference**

The work was presented at the HIV R4P (Research for Prevention) conference, in Cape Town (South Africa) at the Cape Town International Convention Centre from the 27 – 31 October 2014. Poster presentation: T.P. Nonodi and D. Meyer: 'NMR Metabonomics in an *in vitro* Model of HIV-1 latency'.

Summary

Background: Metabolic disorders have been identified in patients infected with the human immunodeficiency virus (HIV). These disorders include lipodystrophy, wasting syndrome, cardiovascular disease and glucose intolerance. Highly active antiretroviral treatment (HAART) administered to patients can successfully suppress the virus and decrease the prevalence of opportunistic infections associated with AIDS but increase incidence of metabolic disorders. Glucose tolerance test, dual-energy x-ray absorptiometry and CD4 counts are some of the conventional tests that are used to detect and monitor disease progression and metabolic disorders. These are single result tests that are time-consuming and provide limited information about the metabolic disorder. A metabonomic approach allows for the measurement of multiple metabolites simultaneously; which could lead to the identification of markers of disease progression. Most HIV-metabonomics studies to date used nuclear magnetic resonance (NMR) spectroscopy and mass spectrometry (MS) spectrometry to detect multiple metabolites from blood and urine samples simultaneously, fewer studies utilized cell culture supernatants as metabolite source.

In the body HIV is able to seize control of cellular networks and exists as an active or latent virus. HIV latency is mainly responsible for survival of the virus through the production of reservoirs throughout the body. It is then of great interest to investigate the effects of active and latent virus on cell metabolic networks. *In vitro* cell models such as U1 cells, a promonocyte latently infected with HIV-1 are suitable for such investigations because the models allow for control over activation of the virus with stimulants. To date only one study has compared the metabolic profiles of the active virus against non-infected cells but no study has comparatively investigated actively and latently infected immune system U1 cells, which is what is presented here. In this study a metabonomic approach was used to investigate active and latently infected U1 promonocytic cells and the metabolites were detected by NMR spectroscopy.

Methods: U1 and U937 cells were cultured and lysed by the freeze-thaw method to extract the supernatant, the extent of cell lysis was determined through flow cytometry. NMR spectroscopy was used to detect metabolic profiles of uninfected U937 cells (parent cell line from which U1 cells were derived) as well as actively and latently infected U1 cells. Phorbol myristate acetate (PMA) was used as a stimulant to activate the virus. NMR data was preprocessed for statistical analysis with Mestrenova 10.0 software, and the metabolites were putatively identified with the use of Chenomx software, literature searches, human metabolome database (HMDB) and Kyoto encyclopedia of genes and genomes (KEGG). For statistical data analysis SPSS 20.0 software was used to determine group separation and metabolic profile differences.

Results: Glucose, lactate, glutamine/glutamate, leucine, alanine, choline, phosphocreatine and lipid are some of the metabolites that were detected by NMR spectroscopy and through ANOVA analysis the metabolites were determined to be significantly different (P-value<0.05) between the three groups. A multiple comparison table presented the group significant differences and LDA correctly classified the experimental groups with 100% accuracy. U937 and actively infected cells produced similar results to what was seen in other investigations where sera and plasma were used as metabolite source. Latently infected cells produced the more distinguishable separation among the experimental groups and the metabolites responsible for this separation were those mainly involved in glycolysis and lipid biosynthesis pathways. All the cell lines were treated with lactate to evaluate the influence of one prominent metabolite on the virus and cell metabolism. Lactate was selected because the metabolite was found to be significantly present in the initial experiments and for its role in glycolysis (indicates anaerobic respiration). Cysteine, an indicator of oxidative stress was produced and some of the metabolites such as alanine and taurine were no longer detectable.

Conclusion: NMR spectroscopy successfully elucidated metabolic profiles of U937 cells, U1 cells (latent virus) and PMA induced U1 cells (active virus). The technique was highly reproducible with minimal sample preparation. Most metabolites that were detected are those primarily associated with metabolic disorders involving glycolytic energy metabolism. Through multiple comparisons it was determined that latent HIV-1 infection had a profound effect on cell glycolysis as seen by the significant alteration of lactate and the occurrence of aerobic glycolysis and mitochondrial disruption. In this study, it was observed that the virus supports biosynthetic pathways more than the production of energy through oxidative phosphorylation. Cells that were exposed to lactate produced a different metabolic profile from those that were not treated, this indicated that an increase or decrease in concentration of a particular metabolite can affect cell metabolism in HIV infected cells.

Table of Contents

List of figures

List of tables

Abbreviations

ADP   Adenosine diphosphate

AIDS   Acquired immunodeficiency syndrome

ANOVA   Analysis of variance

ART   Antiretroviral treatment

ATP   Adenosine triphosphate

BCAA   Branched-chain amino acids

CDC   Centers for disease control

CNS   Central nervous system

CVD   Cardiovascular disease

DNA   Deoxyribonucleic acid

D_2O Deuterium oxide

EGIR   European Group for the Study of Insulin Resistance

FT-IR   Fourier transform infrared spectroscopy

GFP   Green fluorescent protein

HAART   Highly active antiretroviral therapy

HDAC2   Histone deacetylase 2

HDL   High density lipoprotein cholesterol

HERMES   HIV exposure and risk of metabolic syndrome

HIV   Human immunodeficiency virus

HK   Hexokinase enzyme

HMBD   Human metabolome database

HOMA   Homeostasis model assessment of insulin resistance

KEGG   Kyoto encyclopedia of genes and genomes

LDA	Linear discriminant analysis
LDL	Low density lipoprotein cholesterol
LTR	Long terminal repeats
Mtb	Mycobacterium tuberculosis
MDM	Monocyte derived macrophages
mRNA	messenger ribonucleic acid
MS	Mass spectrometry
MVDA	Multivariate data analysis
NAD	Nicotinamide dinucleotide
NADPH	Nicotinamide dinucleotide phosphate
NCE ATP III	National Cholesterol Education Program-Adult Treatment Panel III
NNRTI	Non-nucleoside reverse-transcriptase inhibitors
NRTI	Nucleoside reverse-transcriptase inhibitors
OS	Oxidative stress
PAF	Platelet-activating factor
PCA	Principal component analysis
PI	Protease inhibitors
PMA	Phorbol-12-myristatic-13-acetate
PPM	Parts per million
PPP	Pentose phosphate pathway
RNA	Ribonucleic acid
RT	Reverse transcriptase
SIV	Simian immunodeficiency virus
SMART	Strategies for management of antiretroviral therapy
SPSS	Statistical package for the social sciences

TCA	Tricarboxylic acid
TSP	Trimethylsilyl propionate
VCC	Virus-containing compartment
VLDL	Very low density lipoprotein
WHO	World Health Organization

Chapter 1: Introduction

HIV is one of the most virulent opportunistic pathogens due to its ability to overpower and control the immune system of its host (UNAIDS 2014). The virus is able to attack and survive within immune system cells for a very long period of time (Kumar, Abbas, and Herbein 2014). Viral latency allows the virus to evade immune system defenses and over time the virus weakens the immune system resulting in a compromised immunity against other infections (Sleasman and Goodenow 2003; Siliciano and Greene 2011).

In 2013 an estimated 35 million people worldwide were infected with the virus and about 2.1 million people were newly infected (close to 240 people every hour) (UNAIDS 2014). The mortality rate was 1.5 million people in 2013 alone (UNAIDS 2014). Presently, there is no cure; though great strides have been made in the treatment of HIV disease, through implementation of Antiretroviral therapy (ART) in 1986 and HAART in 1996 (Delaney 2006; Rathbun 2015). The treatment has decreased the mortality and morbidity rates of HIV infection and in 2013, 12.9 million people world-wide had access to the antiretroviral therapy (UNAIDS 2014). By the late 90's people on treatment were reported to have developed metabolic disorders, which were observed with changes in lipid distribution, insulin resistance, cardiovascular disease, diabetes and glucose intolerance to name a few. What should be highlighted is that before implementation of HAART these metabolic disorders were already identified in HIV-1 infected patients but HAART exacerbates the situation (Carr *et al.* 1998). A combination of three or more metabolic disorders result in what is described as a metabolic syndrome (Slama *et al.* 2009).

Currently, single metabolite tests such as glucose/insulin tolerance and dual-energy x-ray absorptiometry as well as magnetic resonance imaging (MRI) scans (for lipid distribution) are used to detect and determine the risk factors associated with metabolic disorders. Usually a single test measures a single metabolite; which can be a time-consuming and tedious task, prone to inaccuracies. Many risk factors are associated with HIV-1 related metabolic disorders, requires that methods be developed for quick detection of metabolite fluctuations so medical intervention strategies can be implemented.

Metabonomics, defined by Jeremy Nicholson as "the quantitative measurement of the multiparametric time-related metabolic responses of a complex (multicellular) system to a pathophysiological intervention or genetic modification," is a possible solution. In a nutshell it is a study that provides a "snapshot" of metabolic profiles at a particular time within an organ/cell (Lindon, Nicholson, and Holmes 2007). By detecting and understanding a particular set of metabolic profiles obtained at certain periods of time, disease progression can be monitored.

High throughput, sensitive, and robust techniques are used in metabonomic studies, these are mainly nuclear magnetic resonance spectroscopy (NMR), hyphenated mass spectrometry (-MS), Raman and infrared spectroscopy (Lindon, Nicholson, and Holmes 2007; Stuart 2005). Overall these techniques are used to detect metabolites in either gas, aqueous, or solid state but the raw data from the instrument must be processed and interpreted through chemometric (statistics and mathematics) and bioinformatics (mathematics and computer science) tools. Widely used statistical methods for the analysis of biological data are univariate analysis of variance (ANOVA), linear discriminant analysis (LDA) and other multivariate analysis.

Metabonomics was applied in many HIV metabolic profile investigations using biological samples such as urine, saliva, cells, tissue, blood serum and plasma and distinctive metabolites were identified as markers of disease (McKnight et al. 2014; Hewer et al. 2006). A number of publications including in our group have identified biomarkers from HIV negative and positive blood sera and plasma from patients on/ not on HAART (Hewer et al. 2006; L. J. Sitole, Williams, and Meyer 2013; McKnight et al. 2014). Very few studies have investigated the effect of HIV infection on cell culture supernatant metabolic profiles (cell supernatants provide information about metabolites that remain in the cell not only secreted metabolites) and even less studies have been done for latently infected cells. HIV is able to evade the immune system by integrating its DNA into the cell's genome and becoming latent (Siliciano and Greene 2011). Over time an increase in latent virus cells which resemble the normal host immune cells and thus cannot be recognized by host defenses, create reservoirs throughout the body that are resistant to HAART and host defenses (Chavez, Calvanese, and Verdin 2015).

In this study, metabolic profiles of latently and actively infected HIV-1 positive U1 cells and HIV negative U937 cells (of promonocytic origin) were determined by NMR spectroscopy. NMR data was preprocessed with Mestrenova lab software, HMDB/KEGG and Chenomx software were used to putatively identify metabolites and statistical package for the social sciences (SPSS) software was used to determine significant differences between experimental groups.

In the next chapter (chapter 2) a detailed background of topics related to the study is provided. This chapter ends with the objective and aims of the investigation. Chapter 3 presents a workflow diagram and the methodology of the study. Results are presented in chapter 4 and then a detailed discussion follows in chapter 5. Chapter 6 and 7 provides the overall conclusion and future perspectives, respectively. These are followed by the references and an appendix, presenting additional data.

Chapter 2: Literature Review

2.1 Introduction to HIV

The *Retroviridae* family is classified as viruses that carry a reverse transcriptase enzyme that converts a single stranded RNA genome into double stranded DNA, which can then be inserted into the infected cell's genome (Johnson *et al.* 2008). The *Retroviridae* family has the *Lentivirus* genus which HIV belongs to. Generally, *Lentiviruses* affect many mammals but the virus/strain with the largest impact to humans is HIV-1, which accounts for more than 35 million infections worldwide (UNAIDS 2014; Gyorkey, Melnick, and Gyorkey 1987).

There are two types of HIV, HIV-1 and HIV-2, which are divided into groups M, O, N and A to H respectively. Group M from HIV type 1 is the most prevalent in the world, with 9 subtypes and 43 variants (Tebit *et al.* 2010). HIV has a link of origin to monkeys and chimpanzees (infected with SIV) and through the years it has mutated to the virulent subtype M that largely affects Africa (Tebit *et al.* 2010). Current statistics show that more than 2.1 million people were newly infected with the virus in 2014 (UNAIDS 2014). The HIV genome consist of three main genes that are commonly found within retroviruses; these are *gag, pol and env* genes which encode for long-terminal repeats which flank the main genes, accessory genes non-structural and structural proteins (fig 2.1) (Tebit *et al.* 2010).

4
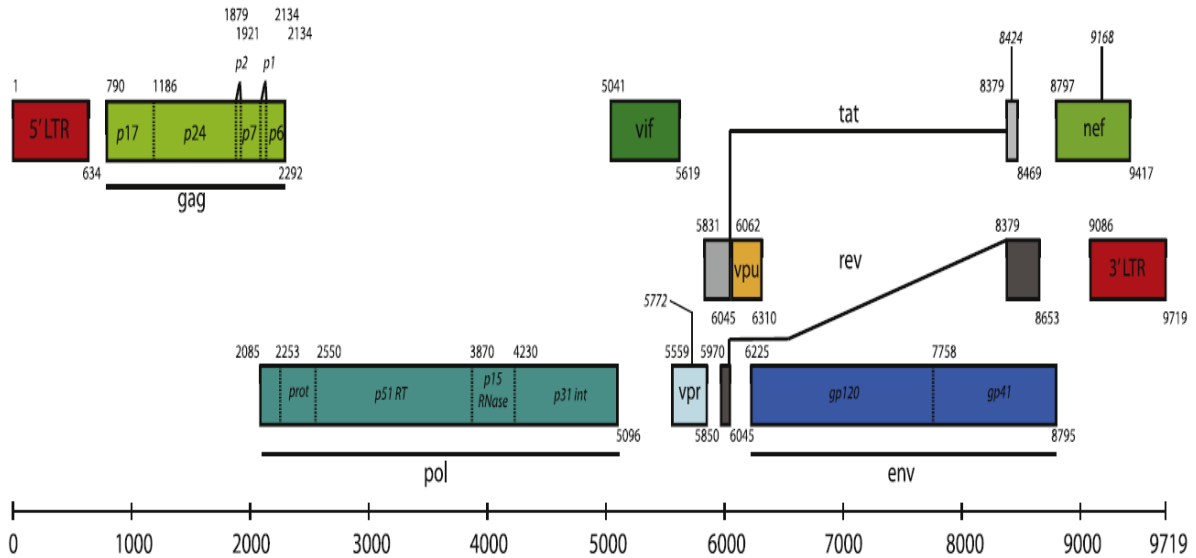
Figure 2.1: The HIV genome and its genes which play a major role in HIV infection. The three main genes gag (light green), pol (turqoise) and env (dark blue) genes are commonly found in retroviruses. (Tebit et al. 2010)

2.2 Mechanism of HIV infection

Primary infection occurs when the virus infects circulating dendritic cells of the immune system at the site of infection, these cells then transport the virus to other cells such as the CD4$^+$ T lymphocyte cells and to the more localized macrophages. The virus infects the cells mainly by the interaction that occurs between the viral gp120 glycoprotein (protein encoded by the HIV *env* gene) and host CD4 receptors of the immune system cells. This in turn, increases the binding affinity of the virus to the trans-membrane co-receptors CCR5 or CXCR4 of the cell (Sleasman and Goodenow 2003). The binding of receptors results in the fusion between the virus lipid envelop and the cell membrane, subsequently the viral core is released into the cell cytoplasm.

The viral core contains enzymes, proteins and two of each single-stranded RNA genomes. Reverse transcriptase enzyme transcribes the RNA molecule to double-stranded DNA. The dsDNA is transported to the nucleus and integrated into the cell's genomic DNA by the integrase enzyme (Sleasman and Goodenow 2003;

5

Maiuri *et al.* 2011). HIV can either remain in this dormant/latent form, or become active and overtake the cell's transcriptional machinery to produce more viruses, which will bud out through the cell membrane taking parts of the cell membrane into its envelope. The viruses mature outside the cell through cleavage of the Gag polyproteins by virus protease enzyme and thereafter HIV will find more immune cells to infect (Sleasman and Goodenow 2003). Figure 2.2 provides a schematic diagram of the viral life cycle.
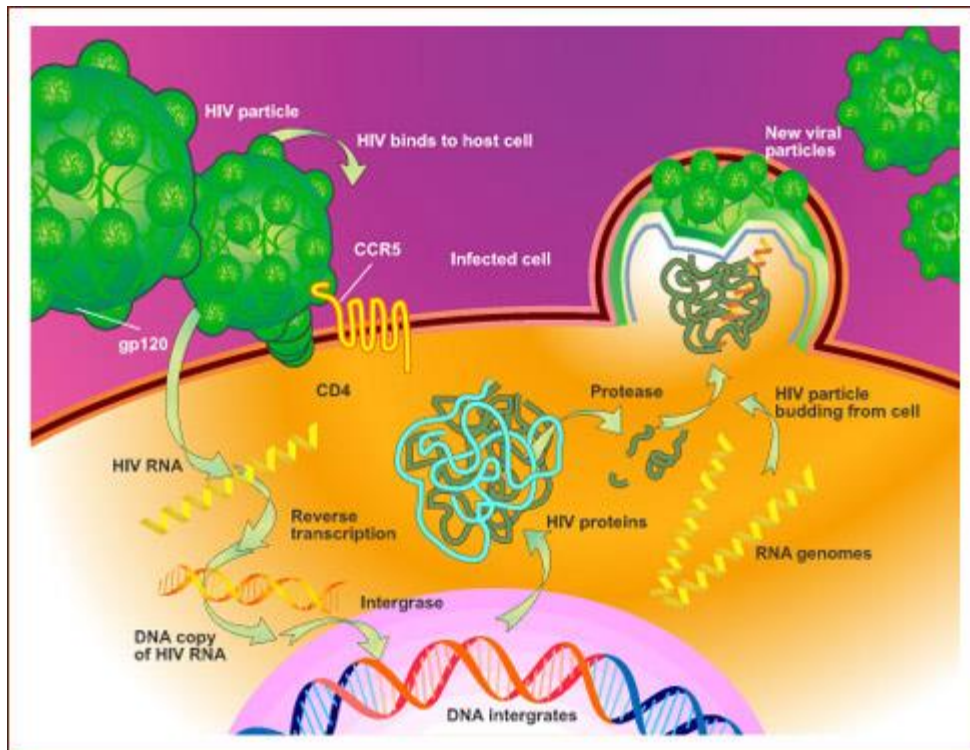
Figure 1.2: A schematic diagram of the HIV replication cycle. The virus enters the cell through binding of viral and host cell receptors. Once in the cell the virus generates DNA strands which are transported to the nucleus. In the nucleus the viral DNA is either left embedded in the host genome as latent or replicated for virus assembly. Then these new viruses bud out of the cell for maturation. (Raghava 2015)

2.3 Stages of HIV infection

In general, HIV infection occurs in three stages, primary, latent and apparent disease. During primary infection the virus replicates at high rates and infects a large number of cells. The virus then enters into a state of latency where it remains embedded into the host's genome, resultantly creating viral reservoirs (Siliciano and Greene 2011). Though HIV uses different escape mechanisms (for example, rapid gene mutations); HIV latency provides a more stable and longer lasting evasion mechanism (Kumar, Abbas, and Herbein 2014). In the presence of an external or internal stimulus the virus is reactivated and this could lead to the 'apparent disease' stage (fig 2.3).

2.3. Insert. Recently, RT-PCR showed that viral latency occurs early in infection and that the virus remains active throughout all stages of infection. Different to what was previously thought.
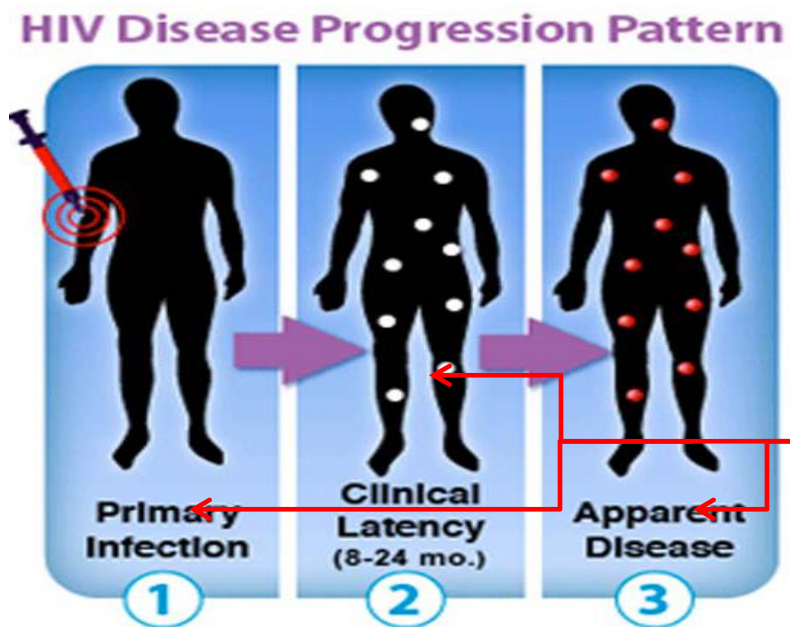
Figure 2.2: Disease progression of HIV infection. In general, HIV progression occurs in three stages. First is the primary infection which can occur through the use of non-sterile infected syringes. Latency occurs when the virus embeds the DNA into the cell's genome. If left untreated the patient runs the risk of the infection developing into the apparent disease phase, characterized by the presence of opportunistic infections. (Huber 2013)

The apparent disease is characterized by an increase in viral load, decline in immune system cells and presence of opportunistic infections such as *Mycobacterium tuberculosis* (*Mtb*), *Mycobacterium kansasii, Pneumocystis carinii and Histoplasmosis capsulatum*, as well as metabolic syndrome (for example wasting syndrome); this stage is also known as the acquired immune-deficiency syndrome (AIDS), which occurs when CD4 cell count is below 200 cells/mm^3 (Orenstein 2001; UNAIDS 2014).

The three stage process might be true for a very small (about one out of 10^6-10^7) population of CD4+ T lymphocytes and monocytes/macrophages, recent RT-PCR studies show that HIV-1 establishes latency early during primary infection and still remains active throughout all the stages of infection (fig.3.insert) (Finzi *et al*. 2012; Siliciano and Greene 2011; Kumar, Abbas, and Herbein 2014; Chun and Fauci 1999; Redel *et al*. 2010). How the virus achieves latency is presented in the next section.

2.4 HIV latency

HIV latency was observed by Folk *et al* (1986) through *in vitro* studies of transformed cells; whereby surviving infected cells had reduced viral replication (Siliciano and Greene 2011; Folks *et al.* 1986). HIV latency is a state of viral replication dormancy that provides a way for the virus to evade host defenses (Siliciano and Greene 2011). Viral latency is established when activated CD4$^+$ T cells (main targets of HIV infection) are infected but survive and return to a resting state (Siliciano and Greene 2011) (Chavez, Calvanese, and Verdin 2015). This process occurs during viral genome integration whereby viral proteins are not transcribed, therefore cytoplasmic effects of the virus do not occur and cell death is prevented. Chavez *et al* (2015) used a dual reporter virus (HIV Dou-Fluo I) which identified latently infected cells early in infection, after directly infecting resting CD4$^+$ T cells (Chavez, Calvanese, and Verdin 2015). Resting CD4$^+$ T cells (most abundantly found in reservoirs) have a long half-life, which enables the virus to

survive for long periods of time unlike activated CD4$^+$ T cells (Chavez, Calvanese, and Verdin 2015).

Cells of the monocyte/macrophage lineage also serve as robust viral evasion agents due to the ability to resist cell apoptosis induced by HIV infection (Kumar, Abbas, and Herbein 2014). Because macrophages are found in most tissue (including the brain as microglia) HIV is able to create reservoirs throughout the body (Kumar, Abbas, and Herbein 2014). Viral reservoirs were described by Blankson (2002) as a 'cell type or anatomical site where replication-competent' viruses accumulate and survive longer than the actively replicating viruses (Blankson 2002). HIV reservoirs are found in many tissues and organs around the body such as the lymph nodes, central nervous system (CNS), bone marrow and the genital tract as depicted in (fig 2.4) (Dahl, Josefsson, and Palmer 2010). Infected cells are not detected by the immune system cells because the virus is embedded in the host genome and does not produce cytopathic compounds, thus is able to escape host immune defenses and HAART (which target the activated virus and compounds produced during replication).

HIV infected macrophages contain virus containing compartments (VCCs) and release cytokines and chemokines to recruit CD4$^+$ T cells. When the infected macrophage and uninfected CD4$^+$ T cells come into contact, virological synapses form and the virus (VCC) is transferred to the uninfected CD4$^+$ T cells. This event in turn promotes viral latency and reservoir formation. The presence of monocyte/macrophage lineage cells, cytokines and resting/memory CD4$^+$T cells together enhance the stability of viral reservoirs (Kumar and Herbein 2014)
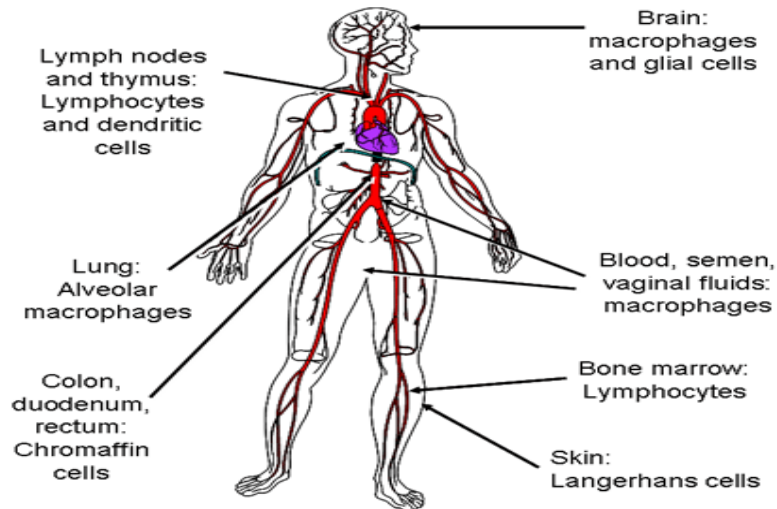
Figure 2.3: Diagram depicting various HIV reservoirs in humans. It is through the establishment of these reservoirs that the virus is able to evade HAART and host cell defenses because they contain the latent virus. (Hunt 2013)

HIV is able to establish and maintain latency through epigenetics, chromatin remodeling and gene silencing, these are explained in the following section (Siliciano and Greene 2011; Kumar, Abbas, and Herbein 2014).

2.4.1 HIV latency mechanisms

There are two types of latency mechanisms; pre-integration and post-integration latency (Kumar, Abbas, and Herbein 2014). The virus undergoes pre-integration latency, after transcription of viral ssRNA to a dsDNA; it is transported as a PIC complex (which comprises of viral integrase, matrix, capsid and Vpr proteins) to the nucleus (Kumar, Abbas, and Herbein 2014; Siliciano and Greene 2011). Upon entering the nucleus, the virus may be deemed latent without integration due to transcribing errors of reverse transcriptase (RT) or due to inhibition of PIC by host restriction factors (MX2 and APOBEC3), rendering the virus latent/inactive before integration (Kumar, Abbas, and Herbein 2014). Post-integration latency involves epigenetic, transcriptional and post transcriptional gene silencing of the provirus genome after integration, this method is also used to maintain viral latency and is

10

most responsible for viral persistence (Kumar, Abbas, and Herbein 2014; Goldsmith *et al.* 2010).

There are a few ways that HIV latency is maintained one is the site of viral genome integration into the host's DNA. The host's genome folds into two regions: heterochromatin that is tightly compact and transcriptionally inactive, and euchromatin which is less compact and is transcriptionally active (Kumar, Abbas, and Herbein 2014; Siliciano and Greene 2011). Non-coding genes are commonly found within the heterochromatin (which hinders binding of transcriptional factors to DNA).

Jordan *et al* 2001 saw in an HIV latency model (J-Lat), provirus DNA was integrated into the heterochromatin (Kumar, Abbas, and Herbein 2014; Siliciano and Greene 2011; Albert Jordan, Bisgrove, and Verdin 2003). *In vivo* studies were conducted to test the accuracy of Jordan *et al* (2001) findings because, prior to that study the general assumption was that HIV would not integrate into the non-coding region. Jordan *et al* (2001) concept was reconsidered when the work could not be reproduced but showed the virus had integrated itself within the coding euchromatin region of resting CD4^{+} T cells and macrophages as opposed to heterochromatin (A Jordan, Defechereux, and Verdin 2001; Mack *et al.* 2003; Kumar, Abbas, and Herbein 2014; Siliciano and Greene 2011). This proved that heterochromatin does not play a role in establishing HIV latency. They also found that chromatin remodeling was involved in the maintenance of HIV latency. Chromatin comprises of nucleosomes, which are complexes of histone proteins surrounded by DNA, therefore nucleosome structures determine chromatin modelling (Kumar, Abbas, and Herbein 2014; Siliciano and Greene 2011).

During chromatin remodeling nucleosome nuc-0 and nuc-1 overlap the 5' LTR region of HIV provirus thus play a role in regulating HIV gene expression. In J-Lat and CD4$^+$ T cells the presence of methyl CpG binding domain protein-2 (MBD2) and HDAC2 found on CpG islands flanking the provirus start site promote gene silencing, which consequently induce latency (Blazkova *et al.* 2009; Kauder *et al.* 2009).

Micro RNAs are derived from either host or viral RNA, they are small non-coding RNA molecules that can regulate the expression of specific coding genes (Huang *et al.* 2007). Huang *et al* in 2007 discovered that miR-28, miR-125B, miR-150, miR-223 and miR-382 (cellular micro RNAs (miRs)) within resting CD4$^+$T cells were more abundant than in active CD4$^+$T cells and that the miRs could inhibit HIV-1 production and so induce viral latency (Huang *et al.* 2007).

2.4.2 Reactivation of the virus

Viral latency is disrupted by internal and external influences on the infected cells. Internal simulants such as transcription factors, cytokines and chemokines cause viral reactivation by inducing cell differentiation or division, prompting HIV replication (Kumar, Abbas, and Herbein 2014; Dahl, Josefsson, and Palmer 2010). During replication cytopathic compounds could either induce cell death directly or attract cytotoxic T cells for cell death (Pace *et al.* 2011; Dahl, Josefsson, and Palmer 2010). External influences such as co-infection by opportunistic pathogens increase NF-κB production that induce expression of TNF-α and chemokines, which in turn increase viral replication within macrophages (Orenstein 2001).

2.4.3 In vitro models of HIV-1 latency

Investigations into HIV latency make use of latency models because of the difficulties of investigating latency within the body. Virus eradication methods can be explored through *in vitro* latency models without patient risk (Pace *et al.* 2011). The ease of manipulation between latency and activation and how readily the cells are infected with HIV makes latency models the best option for latency studies

12

(Pace *et al*. 2011). There are many HIV latency models available which include thymocyte, activated and resting CD4$^+$ T cells, HT-29 cells and U1 cells (Pace *et al*. 2011; Lutz *et al*. 1997; Hollenbaugh, Munger, and Kim 2011). For example the activated CD4$^+$ T cell model has been used to investigate epigenetic silencing and P-TEFb restriction which induce latency (Tyagi, Pearson, and Karn 2010). Resting CD4$^+$ T cells were used for direct HIV infection studies to determine the different mechanisms of latency induction (Pace *et al*. 2011). U1 cells are subcloned promonocytic cells that were obtained from a histiocytic lymphoma cell line U937 (Tiemessen, Kilroe, and Martin 1998; Aoki and Nakashimab 1994). The cells are chronically infected with HIV-1 and contain two integrated viral DNA copies (Amet *et al*. 2008). The U937 are the HIV-1 negative parent cells of U1 cells and are mostly used in research as controls.

Several cytokines, such as tumor necrosis factor-alpha (TNF-α) and phorbol esters are used to induce activation, increase gene expression and release the virions from within the cells (Amet *et al*. 2008). In the presence of an external stimulus or histone acetylation, nuc-1 undergoes remodeling and the virus is reactivated. This was observed through the inhibition of histone deacetylase (HDAC) enzyme from binding to histones (Kumar, Abbas, and Herbein 2014; Siliciano and Greene 2011). HIV latency was prevented and RNA Pol 2 recruited for RNA synthesis, concluding that in HIV-1, re-modeling of nuc-1 is necessary for gene transcription (Van Lint *et al.* 1996; Siliciano and Greene 2011; Kumar, Abbas, and Herbein 2014; S. A. Williams *et al*. 2006) The U1 cells have been used widely for the study of HIV-1 expression inducers and inhibitors.

 As an example Aoki *et al* (1994) used HIV-1 infected U1 cells to induce apoptosis, whereas Amet *et al* (2008) recently discovered that exposure of the cells to statins suppresses the release of virions from the U1 cells (Tiemessen, Kilroe, and Martin 1998; Amet *et al*. 2008; Aoki and Nakashimab 1994). All these cells are used to mimic what could be happening with the body.

13

2.5 Immune system cells affected by HIV

HIV infects immune system cells, mainly T lymphocytes, dendritic cells and macrophages (Kondo 2010). These cells are differentiated from hematopoietic stem cells that differentiate to multipotent lymphoid and myeloid lineages (Kondo 2010). The lymphoid lineage gives rise to T, B and natural killer cells, while the myeloid lineage produces megakaryocytes, erythrocytes, granulocytes and monocytes; monocytes further differentiate into macrophages and dendritic cells shown in (fig 2.5) (Kondo 2010). These cells are responsible for eliciting an immune response against pathogens such as HIV. Macrophages are localized immune cells involved in activating T cells and inducing inflammatory responses, while dendritic cells collect antigens around the body and transports them to the lymph nodes (immune system cell site) (Daigneault *et al.* 2012). T cells secrete cytokines that induce antibody production and regulate macrophage phagocytosis (Daigneault *et al.* 2012).

Cells of the Immune System
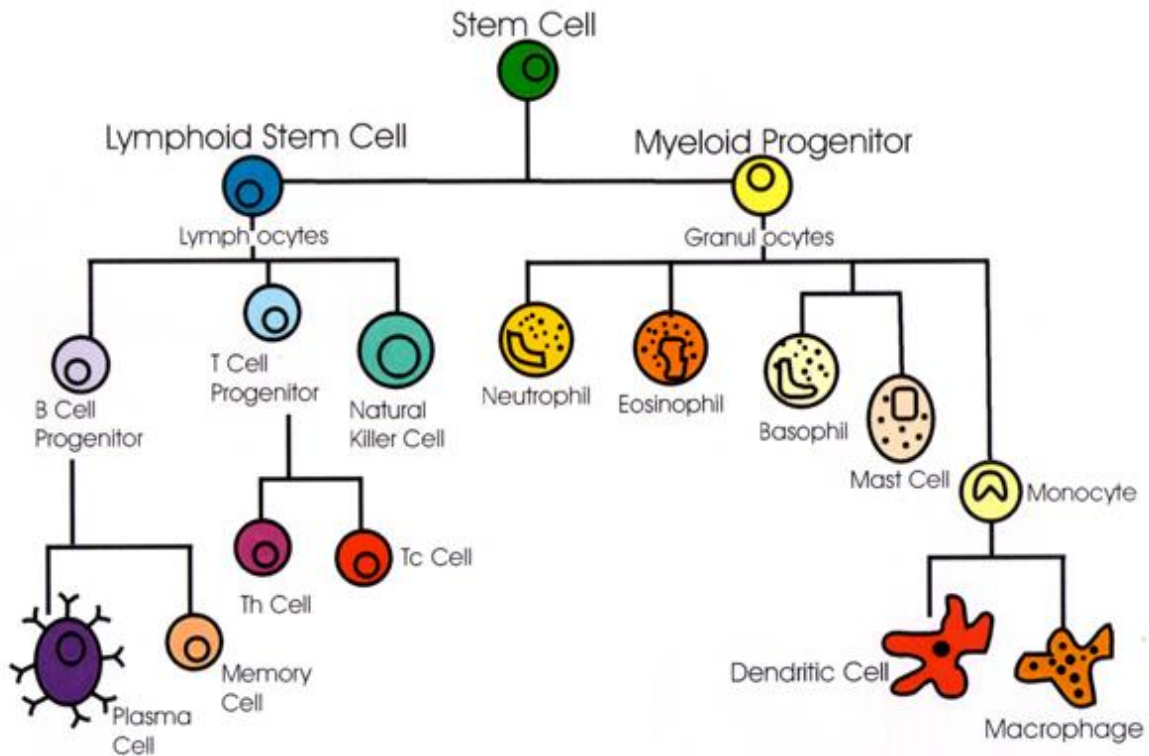
Figure 2.4: Hematopoietic stem cell lineage of immune system. Monocytes, dendritic cells and macrophages from the myeloid lineage as well as T-lymphocytes from the lymphoid lineage are the main cells which HIV infects. Through these cells the virus is able to survive, travel and multiply within the body. (Smith 2015)

2.6 HIV suppression by HAART

$CD4^+T$ cells, monocyte/macrophage derived cells and other immune system cells elicit an immune response against viral antigens during an infection, but eventually the immune system is weakened and results in the progression of HIV infection to AIDS (Avert 2011). To counteract this, there were about 25 different drugs developed, which are divided into six different classes of antiretroviral treatment (ART). ART consist of integrase inhibitors, nucleoside reverse-transcriptase inhibitors (NRTIs), non-nucleoside reverse-transcriptase inhibitors (NNRTIs) protease inhibitors (PIs), fusion inhibitors and a variety of fixed dose combination

15

drugs as well as the CCR5 receptor antagonists and maturation inhibitors (Zolopa 2010; Bhattacharya and Osman 2009).

The drugs have different mechanisms of suppressing HIV replication and consequently have largely decreased the morbidity and mortality rate of infected individuals (Worm *et al.* 2010; Zolopa 2010). Introduction of HAART brought a better application of these drugs by forming combination treatments of the ARV drugs to manage disease progression and viral resistance rates (Zolopa 2010). In an *in vitro* study by Brown *et al* (2006) GFP tagged HIV-1 genome was used to trace the fate of the virus and found that in HIV positive patients on HAART, 0.05% of macrophage population in the lymph nodes were still infected with HIV, which indicated viral latency (A. Brown *et al.* 2006). This led to the chronic use of HAART because the drugs do not completely eliminate the virus (Chavez 2015). Long term application of HAART has resulted in the development of metabolic disorders (Worm and Lundgren 2011). PI drugs were reported to cause hyperglycaemia, dyslipidemia and diabetes mellitus; the NNRTI drugs were associated with the development of dyslipidemia (Worm *et al.* 2010). Long term infection by the virus is considered the root cause of these metabolic disorders, then which are augmented by HAART and physiological risk factors (Chow and Day 2006, Lichtenstein 2003, Bacchetti 2005). The following section presents classification and examples of HIV related metabolic disorders.

2.7 HIV related metabolic syndrome

According to the World Health Organization (WHO) and European Group for the Study of Insulin Resistance (EGIR) the metabolic syndrome is classified by the development of insulin resistance. For general practice the National Cholesterol Education Program-Adult Treatment Panel III (NCEP-ATP III) classifies metabolic syndrome as the presence of any three disorders from abdominal obesity, elevated triglycerides, reduced high-density lipoprotein (HDL) cholesterol, elevated blood pressure and elevated fasting glucose risk factors (Slama *et al.* 2009). These

16

classifications where adapted from Reaven's term 'syndrome x' which he described as a cluster of occurring disorders for example dyslipidemia, obesity, impaired glucose tolerance and hypertension that independently relate to cardiovascular disease (Reaven 1997; Drelichowska *et al*. 2014).

Currently, metabolic syndrome refers to disorders that produce a high risk for the development of cardiovascular disease, atherogenesis and diabetes; but there is controversy around the definition and whether inflammation of cardiovascular disease and hepatic disorders should be included (Slama *et al*. 2009; Drelichowska *et al*. 2014).

Metabolic syndrome was identified in treatment naïve individuals even before the development of HAART (Slama *et al.* 2009). Obesity, lack of physical activity and excessive weight gain are used as predictors of metabolic syndrome (Worm and Lundgren 2011). Most HIV infected people have increased levels of triglycerides and low high density lipoprotein cholesterol (HDL) but in developed countries increase in waist circumference resulting from an increase in fat was the risk component (Worm and Lundgren 2011). Because metabolic syndrome is caused by HIV, HAART and possibly other diseases/illnesses; it is difficult to distinguish how and to what scale these contribute to the metabolic syndrome. A single component measurement of metabolic syndrome (performed by either glucose tolerance test, dual-energy x-ray absorptiometry or MRI) prediction is unreliable (Worm et al. 2010).

According to strategies for management of antiretroviral therapy (SMART) an increase in viral RNA load (> 100 000 copies/ml) and low CD4 cell count (< 100 cells/mm^3) has been associated with the development of metabolic syndrome but these results are still not conclusive (Worm and Lundgren 2011; Bonfanti *et al.* 2010).

A detailed account of the major component diseases of metabolic syndrome is provided next.

2.7.1 Insulin resistance

Insulin is a hormone produced in the pancreas by the beta cells in the islets of Langerhans. The hormone is released into the blood to facilitate the translocation of excess glucose from the blood to the liver and peripheral cells where it is stored as glycogen; it also promotes the metabolism of glucose, lipids and proteins in the muscle, liver and adipose tissue (Saltiel and Kahn 2001; Newsholme *et al.* 2003; Clearinghouse 2014). Insulin resistance occurs when muscle, fat or liver cells cannot respond to insulin, resulting in high levels of glucose in the blood stream and in turn causing an abnormal increase of insulin, ultimately leading to the development of type 2 diabetes (Bugianesi, McCullough, and Marchesini 2005; Clearinghouse 2014). Low HDL cholesterol and high triglyceride levels are characteristics that indicate prediabetes, because insulin regulates adipocyte metabolism by promoting storage of adipocyte triglyceride, lipogenesis, differentiation of preadipocytes and inhibiting lipolysis (Khan, Collins, and Keane 2000).

A homeostasis model assessment of insulin resistance (HOMA) reported high insulin resistance in HIV positive individuals with metabolic syndrome compared to those without during the HIV exposure and risk of metabolic syndrome (HERMES) study (Bonfanti *et al.* 2010). The researchers also found irregularities in blood glucose (Bonfanti *et al.* 2010). In another study HIV positive individuals had increased rate of insulin clearance and peripheral tissue sensitivity to insulin (El-Sadr *et al.* 2005). Insulin resistance in HIV infected individuals is also a risk factor for cardiovascular disease (Taiwo 2005)

2.7.2 Cardiovascular disease (CVD)

Cardiac abnormalities were identified in both adults and children infected with HIV and these manifestations were altered when HAART was introduced, this raised concerns about the virus itself and its influence in the presence of HAART, as more CVD cases were on the increase (Barbaro 2002). HIV affects the heart of HIV positive individuals in multiple ways. These include pericardial effusion, disturbance of rhythm, malignant infiltration, marantic endocarditis and heart muscle disease (Currie *et al.* 1994). Pericardial effusion or tamponade refers to the excessive production of fluid within the pericardium lining of the heart, caused by either opportunistic infections (*Mtb*) or malignancies (Kaposi sarcoma) related to HIV (Barbaro 2002). The build-up of fluid was seen to be enhanced by cytokine expression at a later stage of HIV infection (Barbaro 2002). Bonfanti deducted that activation of pro-inflammatory cytokines and the coagulation cascade may play a role in increasing the risk of CVD, due to elevated IL-6 (Bonfanti *et al.* 2010).

Abnormalities in the heart muscle (cardiomyopathy) especially dilated cardiomyopathy was recognized in HIV positive patients as caused by HIV itself before HAART was implemented (Barbaro 2002). About 30% of patients with HIV related cardiomyopathy had autoantibodies (anti-α myosin autoantibodies) which suggested left ventricular dysfunction (Barbaro 2002).

2.7.3 Lipodystrophy

Lipodystrophy also known as lipomatosis, central fat accumulation and peripheral lipotrophy is caused by HIV infection (and certain HAART drugs) that results in disfigurement of some HIV positive individuals (A. Carr 2010). These are changes in fat distribution around the body with fat accumulating in the abdomen, breasts, face, limbs and dorso-cervical spine (van der Valk et al. 2001; A. Carr *et al.* 2003). The associated risk factors are low HDL cholesterol, lactic acidaemia, hepatic transaminases and insulin resistance (A. Carr *et al.* 2003). Dyslipidemia is a lipoprotein metabolic disorder that is characterized by elevated levels of LDL

19

cholesterol and triglycerides as well as low concentrations of HDL cholesterol, typical of all metabolic syndrome risk factors (A. Carr *et al.* 2003).

2.7.4 Atherosclerosis

Atherosclerosis like other metabolic disorders associated with HIV, develops where there is an increase in LDL, triglycerides and decrease in HDL as well as the development of risk factors like diabetes mellitus and hypertension (Reape and Groot 1999). Atherosclerosis is a disorder whereby the arteries are blocked, eventually preventing blood circulation; the blockage is caused by high concentrations of LDL that result in a large number of sub-endothelial spaces (Reape and Groot 1999; Schillaci *et al.* 2005). Within these spaces LDL is oxidized by reactive oxygen species (produced by resident macrophages) and recruits leukocytes and adhesion molecules to the vascular wall (Reape and Groot 1999). Low CD4 cell count causes subclinical carotid atherosclerosis in HIV positive individuals (Schillaci *et al.* 2005).

2.7.5 Wasting syndrome

In 1987 the centers for disease control (CDC) classified the wasting syndrome as an AIDS-defining illness (Coodley, Loveless, and Merrill 1994). It is described as involuntary loss of 10% of body weight in HIV positive individuals; this is due to either chronic diarrhea, weakness and fever (Coodley, Loveless, and Merrill 1994). The decrease in body mass is primarily caused by a loss in body muscle as opposed to fat (Coodley, Loveless, and Merrill 1994). Cytokine effects, endocrine dysfunction and primary muscle disease are thought to cause wasting in patients (Coodley, Loveless, and Merrill 1994).

To understand these HIV-related metabolic disorders, we need to understand the influence the virus has on metabolites (risk factors), metabolic pathways and overall metabolism of the infected cells. Generally the risk factors for all the disorders are studied in isolation due to the limitation of available techniques, this is very challenging because the metabolome contains thousands of metabolites. A solution

would to be to find a system or technique that enables evaluation of multiple metabolites. Metabonomics carries such promise due to the holistic approach of the study. In the following section the definition and principles of metabonomics are presented.

2.8 The different 'Omics'

Through the years 'Omics' studies have been on the increase because not only do they generate comprehensive data but generally not all parameters being investigated need to be known to acquire useful data (Robertson *et al*. 2005) The 'omics' is a study of a wide range and a large scale of molecules such as DNA (genomics), RNA (transcriptomics), amino acids/proteins (proteomics) and metabolites (metabolomics/metabonomics). The main 'omics' presented in fig 2.6 are mentioned, but there is a vast range of other 'omics' such as pharmacometabolomics, nutriomics and fluxomics to name a few that describe subsets of metabolites in specific scenerios (Claudino *et al.* 2012; Juan Manuel Cevallos-Cevallos and Reyes-De-Corcuera 2012).
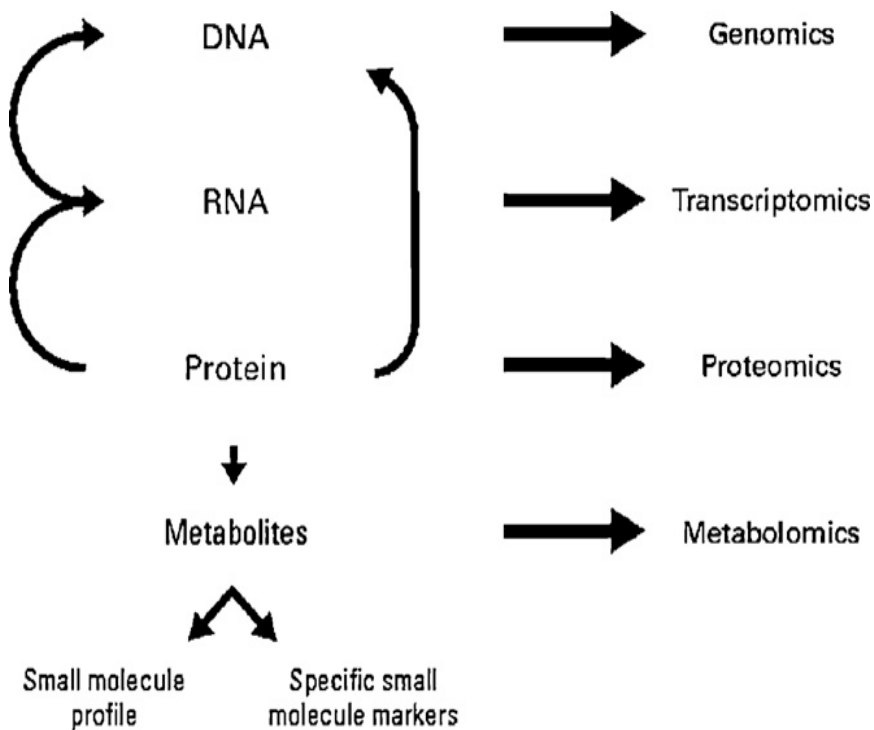
Figure 2.5: The main 'omics' (Claudino *et al.* 2012)

2.8.1 Metabonomics defined

Wishart *et al* (2011) emphasized the big difference in the number of metabolites produced compared to the number of proteins and nucleotides, by highlighting that 4 different bases in the genome make 20 different amino acids and subsequently thousands of different metabolites. This is why it is then said that metabonomics studies give an overall "instantaneous snapshot" of the cell physiology (Wishart 2011; Gambari and Lampronti 2006). A metabolite can be defined as a low molecular weight (<1,000 Da) organic molecule that is produced from metabolism (Roux et al. 2011; Van Der Werf, Jellema, and Hankemeier 2005). There are two types of metabolites, endogenous and exogenous. Endogenous metabolites are molecules that are produced in the body as metabolic pathway intermediates, these metabolites are produced as primary and secondary metabolites, essential for growth and development of an individual (Roux et al. 2011). Exogenous metabolites

arise from the metabolism of compounds acquired from the external environment (food and drugs) which are either enzymatically converted or modified for specific biological functions within the body (Roux et al. 2011). According to Gambari and Lampronti (2006) the metabolome is described as a collection of metabolites that result from gene expression (Gambari and Lampronti 2006). Metabonomics is thus a study of profiling multiple metabolites and the concentration changes due to genetic modification, drugs, stimuli or pathogens (Beckonert et al. 2007).

Generally Metabonomics and Metabolomics are used interchangeably. Practically, Metabolomics is used for plant studies and is defined as the 'systematic investigation of the unique chemical fingerprints that specific cellular processes leave behind'. Metabonomics, used for human and animal studies is defined as 'the study of the metabolic response of organisms to disease, environmental or genetic modification' (Roux *et al.* 2011; Gambari and Lampronti 2006; Lindon *et al.* 2000). Metabonomics is relatively new compared to the other main "omics" but provides a much more comprehensive view of the state of an organism (Gambari and Lampronti 2006; Beyoğlu and Idle 2013).

Metabonomics can be applied to determine metabolic profiles and patterns of diseased and healthy subjects, animal and human metabolic databases and used to investigate drug toxicity (Lindon, Nicholson, and Holmes 2007). Metabonomics investigations are conducted through analysis of blood serum/plasma, urine, saliva, tissue extracts, bile and cell culture supernatants (Lindon, Nicholson, and Holmes 2007). Metabolites are detected from these samples with analytical techniques such as nuclear magnetic resonance (NMR) spectroscopy, hyphenated mass spectrometry (-MS), infrared (IR) and Raman spectroscopy (Jankevics *et al.* 2012). Data from these is interpreted with statistical tools. A simplified metabonomics process is presented in fig 2.7. The next section will provide details of the techniques and statistical tools used for metabonomics.

sample collection, preparation and extraction

Spectroscopy/Spectrometry data acquisition

data and statistical pre-processing

statistical analysis

identification/quantification of differences between metabolites of different groups
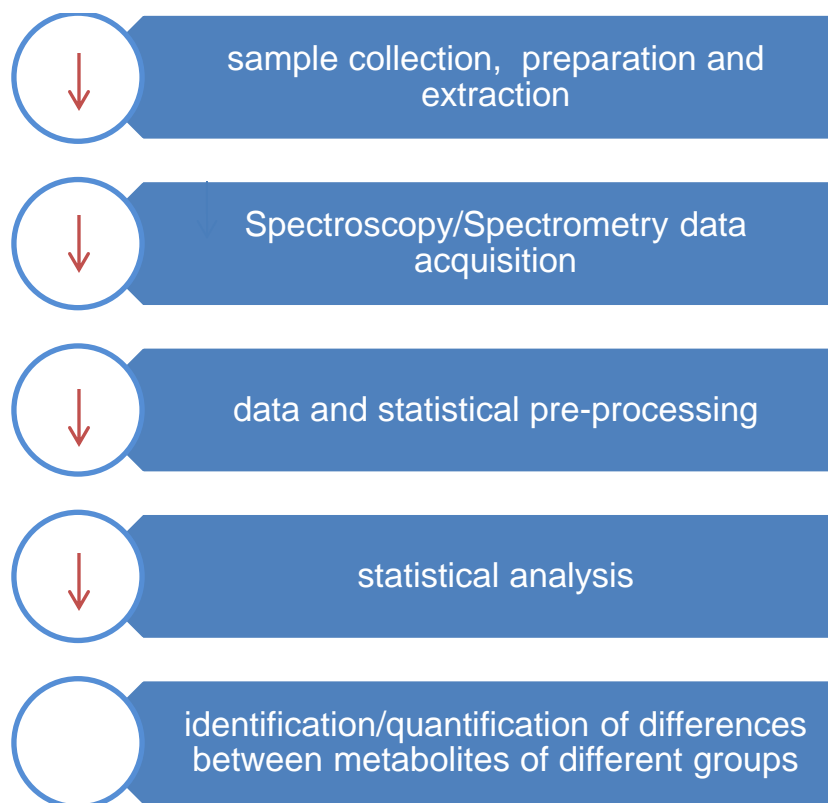
Figure 2.6: Metabonomic study process, essentially involves collecting of the sample and the use of high-throughput techniques such as spectroscopic techniques to acquire data. Statistical analysis is then applied to the data, which allows for the identification of metabolite differences within a particular sample.

2.8.2 Metabonomics investigations of HIV-1 infected cells/fluids

Metabonomics has been applied to many HIV infection studies, these studies are described below.

2.8.2.1 Blood based metabonomics

In our group Hewer *et al* (2006) used NMR spectroscopy to observe if NMR can detect differences in metabolic profiles of HIV infected/HAART and negative blood sera (Hewer *et al*. 2006). The authors found that that indeed there were significant differences between the group and that NMR successfully identified the metabolic profiles (Hewer *et al*. 2006). HAART treated HIV infected sera showed a large distinction between the experimental groups; lipids, glucose and amino acids were

24

discovered as significantly different. These findings were confirmed by Phillipeos *et al* (2009) NMR study of HIV infected, on HAART and HIV negative sera. LDL and VLDL lipids were identified. All these metabolites have been identified as risk factors associated with HIV related metabolic disorders such as lipodystrophy and diabetes (Philippeos, Steffens, and Meyer 2009). Another metabolite that was found to be significantly altered was choline. The authors highlighted that choline is a neural metabolite, which increased levels were associated with dementia (Philippeos, Steffens, and Meyer 2009).

Subsequently a gas chromatography-mass spectrometry (GC-MS) study was conducted on HIV positive and HIV negative sera. Statistical differences in metabolites involved in lipid, amino acid and glucose metabolism between the groups were identified (A. Williams *et al*. 2012). The authors also evaluated cell apoptosis (an indication of mitochondrial dysfunction) of peripheral blood mononuclear cells (PBMCs) and found that HIV infected cells had increased levels of apoptosis relative to non-infected cells (A. Williams *et al*. 2012).

An article by Eck *et al* (1989) found variable and elevated plasma and extracellular glutamate concentrations in HIV-1 infected cells (analysed with an amino acid analyser) that inhibited macrophage and lymphocyte functions compared to uninfected cells (Eck, Frey, and Droge 1989). Glutamate prevents the release of cysteine from macrophage, monocytic and fibroblast cells, which is involved in cell activation, division and other functions (Eck, Frey, and Droge 1989). In another study Hortin *et al* (1994) compared amino acid plasma concentrations of HIV-1 infected and uninfected individuals (Hortin, Landt, and Powderly 1994). The samples were analysed by post-column reaction with o-phthalaldehyde and fluorescence to detect the amino acids. The authors compared 21 different amino acids among HIV positive and negative plasma samples. Cysteine, methionine and tryptophan concentrations were decreased; taurine and lysine were increased in HIV infected plasma compared to HIV negative (Hortin, Landt, and Powderly 1994).

25

2.8.2.2 Cell culture supernatant based metabonomics

LC-MS analysis was used to determine the metabolic profile differences of activated CD4^{+} T cells and activated U1 derived macrophages compared the uninfected counterparts (Hollenbaugh, Munger, and Kim 2011). In the study glucose uptake was increased in actively replicating CD4^{+} T cells and decreased in activated U1 macrophages. This proves that the fate of the two immune system cells have different outcomes of HIV infection (Hollenbaugh, Munger, and Kim 2011). Glucose-3-phosphate was also reduced in U1 macrophages but pyruvate was increased, the authors hypothesized that this could be due to the slow functioning of mitochondrial related TCA cycle or other carbon sources from amino acids that increase pyruvate concentrations (Hollenbaugh, Munger, and Kim 2011).

Lutz *et al* (1997) used high resolution ^{1}H, ^{31}P and ^{13}C NMR to analyse possible changes of glucose metabolism in human intestinal epithelial cells (HT-29) that were chronically and acutely infected with HIV-1, as well as uninfected cells (Lutz *et al.* 1997). They found that chronically infected HT-29 cell morphology was still typical, consisting of microvilli and tight junctions on apical brush borders (Lutz *et al.* 1997). Actively replicating infected cells produced growth retarded microvilli and hypertrophy of the Golgi apparatus, which is responsible for terminal glycosylation of glycoproteins (Lutz *et al.* 1997). Chronically infected cells had 181% increased glucose and 66% decreased fructose-1,6-diphosphate levels compared to controls (similar results to sera/plasma studies) (Lutz *et al.* 1997). Acutely infected cells had a 33% increase in nicotinamide adenine dinucleotide levels compared to the controls. An increased glucose production within HIV replicating HT-29 cells indicated that increased energy is required for replication (glucose is the main source of energy through glycolysis and other pathways) (Lutz *et al.* 1997). The authors then concluded that HIV may cause metabolic disorders by affecting the carbohydrate and lipid metabolism of intestinal epithelial cells in AIDS patients (Lutz *et al.* 1997).

2.8.2.2.1. Flow cytometry for cell culture experiments

In cell based NMR experiments and particularly in this study, it is vital to have the metabolites released into the cell supernatant for NMR analysis. By employing cell lysis methods, the extent of cells lysis thus metabolite release, can be determined by flow cytometry. Flow cytometry is a technique used to sort and measure the viability of cells through their individual properties, by streaming the suspended cells in a single file within a stream of fluid (Díaz *et al.* 2010). The cells are passed through a beam of light that is then scattered by the cells at different angles that distinguish differences in size and density (Díaz *et al.* 2010). Specific dyes are used to label cells to indicate the different stages of cell death, which fluorescence of these dyes is detected at particular wavelengths (Díaz *et al.* 2010). Measurements are made on individual cells therefore sample heterogeneity can be quantified and subpopulations of cells can be identified for any contamination (Díaz *et al.* 2010). A high number of cells are measured per second (Díaz *et al.* 2010). It is a rapid analysis that allows information to be obtained qualitatively and quantitatively (Díaz *et al.* 2010).

Many articles have employed the use of flow cytometry; Riscoe *et al* 2004, used the high-throughput technique to determine the effect of existing, new and combination of antimalarial drugs on *Plasmodium falciparum* in red blood cells by using fluorescent dyes, they were able to track a linear correlation between the level of fluorescence and the level of parasitemia. Niki *et al* 2003, measured the extent of cell death with flow cytometry and fluorescent dyes of Jurkat cells deprived of selenium, an essential trace element which plays a role in cell survival and proliferation (Niki *et al.* 2003). The fluorescent dyes annexin V- FITC and Propidium Iodide are the most commonly used to determine the extent of cell death by indicating apoptosis (programmed cell death) and cell necrosis respectively (Niki *et al.* 2003). Annexin V- FITC binds to exposed phosphatidyl serine of the cell membrane which this process usually occurs during cell apoptosis, while PI binds to exposed nucleic acids thus indicating cell death and lysis. There are a number of

27

methods that can be used to cause cell death, cells can either be chemically (methanol and auranofin) or mechanically (sonication and freeze-thaw) treated (Chen 2014; Basu 2000; Hutcheson *et al*. 2010; Mellerick & Liu 2004). For NMR experiments mechanical lysis such as freeze-thaw method is preferred because unlike methanol which could distort metabolic profile results the supernatant is left as is. The freeze-thaw method involves freezing samples in liquid nitrogen and then thawing in a waterbath for a number of cycles, this causes the cells membrane to disrupt and release their contents (Basu 2000).

2.8.3 Instrumentation used in metabonomic investigations

To characterize disease states in response to an external influence such as a viral pathogen, a large number of metabolites can be analysed through the use of metabonomics instruments such as NMR, MS, Fourier transform infrared (FT-IR) and Raman spectroscopy (Sitole, Williams, and Meyer 2013). These are high resolution and high throughput analytical tools, which enable identification and quantification of many metabolites produced from metabolism (Sitole, Williams, and Meyer 2013). In a metabonomics study design, the sample determines the type of technique to be used whether it is LC-MS spectrometry, NMR, IR or Raman spectroscopy. The objective of the study should be to get the maximum amount of information with a low number of experimental runs at a lesser time, which in clinical practice could reduce the amount of time that metabolic disorders are detected and identified (Trygg, Holmes, and Lundstedt 2007). The properties of the instrumentation used in metabonomic studies are presented and compared in table 2.1.

Table 2.1: Presents metabonomics instrumentation properties

Instrument	Properties
FT-IR	Identifies functional groups, time consuming
Raman	Weak signals
MS	Sample destruction, intensive sample preparation, sensitive
NMR	Detects fine structural components, quantitative and qualitative, minimal sample preparation, highly reproducible

2.8.3.1 Vibrational spectroscopy

FT-IR and Raman spectroscopy are classified as vibrational spectroscopy techniques, these are used to identify compounds according to molecular vibrations and rotations (Stuart 2005).

(1)FT-IR and Raman spectroscopy

FT-IR spectroscopy is a technique were infrared radiation is passed through a sample and the bonds of the functional groups within the sample absorbs the energy, causing rotations and vibrations by either stretching, bending of bonds or a combination of both (changing its molecular dipoles) (Ellis and Goodacre 2006). The vibrations through Fourier transformation are transformed into an infrared absorption spectrum which characterizes the bonds and functional groups of biochemical compounds (provides the fingerprint of compounds) (Ellis and Goodacre 2006; Stuart 2005). The infrared spectrum is divided into three regions the far infrared (< 400 cm^{-1}), mid infrared (4000-400 cm^{-1}) and near infrared (14285-4000 cm^{-1}), mid infrared region is generally used in disease diagnostic studies

because it contains more defined peaks such as fatty acids and proteins (Ellis and Goodacre 2006; Stuart 2005).

While FTIR gives a fingerprint for carbohydrates, amino acids, lipids, fatty acids, and polysaccharides, Raman spectroscopy involves the inelastic scattering of light (Ellis and Goodacre 2006; Stuart 2005). A photon is absorbed by a Raman active molecule which in turn re-emits energy at a lower frequency usually within the infrared region (Ellis and Goodacre 2006). This shift provides the vibrational and rotational properties of the sample thus the fingerprint of the sample (Ellis and Goodacre 2006). The disadvantage of using these techniques is that information is functional group specific and in infrared spectroscopy there's an overlap of certain molecules (carbonyl and amides in different proteins) that makes pure samples essential (Ellis and Goodacre 2006).

2.8.3.2 Mass spectrometry

The idea of determining the metabolic pattern is said to be introduced by Williams (1951) who compared urine samples of 200000 mental patients (Roux *et al*. 2011; R. Williams 1951). This was followed by a study of metabolic profiling of urine samples through gas chromatography-(GC-MS) (Roux *et al.* 2011). Metabolite profiling of molecules was done by directly injecting a sample into a mass spectrometer (MS), but profiling of the metabolites using this technique needed the metabolites to be separated prior to detection (Roux *et al*. 2011).

To elucidate the chemical composition of samples, MS uses a mass to charge (m/z) ratio which is different for every compound (Becker 2007). In the MS machine the sample is analysed in a vacuum due to the reactive nature of ions, small amounts of liquids, solids (are vaporized upon entering) and gases are ionized by an electron beam which by assumption gives all the atoms a positive single charge, through the displacement of a single electron (Becker 2007).

Once ionized the sample is accelerated towards a magnetic field with oppositely charged parallel plates. At this point the positively charged molecules are attracted to the oppositely charged plate at different strengths depending on their mass. Therefore the light weight molecules are more deflected. Ions are detected according to charge and chemical data processed (Becker 2007). The technique is highly sensitive but it requires intrinsic sample preparation.

Usually MS is used in conjunction with other techniques such as gas chromatography (GC) and liquid chromatography (LC) to separate the molecules. Sample destruction occurs in MS.

2.8.3.3 NMR spectroscopy

Since the 1980s NMR spectroscopy has been used to determine multiple analytes and the resulting data is interpreted using multivariate statistics to classify samples according to their biological state (Nicholson, Holmes, and Lindon 2007). Diet, lifestyle, environment, genetic and pharmaceutical effects influence the biological state of individuals and can be either helpful or harmful and are said to also contribute to the extent of influence a pathogen will have on a person (Nicholson, Holmes, and Lindon 2007). Since its development (as it relates to metabonomics) NMR has been used for biofluid, tissue and cell metabolic profiling (Salek, Cheng, and Griffin 2011).

NMR spectroscopy is a relatively quick, non-destructive, highly reproducible technique that requires minimal to no sample preparation and also uses small sample volumes for both pure compounds and mixtures (Nicholson, Holmes, and Lindon 2007). The principle of NMR relies on certain atoms such as ^{1}H, ^{13}C, ^{15}N, ^{31}P and ^{19}F with an odd number of protons, thus possessing a nuclear spin that creates a magnetism around them (Lindon, Nicholson, and Holmes 2007).

When a sample is introduced into NMR equipment an external magnetic field is released causing the atoms to align in the direction of or against (have different

energy states) the external magnetic field. When a high frequency magnetic field (eg F1) is applied the atoms are excited from a low energy state to a higher energy state, the energy to create that transition for each element is different therefore require a different frequency (magnetic pulse) of field F1 (Lindon, Nicholson, and Holmes 2007). As the atoms return to their lower energy state each atom releases different energy frequencies according to their proton (or other nucleotide) composition and the different spatial environment the atoms are in. The data is released as a frequency which is converted to a spectrum; for example a ^{1}H spectrum represents hydrogen atoms in different environments (chemical shifts) (Lindon, Nicholson, and Holmes 2007). Figures 2.8 and 2.9, shows the process for sample analysis and the NMR workstation/instrumentation respectively.
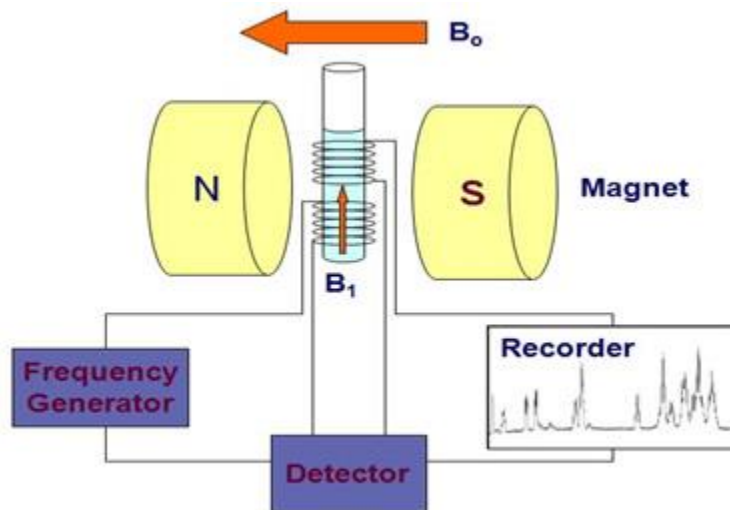
Figure 2.7: a simple depiction of the internal environment within an NMR spectrometer. Each metabolite has its own frequency which can be detected and transformed into peaks observed from the recorder. (Agilent 2013)
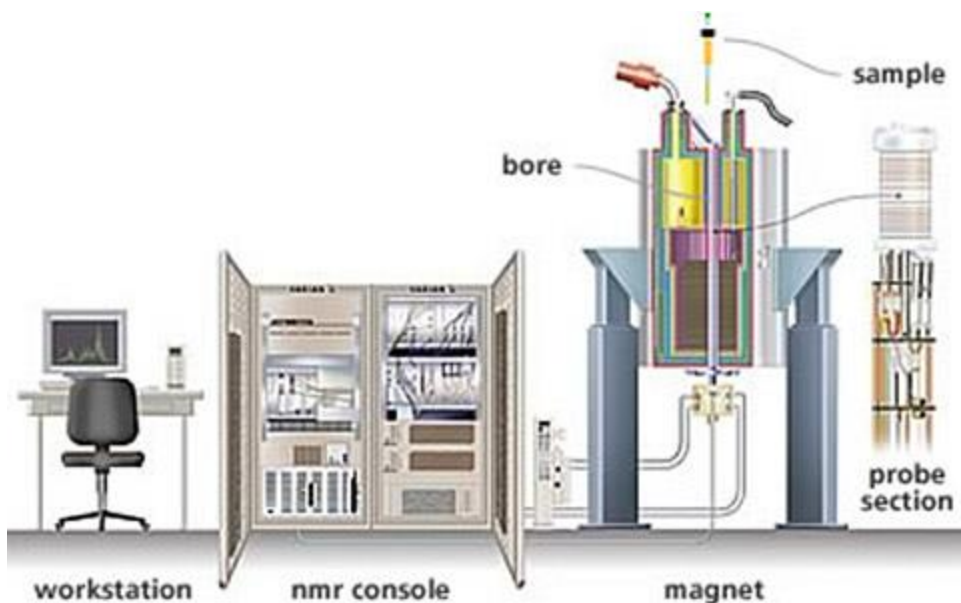
Figure 2.8: NMR spectroscopy facility. The facility includes a spectroscope were the sample is inserted, a console for data transformation and a workstation with a computer to present the data. (Agilent 2013)

2.9 Metabonomics chemometrics/bioinformatics

2.9.1 Data pre-processing

Before any statistical analysis, the raw data is pre-processed to ensure that the most accurate results are presented. Pre-processing includes baseline correction, spectral alignment, water suppression, normalizing and binning (Robertson 2005). Software such as Bruker Topspin and Mestrenova are used for data pre-processing (Mavel *et al.* 2013)

2.9.2 Chemometrics and Bioinformatics defined

Chemometrics is defined as a broad application of mathematical and statistical methods and tools used for spectral processing, peak alignment, outlier detection normalization, solvent suppression (Robertson 2005). Bioinformatics involves the storage, retrieval and analysis of computer-stored information (such as in

33

databases) for biological research; mathematics and computer science techniques are used to organize and form ideas from biological data (Robertson 2005). An overlap in these applications occurs when databases are used to process spectra. Whole spectra are overlaid for pattern recognition instead of looking for matching single areas and can be readily annotated (Robertson 2005). Pattern recognition methods drove to the implementation of COMET consortium where the spectra and not the pattern are processed to obtain component identification, but this method is costly and time consuming (Robertson 2005). This lead to the establishment of multivariate analysis such as PCA and LDA, these tools enable a large set of data to be processed at a short period of time (Robertson 2005).

Metabolic analysis is divided into three categories; discriminative, informative and predictive analysis. Discriminative is based on finding differences between sample groups without necessarily elucidating the metabolic pathways that are responsible for the differences and also without creating statistical models (Cevallos-Cevallos *et al*. 2009). This analysis is achieved through the use of principal component analysis (PCA) and other multivariate data analysis (MVDA) (Cevallos-Cevallos *et al*. 2009). Informative analysis is used to identify and quantify metabolites to acquire essential information about their metabolic pathways and influences, usually the results from this type of analysis are included in databases. In predictive metabonomic analysis, statistical models and information on the metabolic profiles are used to predict the outcome of a certain variable for example partial least squares (PLS) statistical analysis is used (Cevallos-Cevallos *et al*. 2009).

There are two types of statistical analysis of observations. Descriptive statistics involves organizing of observations into a form that can be described by a few key parameters (standard deviation, mean) and inferential statistics compares and derives conclusions about two groups to determine if they are different or not (Brown 2005).

2.9.2.1 Analysis of variance (ANOVA)

Analysis of variance (ANOVA) is inferential statistics that compares if there are differences in means from three or more groups and whether the null hypothesis can be reject (which states that the means of the group are the same). One-way ANOVA uses a single independent variable to compare the means and factorial ANOVA uses multiple independent variables (Brown 2005). An ANOVA analysis is said to calculate the 'overall variation between the groups and the overall variation within the group.' In order to identify which of the group means contributes to the difference multiple, more calculations should be conducted (Brown 2005). *Post hoc* tests are conducted to determine the differences between any pair of group means; among these tests (Dunett's, Fisher's and Scheffe's test to name a few) is the Tukey's test (Brown 2005).

A Tukey's test (also known as honesty significant differences (HSD) method) is designed to compare means in a stepwise manner while maintaining the error rate of α level (describes how different the group means are; if the difference is equal to or less than 5% the null hypothesis is rejected) (Brown 2005). For example in a group of nine there are 36 possible comparisons, which is the critical value. Tukey's test is generally used because it tests in a wide range of situations (including unequal group sizes) using a single critical statistic and remains conservative fig 2.10 (Brown 2005).

SPSS, GraphPad Prism and SigmaPlot are statistical computer programmes used to acquire ANOVA results (Brown 2005).

Step 1	Null hypothesis states that the group means from which k samples are selected are equal
Step 2	Compute the F ratio
Step 3	Set the criteria for rejecting Null hyothesis.p
Step 4	Decide to reject Null hypothesis if F ratio > F distribution at $\alpha = 0.05$
Step 5	Select appropriate post-hoc test
Step 6	Compute test statistic
Step 7	Set criteria based on Critical statistic
Step 8	Compare test statistic with Critical statistic to determine significance

Figure 2.9: Sequential steps for a post hoc test such as a Tukey's test. The process involves the calculation data significance (Brown 2005)

2.9.2.2 Principal component analysis (PCA)

In a metabonomic study, principal component analysis (PCA) divides the spectrum into small regions of widths associated with metabolites (in biofluids water regions are excluded from the spectrum). These 'bins' are typically around 0.04 ppm in width; which can produce about 200-250 'buckets' in a 10 ppm NMR spectrum (Robertson 2005). In an NMR spectrum different bins may correspond to a single metabolite making the spectrum highly correlated. PCA, a statistical tool, reduces the number of variables that are usually correlated into a lower number of uncorrelated variables. The first principal component provides the most variable data and the second component provides variable data that is not dependent on the first so does the third and so forth, are all independent to one another (Robertson 2005). PCA produces the results as dot plots, each dot representing two variables on a two dimensional plot (Robertson 2005). On the plots the dots with similarities are clustered into groups a representation is provided in fig 2.11 (Szefer 2003; Trygg, Holmes, and Lundstedt 2007). The disadvantage of PCA is the lack of the component's physical and chemical information making it difficult to interpret (Szefer 2003). PCA gives an overview of multivariate profiles and can reveal grouping, trends and outliers as depicted in fig 2.12 (Trygg, Holmes, and Lundstedt 2007).
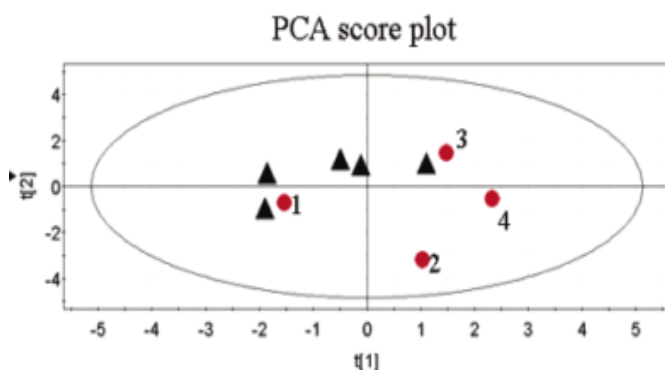
Figure 2.10: Simplified PCA plot which shows grouping of the samples; triangles (above the x-axis) and circles (are below the x-axis). (Trygg, Holmes, and Lundstedt 2007)
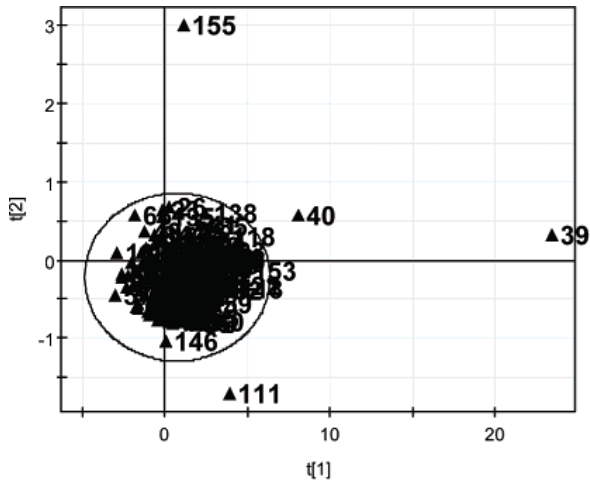
Figure 2.11: PCA plots with outliers (Trygg, Holmes, and Lundstedt 2007)

2.9.2.3 Linear discriminant analysis (LDA)

LDA is a multivariate and supervised statistical tool that separates groups/classes by finding linear discriminants that maximize the ratio of between-class variance and minimizes the ratio of variance within class (Dobrowolski *et al.* 2014). Unlike PCA, LDA data is pre-categorized into classes were it is trained to separate species according to class (Dobrowolski *et al*. 2014). Figure 2.13 represents LDA generated group clusters.

(a)
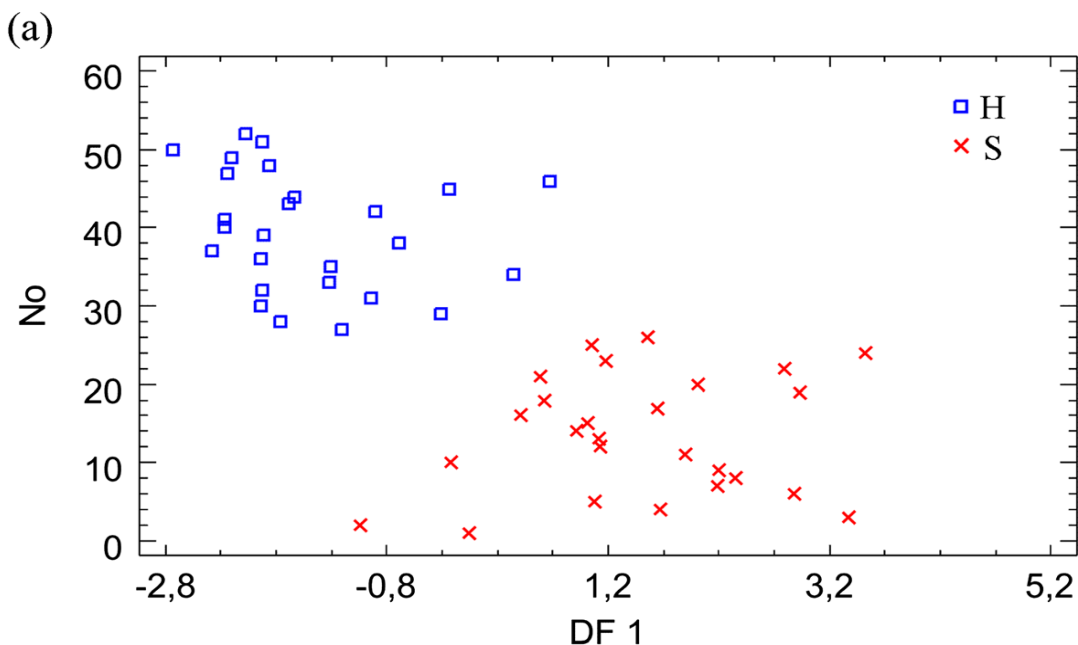
Figure 2.12: Example of an LDA plot which shows distinguishable group clusters of H (blue) and S (red) (Dobrowolski *et al*. 2014)

2.10 Rationale

As demonstrated in other studies, metabolic profiles of latently infected immune cells and global metabolite analysis is possible. Metabonomic studies using cell supernatants as metabolite source (instead of blood/urine) are limited. Currently, there are no studies that have compared the metabolic profiles of latently infected U1 cells to the active virus counterpart. Due to the elusive nature of latent virus and the effect of the virus as a whole on metabolism, it is of importance to understand which cellular pathways the virus influences. In this study through NMR spectroscopy analysis, metabolic profiles of HIV-1 latently and actively infected U1 cells were investigated and the data statistically analysed with chemometric and bioinformatics tools to determine the statistical differences between cell lines and potential biomarkers of HIV-1 latency and the associated metabolic disorders. In the next section the objective and aims of the study are presented.

39

2.11 Hypothesis

In general, metabonomics is considered a hypothesis generating field; whereby, a new hypothesis could be derived from the initial findings. For this study we propose a possible hypothesis as being 'Metabolic profiles of latently and actively infected U1 cell culture supernatants should be detectable and distinguishable by NMR spectroscopy'. This is done so we have a working hypothesis, fully understanding that the data may lead us to an entirely new hypothesis.

2.12 Objective

The objective of the study was to determine whether NMR spectroscopy could detect significantly different metabolites/ metabolic profiles that differentiate latent HIV-1 positive cells, active HIV-1 active positive cells and HIV-1 negative cells.

2.13 Aims

- The first aim was to determine the growth pattern and extent of cell lysis by flow cytometry. Viability dyes such as trypan blue could have been used but are less sensitive compared to flow cytometry

- In the second aim, due to the robustness of the technique and minimal sample preparation, NMR spectroscopy was selected to determine the metabolic profiles of actively/latently infected U1 cells and HIV negative U937 parent cell line. With the use of statistical analysis, differences in metabolic profiles of cell supernatants were also investigated.

- The influence of an increase in a metabolite in this case, lactate on the metabolic profiles of infected U1 and uninfected cells U937 cells was investigated to observe how fluctuations of metabolite concentrations could affect the infected cell's metabolism.

Chapter 3: Materials and method

3.1 Introduction

Chapter 3 presents the background and methods of experiments conducted for this study. In the first experiment metabolic profiles from U937 and U1 (PMA induced and non-induced) cell supernatants were elucidated through NMR spectroscopy, to determine metabolite differences between the samples. In the second section of the work U937 and U1 (PMA induced and non-induced) cells were treated with lactate, to observe the effect of increased lactate concentration would have on cell metabolism. The latent virus in U1 cells is activated with PMA. The data acquired from these experiments were analysed by bioinformatics and chemometric tools to identify metabolites and determine significant differences between the sample groups. Section 3.1 indicates a summarized annotated diagram of the work flow fig 3.1.

(1) Experimental design
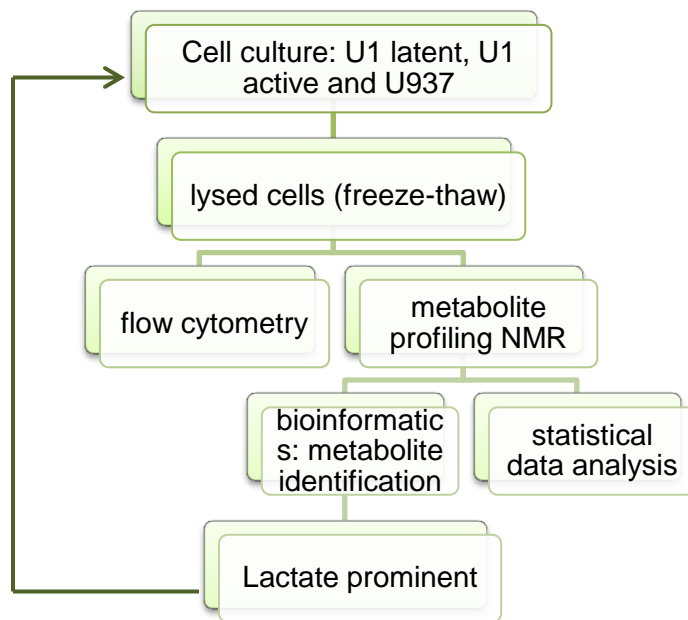
Figure 3.1: Experimental design

3.2 Cell culturing

U1 cells were obtained from the AIDS Research and Reference Reagent Program, NIAID, National Institute of Health (Rockville, MD) and U937 cells, from Highveld Biological (Pty) Ltd (Sandringham, South Africa). The cells were grown in RPMI-1640 media (Sigma Aldrich, Missouri, USA) supplemented with 1% of 100 U/ml penicillin with 100 µg/ml streptomycin (Thermo Scientific, HyClone®, UT, USA), 2.5% Hepes buffer (Thermo Scientific, HyClone®, UT, USA), 2g/L $NaHCO_3$ (Merck) and 10% fetal bovine serum (FBS) (Thermo Scientific, HyClone®, UT, USA) at pH 7.1 and incubated (Nuaire, Nu-4850E) at 37ºC, 5% CO_2, 90% humidity for two days.

HIV-1 was activated by stimulating 2×10^6 cells/ml of U1 cells with 2 nM Phorbol-12-myristic-13-acetate (PMA) dissolved in RPMI-1640 media (prepared as described earlier). PMA is a protein kinase C-activating phorbol ester used to stimulate U1 cell differentiation to induce activation of HIV-1 (Kulkosky et al. 2001)Adams *et al.* 1994). U937, Stimulated and unstimulated U1 cells (2×10^6 cells/ml) were plated into 12-welled plates to a total volume of 2ml/well of RPMI media. All the samples were incubated at 37ºC incubator for 48 hrs. After metabolic profiling of the samples, cells were prepared as above but 10 mM (the anaerobic threshold for lactate concentration in 4 mM) of lactate was added to the samples into each well before 48 hrs of incubation (De Feo et al. 2003). The experiment was performed to assess how HIV-1 affects cell metabolism in response to an increase in metabolite (lactate) concentration. Lactate plays an important role in glycolysis and was found to be significantly present in the initial experiments and thus was selected for this investigation.

3.2.1 Metabolite extraction and optimization

After 48 hrs of incubation (unstimulated and stimulated) U1 and U937 cells (2×10^6 cells/ml) were transferred into 10 ml tubes and centrifuged for 5 min at 1200 rpm (Allegra 25 R, Beckmann coulter). The cell pellet was re-suspended and washed

twice in 1% phosphate buffer saline (PBS). After washing the cells were centrifuged and the pellet was re-suspended in 1ml D_2O/PBS (deuterium oxide, 99.9% atom, Sigma Aldrich, South Africa/PBS) solvent solution. Metabolites were extracted from the cells by 5x freeze thaw cycles through freezing in liquid nitrogen and thawing in a 37 ⁰C waterbath (Labtech). Between each cycle after thawing the cells were vortexed. The cells were then centrifuged and the supernatant transferred into 1mm (diameter) NMR tubes (Bruker, Billerica, MA, United States of America) for NMR analysis (Bruker, Billerica, MA, United States of America), the cell pellets were transferred into 5 ml glass tubes for flow cytometry analysis. The first attempt at cell lysis; sonication was used, this data is presented in the Appendix (fig.1 & 2).

3.3 Determination of cell lysis through flow cytometry

Flow cytometry (Becton Dickinson South Africa) was used to assess the extent of cell lysis. Annexin V and propidium iodide (PI) (Becton Dickinson South Africa) are stains used in flow cytometry (Beckman Coulter cytometer, BD Biosciences) to determine the extent of cell lysis through staining of the cell membrane phosphatidyl serine and DNA respectively, during cell death.

Control cells pre-treatment

Annexin control (the stain was used to detect cells undergoing apoptotic cell death): U1 and U937 cells (2 x 10^6 cells/ml) in 10 ml of 10% RPMI media with 10 µM auranofin (compound used to induce cell death) were incubated in a 37⁰C, 5% CO_2 and 90% humidity incubator for three days. On the day of experiments, Propidium Iodide (PI) treated control cells were prepared; the stain binds DNA and is used as an indication of necrotic cells. Both these stains provide an indication of the extent of cell lysis and thus the extent of supernatant release. Cell necrosis (PI) control: in 2 x 10^6 cells/ml cells 2 ml of pure methanol was added to the cells to induce cell death and placed in ice for 15 min. The cells were then centrifuged for 5 min at 1200 rpm and washed twice in 1x PBS buffer. The annexin control cells were centrifuged and washed twice in 1x PBS buffer. Viable control cells: Stained

43

(contain Annexin and PI stains) and unstained control cells (2×10^6 cells/ml) were also washed twice in 1x PBS buffer.

Flow cytometry samples

To all the cells 400 µl of 1% Annexin buffer was added including freeze-thaw cell pellet (Section 3.2.1), 1 µl of Annexin stain was added to all cells except unstained and PI control cells. PI stain (5 µl) was added to all cells except unstained and Annexin control cells. After 15 min, 1% Annexin buffer was added and the samples were analysed by a flow cytometer, and 10000 events were recorded for each sample (BD biosciences, FACSCalibur flow cytometer).

3.4 NMR analysis

After preparation, all experimental samples (section 3.2.1) and a NMR standard trimethylsilyl propionate (TSP) in D_2O/PBS buffer standard were introduced into a ^{1}H Bruker Avance II spectrometer with a z-TXI probe operating at 400 MHz (Germany) and analysed at 25 ºC (Department of Chemistry, University of Pretoria). Proton NMR was measured using the spectral width of 20.548 ppm, 64 scans, 256 free induction decays (fid) and an acquisition time of 3.9846 s with 4 s relaxation delay; water resonance was suppressed using nuclear overhauser effect spectroscopy (NOESY).

3.5 Chemometrics and bioinformatics

The spectral data from NMR analysis was pre-processed using Mestrenova 10.0.1 software (Mestrelab Research, Santiago de Compostela, Spain. www.mestrelab.com). Mestrenova software is a user friendly and self-explanatory application that has descriptive tabs for analysis, which allow for spectral data pre-processing. In the Baseline corrections interface 2nd or 3rd order polynomials were applied to the data/spectra. An external standard, Trimethylsilyl propionate (TSP) which is detected at 0 ppm was used to align the spectra to the correct chemical

44

shifts by overlapping the TSP spectrum to that of the samples. The water peak (4.4-5.5 ppm) was excluded from the spectra including the flanking regions where no peaks were found. The spectra were divided into 0.04 ppm width bins and all the spectral data converted into Microsoft Excel data.

Statistical analysis was performed by the Department of Statistics (University of Pretoria) using IBM SPSS 20.0 statistical programme. The data was standardized by determining the Z-score for each segment. Comparisons of experimental sample spectra were performed by using the analysis of variance (ANOVA) with Tukey's *post hoc* test. Statistical differences between sample groups were determined and only cases of a *p*-value less than 0.05 were considered. To classify experimental samples into groups of either HIV-1 negative (U937) cells, latently or actively infected U1 cells, a stepwise linear discriminant analysis (LDA) was applied to the standardized data. Two discriminant functions were determined and presented on scatter plots. HMBD, KEGG and Chenomx (www.chenomx.com) software were used to putatively assign metabolite identities.

In the following chapter the results of the study were presented.

Chapter 4: Results

4.1 Cell lysis profile through flow cytometry

The first aim of the study was to culture and assess the extent of cell viability/lysis through flow cytometry. This was performed to confirm the successful release of metabolites from the cells (2 x 10^6 cells/ml) using the freeze-thaw method by comparing to the number of viable cells to cells that had undergone cell death. The flow cytometry plots were divided into four quadrants Q1 indicated viable cells which did not stain, Q2-3 indicate late and early apoptosis respectively by the staining of annexin (Comp-FITC-A); Q4 indicated necrotic cells stained by the PI stain (Comp-PE-Texas Red-A). In fig 4.1a, after incubation 92% of (2 x 10^6 cells/ml) cells which didn't undergo freeze-thaw cycles were still viable, 8% of the cells were in late apoptosis. In comparison (2 x 10^6 cells/ml) cells after five freeze-thaw cycles, 84% of cells had lysed which indicated that the cell contents were released fig.4.1b. Unstimulated U1 cell results are used to represent all sample data because similar results were observed with all the samples. Fig.4.1c1-3, depicts scatter plots of the control samples, c4 shows the scatter pattern of cells that had undergone freeze-thaw cycles. It was noted that the majority scatter pattern of the freeze-thaw cells did not resemble any of the isolated control populations (c1-3) but produced a different pattern which indicated cell debris (c4).

46
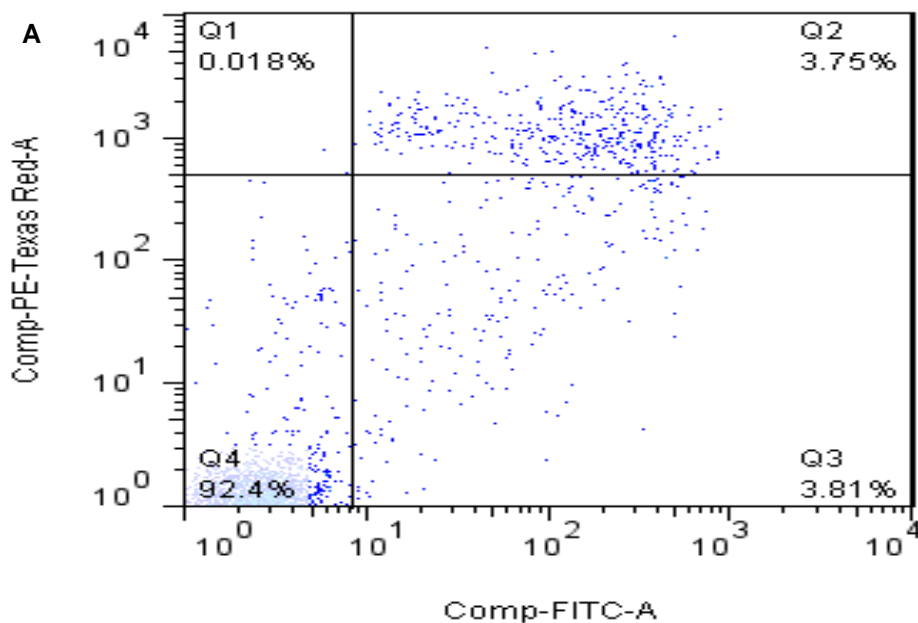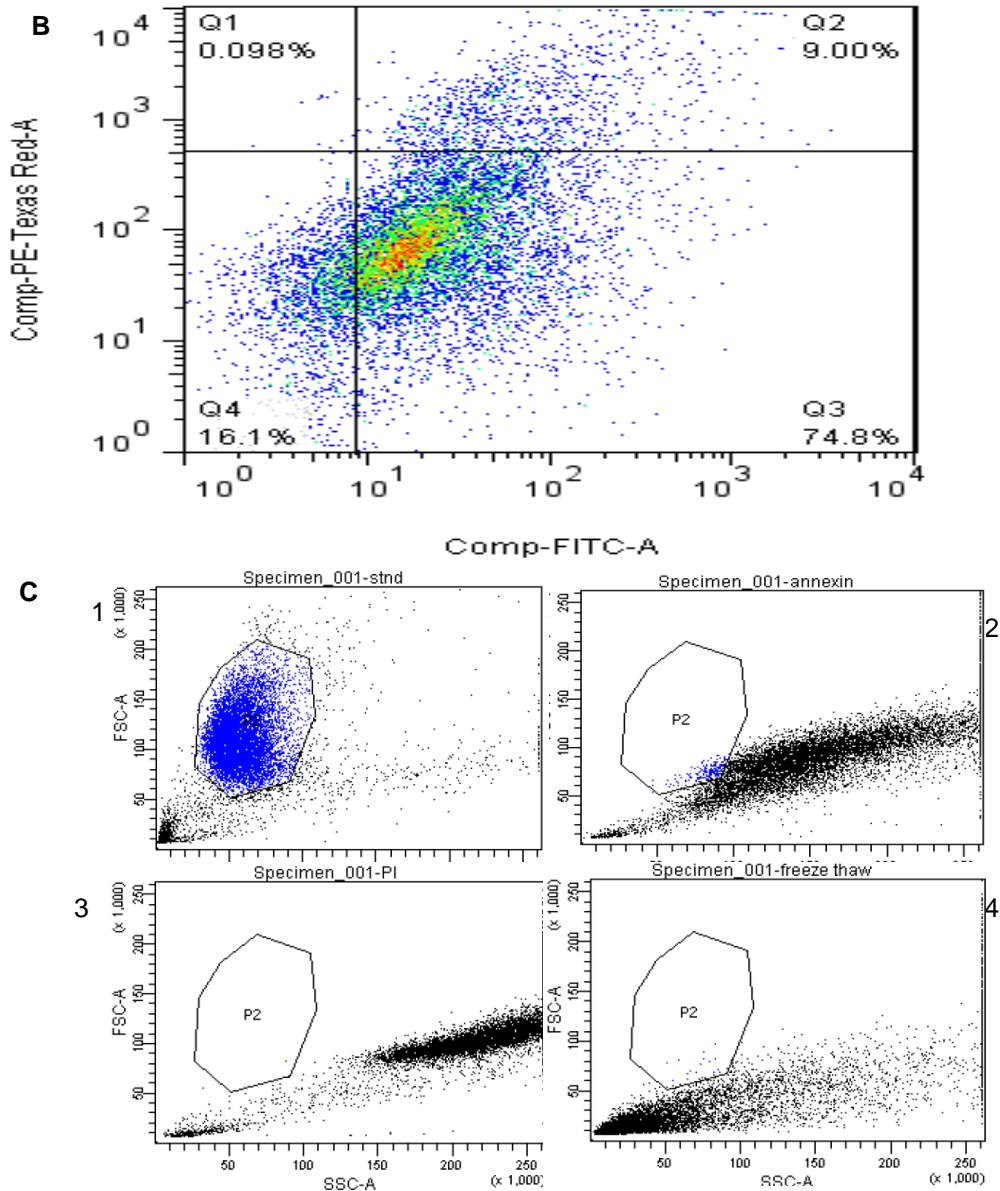
Figure 4.1: Represents flow cytometry scatter plots of viable and lysed cells. After incubation of 48 hrs, aliquots of $2x10^6$ cells/ml U1 cells were transferred into five, 5 ml glass tubes and stained accordingly. A) displays cells that didn't undergo freeze-thaw cycles: more than 92% of the cells were still viable after 48 hrs incubation Q4, B) shows more than 80% of cells had undergone cell death after 5 cycles of freeze-thaw (Q1-3). The first quadrant Q1: indicates necrotic cells that represent exposed DNA bound to PI stain; Annexin positive cells represent apoptotic cells Q2: late apoptosis and Q3: early apoptosis Q4: viable cell region. Comp-FITC-A represents the annexin channel and Comp-PE-Texas Red-A PI channel.C) uncompensated dot plots showing forward and side light scatter patterns of control cells 1) viable, 2) apoptotic, 3) necrotic cells 4) cell debris from freeze-thaw method.

47

4.2 NMR analysis

The second aim was to detect metabolic profiles and identify metabolites from the cell extracts. For any assignments of metabolites to peaks in a spectrum, a standard such as TSP or TMS which are detect at a chemical shift of 0 ppm should be included in analysis as a point of peak reference. Fig 4.2 showed a spectrum of 10% TSP dissolved in D_2O/PBS buffer, appearing at a chemical shift 0 ppm, the peak is characterized by flanking satellites. In this study, TSP was used as an external reference. Metabolites from U937 cells, stimulated and unstimulated U1 cells were detected and metabolic profiles were elucidated. For spectral clarity fig 4.3 is the metabolite assignment of unstimulated U1 cell profile selected as the annotated representative spectrum for all experimental samples. Chenomx software, literature searches, HMDB and KEGG databases were used to putatively identify the metabolites through peak assignments. Fig 4.4, shows baseline corrected and aligned U937, stimulated and unstimulated U1 cell NMR spectra; n=3 for each sample group and the water peaks were excluded from the data. Most of the metabolites identified were those that played important roles in the glycolytic and lipid pathways. Side note: the same buffer was used for all spectra including figure 4.2 which contained a small amount of ethanol from tube cleaning, comparing the signal intensities of ethanol on figure 4.2 and the glucose peaks in figure 4.4 there were differences which indicate 4.2 was an isolated case (about 3.7 ppm), there was a lower intensity for U937 and a much larger peak intensity in U1 unstimulated cells when using the ethanol peak (figure 4.2) as a point of reference therefore eliminating the possibility of peaks being ethanol contamination.
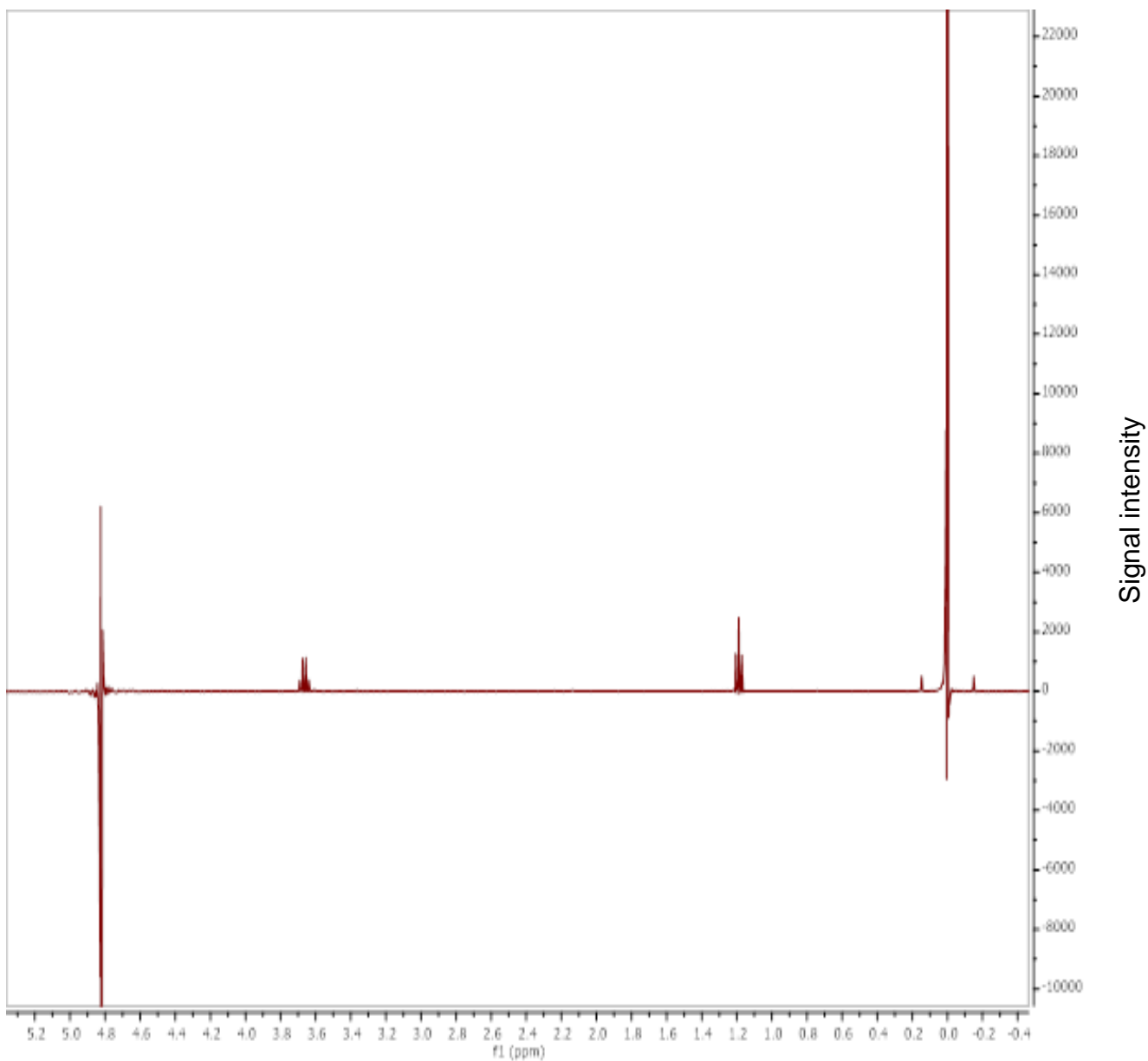
Figure 4.2: **TSP spectrum**. TSP 10% (dissolved in D_2O/PBS buffer) standard measuring at 0 ppm was used as a chemical shift reference; the water peak was identified at 4.8 ppm. The small middle peaks are the ethanol peaks from equipment preparation.
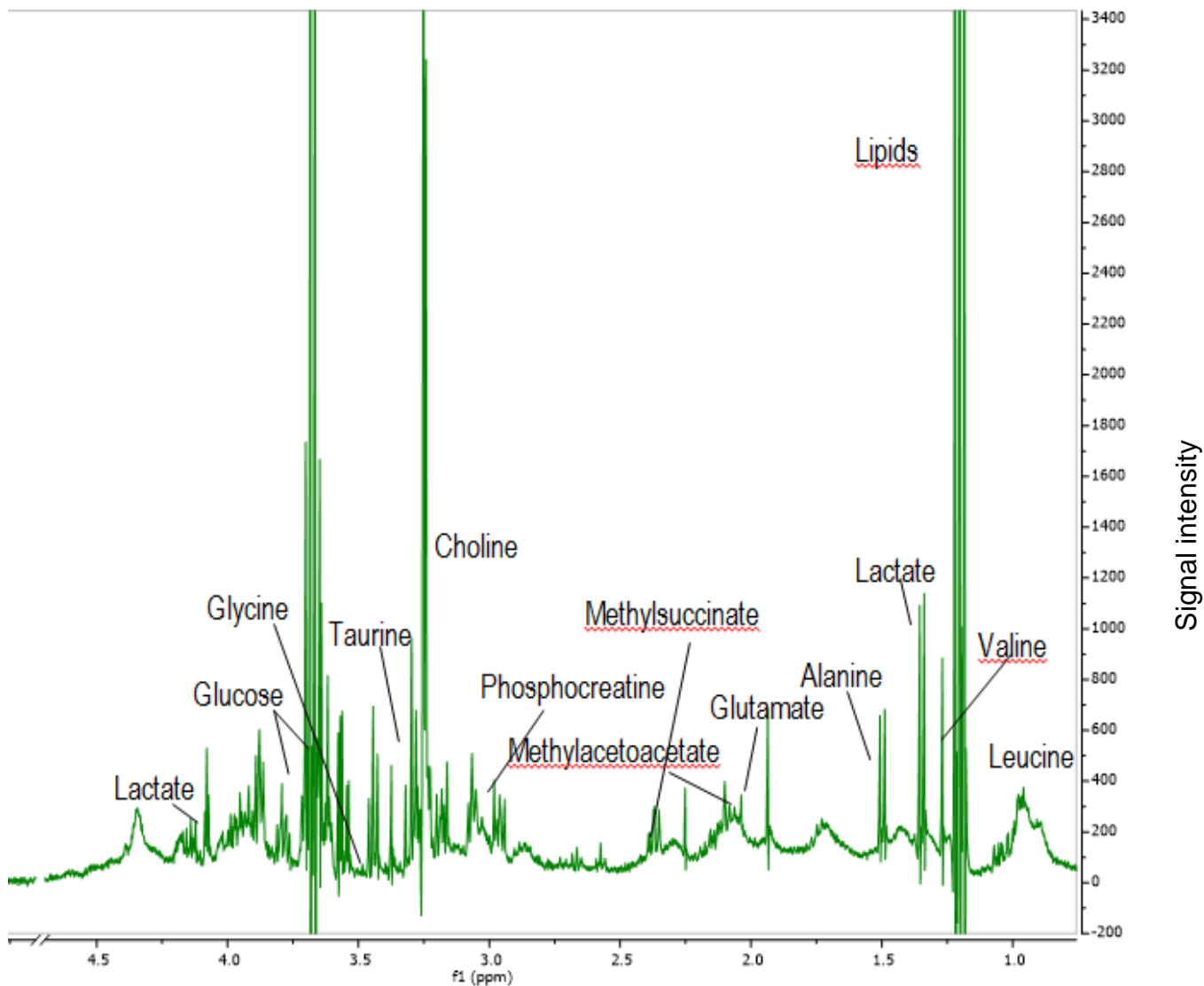
Figure 4.3: **¹H representative spectrum of unstimulated U1 cells** generated by a 400 MHz NMR spectroscope. Significantly prominent metabolites determined by statistical analysis were identified and annotated on the spectrum.
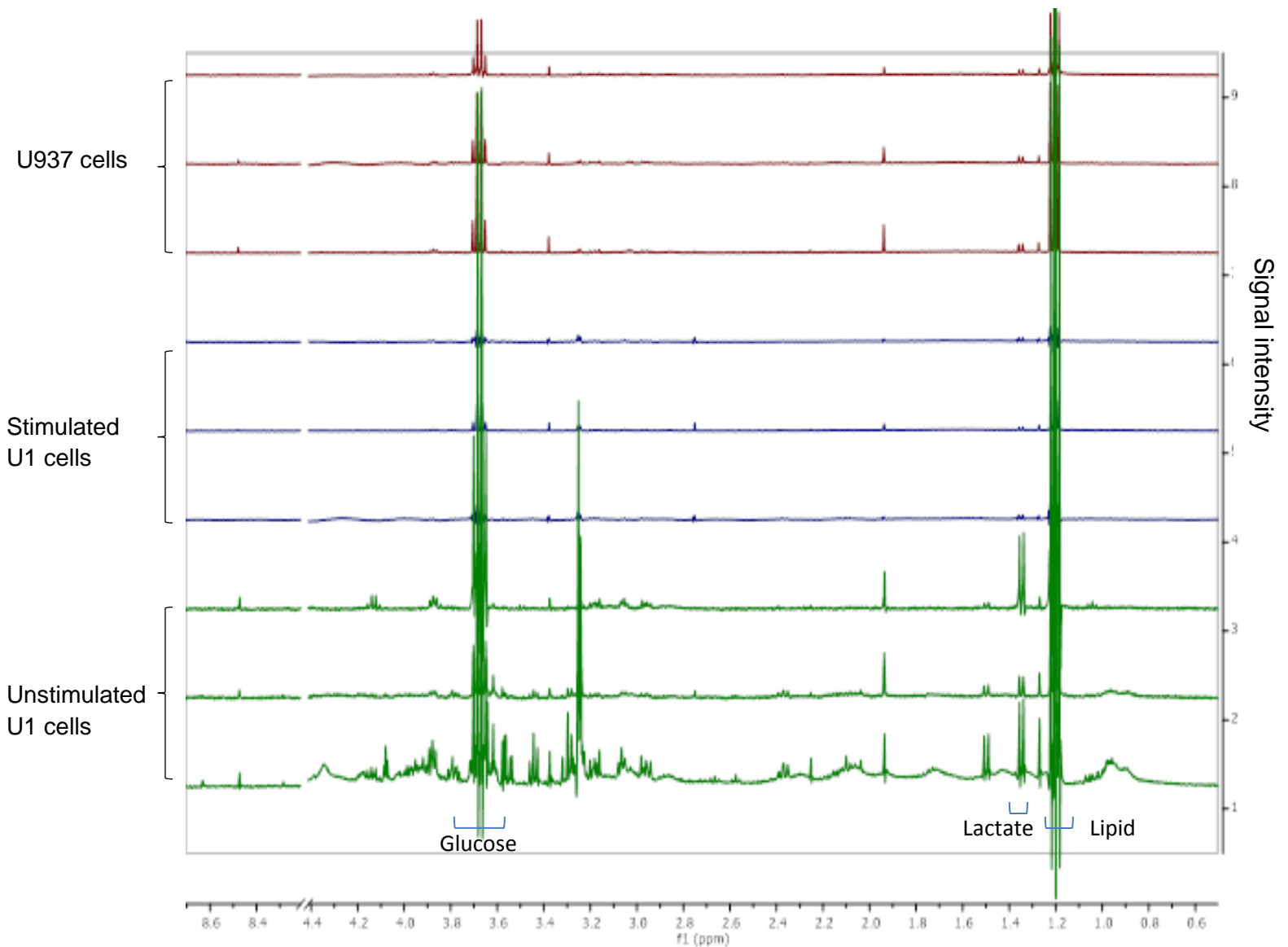
Figure 4.4: **Stacked NMR spectra comparing sample group metabolic profiles of n=3 per group**: PMA (2 nM) stimulated U1 cells (blue), unstimulated U1 cells (green) and U937 cells (red). The water peak (4.4-5.0 ppm) was excluded from the graph. The green spectra had visibly the highest number of peaks with great intensity compared to other samples. These peaks appeared in regions known for lipids, glucose and lactate.

51

4.3 Statistical analysis

The third aim was to conduct statistical analysis on the data to determine group separation and significant differences of metabolites between the groups. LDA was used to classify the samples into groups, a 100% classification of the samples was achieved. Each sample group clustered together and a distinguishable separation was observed, indicating the presence of distinct variables/metabolites fig 4.5. Confirmed in table 4.1 all the samples were classified accurately highlighting the robustness of the cell model and NMR spectroscopy. ANOVA was used to determine the significantly different metabolites (presented in table 4.2), with the peaks and p-values (< 0.05). A more detailed table of multiple comparisons is presented in the Appendix as table 6.
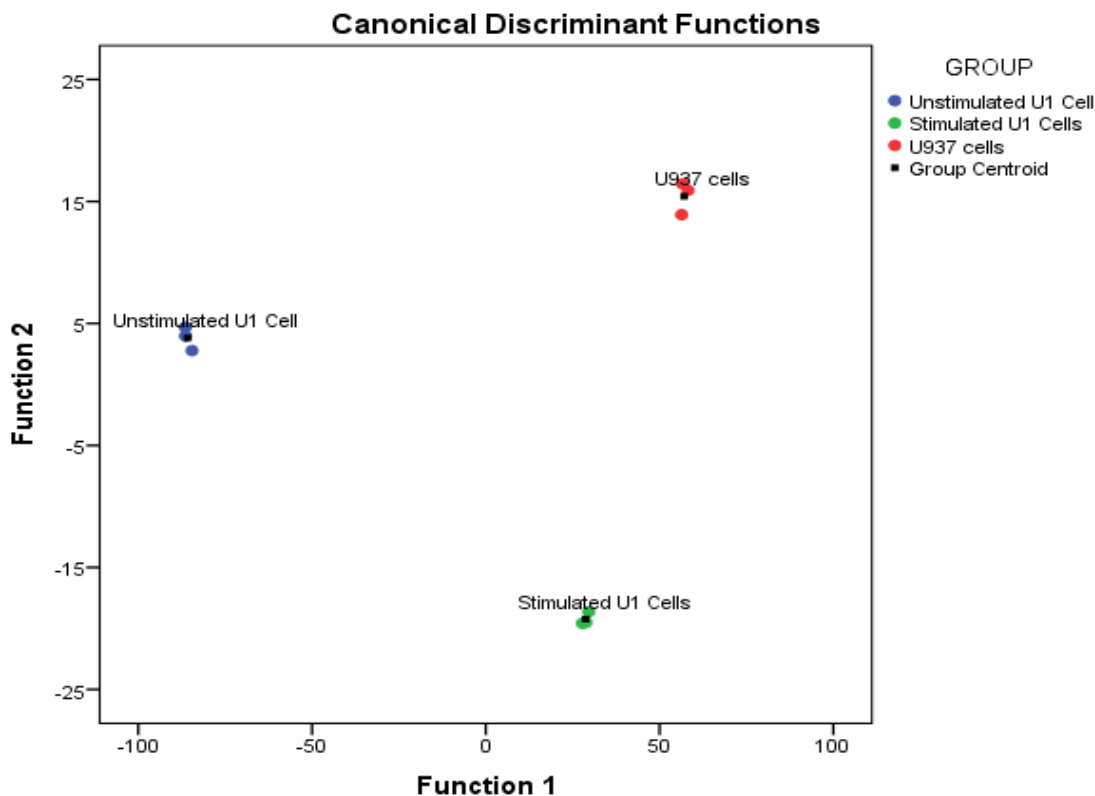
Figure 4.5: **LDA data analysis.** LDA scatter plot of discriminant functions showing the group clustering of U937 (red), stimulated (green) and unstimulated U1 cells (blue) where n=3 for each group.

Table 4.1: A table showing 100% classification of sample groups U937, stimulated and unstimulated U1 cells where n = 3 for each group

Classification Results[a]						
			Predicted Group Membership			
			Unstimulated U1 Cells	Stimulated U1 Cells	U937 cells	Total
GROUP						
Original	Count	Unstimulated U1 Cells	3	0	0	3
		Stimulated U1 Cells	0	3	0	3
		U937 cells	0	0	3	3
	%	Unstimulated U1 Cells	100,0	0,0	0,0	100,0
		Stimulated U1 Cells	0,0	100,0	0,0	100,0
		U937 cells	0,0	0,0	100,0	100,0

a. 100.0% of original grouped cases correctly classified.

Table 4.2: A list of metabolites identified as significantly different (*p*-value < 0.05) between the three experimental groups

Chemical shift (ppm)	Metabolite assignment	P-value < 0.05 (ANOVA)
1.079	Leucine	0,010
1.119	Lipid	0,022
1.199		0,000
1.239		0,000
1.279	Valine	0,001
1.319	Lactate	0,031
1.359		0,005
1.399		0,003
1.439		0,010
4.117		0,003
4.157		0,002
4.197		0,002
1.479	Alanine	0,048
1.519		0,000
1.958	Glutamate	0,006
2.158		0,030
2.198		0,018
2.318	Glutamine	0,023
2.358		0,045
2.558		0,021
3.038	Phosphocreatine	0,020
3.837		0,016
3.278	Choline	0,008
3.358	Taurine	0,003
3.518	Glycine	0,022
3.558	Glucose	0,029
3.598		0,031
3.638		0,014
3.677		0,003

3.717		0,000

Metabolites were identified and assigned by using information available in the literature, Chenomx software and Bioinformatics (HMBD and KEGG) applications. Due to peaks overlapping some metabolites were presented with single or fewer chemical shifts.

4.4 Lactate treated cells

In the final aim the cells were exposed to a higher concentration of lactate in order to determine the influence the change would have on the infected cell in relation to metabolism. In the first investigation lactate was found to be significantly different among the sample groups and due to this metabolite's involvement in the glycolytic pathway it was selected. After 48 hrs incubation the treated samples (n=2) for each group was analysed using NMR, the resultant data is presented in fig 4.6. The peaks in all the samples were pronounced especially in the stimulated U1 cells compared to lactate-untreated data. Again there was a 100% correct classification of sample groups obtained using LDA, with distinct group separation fig 4.7 and table 4.3. Table 4.4 represents metabolites that were found to be significantly different, an interesting thing to note is that some metabolites that were present in the first investigation were not present or significantly altered but a new and significantly different metabolite, cysteine, was identified in the samples.

55
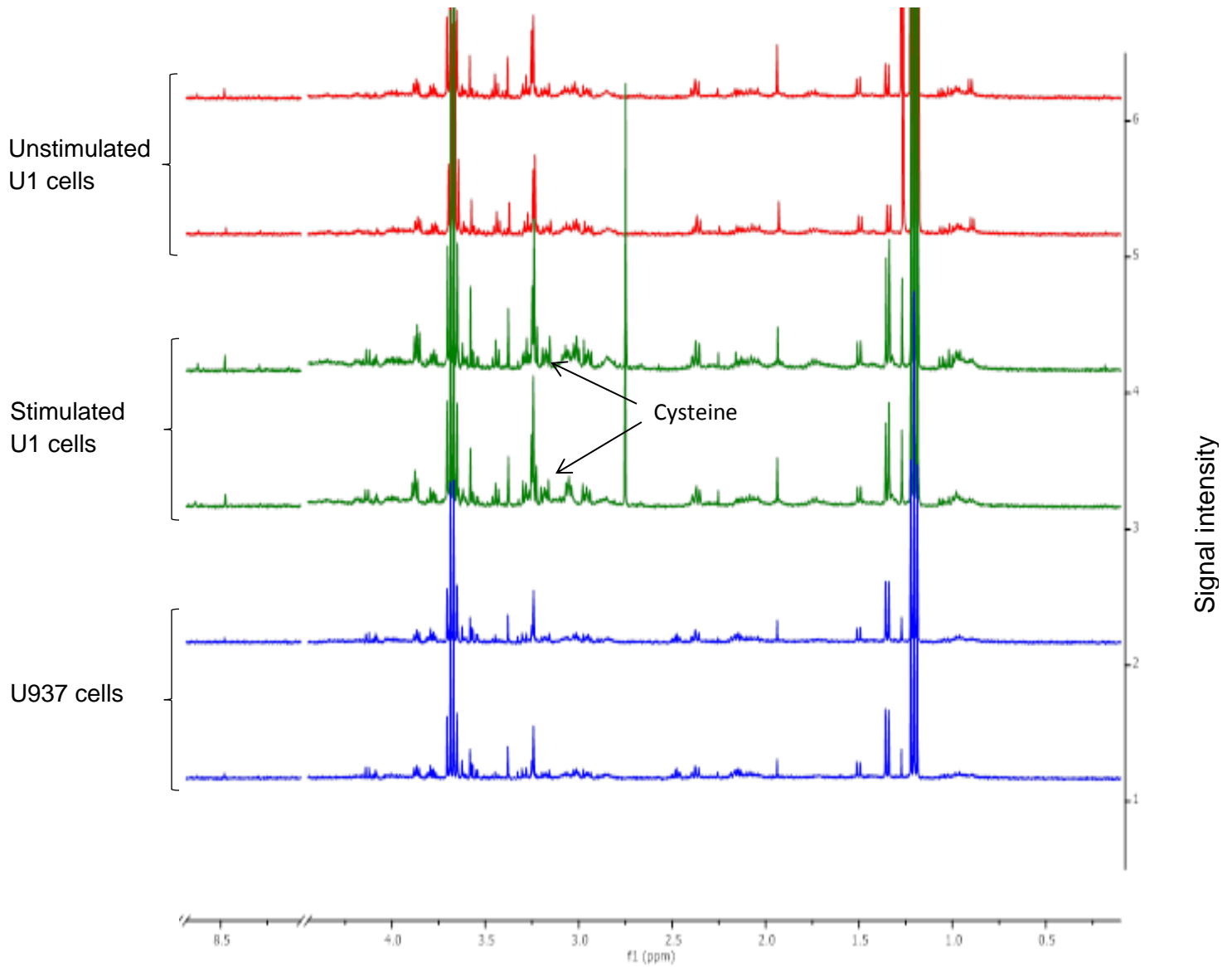
Figure 4.6: **NMR spectra representing lactate treated samples** (2 x 10^6 cells/ml), which were exposed to 10 mM lactate. The red spectra shows the unstimulated U1 cells, green-stimulated U1 cells and blue were the U937 cells. The stimulated U1 cells produced the most prominent metabolic profile.

4.5 Statistical analysis of lactate treated cells
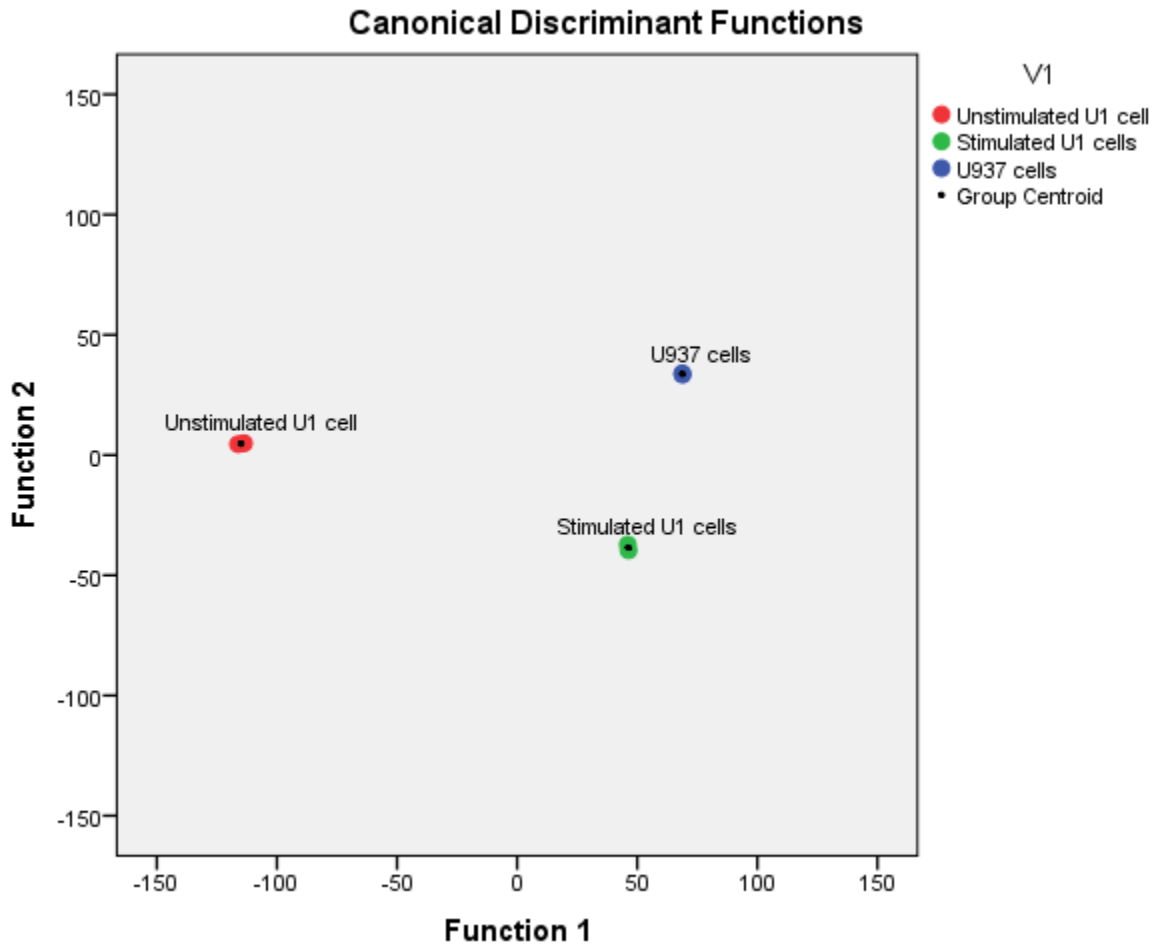
Figure 4.7: **LDA plot of lactate treated cells**. Each sample of 2 x 10^6 cells/ml was treated with 10 mM lactate. Distinguishable group separations of HIV-1 unstimulated U1 cells in red, stimulated U1 cells in green and HIV-1 negative U937 (blue) were observed on the scatter plot.

Table 2.3: Classification of the sample groups treated with 10 mM lactate

Classification Results[a]

| | | | Predicted Group Membership | | | |
		V1	Unstimulated U1 cells	Stimulated U1 cells	U937 cells	Total
Original	Count	Unstimulated U1 cells	2	0	0	2
		Stimulated U1 cells	0	2	0	2
		U937 cells	0	0	2	2
	%	Unstimulated U1 cells	100.0	.0	.0	100.0
		Stimulated U1 cells	.0	100.0	.0	100.0
		U937 cells	.0	.0	100.0	100.0

a. 100.0% of original grouped cases correctly classified.

Table 4.4: Putative metabolite identification and assignment of significantly different metabolites from the investigation of cells treated with 10 mM of lactate

Chemical shift (ppm)	Metabolite assignment	P-value (ANOVA)
1.294	Lactate	0.005
4.292		0.012
4.252		0.003
1.654	Alanine	0.034
1.694		0.021
1.894	Glutamate	0.012
1.974		0.038
2.054		0.008
2.254	Phosphocreatine/	0.035
2.733	creatine	0.041
2.813		0.037
2.893		0.002
2.933		0.017
3.013		0.049
3.093		0.010
3.853		0.001
3.933		0.003
3.133	Cysteine	0.009
3.213		0.011
4.052		0.014
4.092		0.001
3.453	Glucose	0.045
3.493		0.020
3.773		0.011

Literature, Chenomx and Bioinformatics HMBD and KEGG analyses were used to identify the metabolites. Due to peaks overlapping some metabolites were presented with a single or fewer chemical shifts.

Chapter 5: Discussion

The discussion is structured as follows; 1) first a discussion of the investigation determining the metabolic profiles of the uninfected U937, actively and latently infected U1 cells, 2) followed by a discussion of the results from lactate treated cells.

5.1 Changes in metabolites involved in energy metabolism

Glucose, lactate and lipids have been identified as significantly altered metabolites during comparative analysis of infected and uninfected blood sera and plasma in metabonomics analysis (McKnight *et al*. 2014; Hewer *et al*. 2006; Sitole *et al*. 2013). These metabolites were also observed by Hollenbaugh *et al*(2011) using U937 and actively infected U1 cells (Hollenbaugh *et al*. 2011) and again in this current comparative study of uninfected U937 cells and U1 cells with latent or active HIV infections. Lutz *et al* (1997) detected and quantified metabolite concentrations of latently and acutely HIV infected human intestinal epithelial (HT-29) cells. These authors discovered, in latently infected cells a 75% and 181% increase in lactate and glucose concentrations respectively (Lutz *et al.* 1997). In the current study, multiple comparisons ANOVA indicated that latently infected U1 cells compared to the uninfected and actively infected samples contributed the largest difference in glucose, lactate and lipid metabolites observed. In the cell, glucose is the primary source of energy, and undergoes a series of catabolic processes during glycolysis (Zhao *et al*. 2008). According to the traditional dogma, in the absence of oxygen, glucose is converted to lactate by lactate dehydrogenase enzyme (Shaw 2006). In the presence of oxygen, glucose is catabolized into glycolytic intermediates, which are used to generate energy in the form of adenosine triphosphate (ATP) from oxidative phosphorylation that occurs in the mitochondrion.

During glycolysis, glucose is phosphorylated by the hexokinase (HK) enzyme into glucose-6-phosphate (G6P) (Saltiel & Kahn 2001; Zhao *et al*. 2008). G6P is

60

metabolized in the pentose phosphate pathway (PPP) to generate nicotinamide dinucleotide phosphate (NADPH) for lipid biosynthesis. The significant presence of lipids and lactate in latently infected U1 cells suggests that glucose metabolism was mainly directed toward lipid biosynthesis and not mitochondrial energy production. This is supported by the fact that during culturing all the cells were exposed to an adequate and constant supply of oxygen thereby minimizing the possibility that anaerobic respiration was responsible for this reaction. The route of glucose metabolism for lipid biosynthesis is sustained by data produced by Lutz *et al* (1997) where the authors observed that after incubation of over 4 hours of the infected cells, a ^{13}C labelled glucose molecule was catabolised and was discovered to have been utilized for lipid synthesis (Vander Heiden *et al*. 2009; Zhao *et al*. 2008; Lutz *et al*. 1997). Mechanisms that explain these possibilities are explored below.

5.2 Mitochondrion disruption vs the Warburg effect involvement in glycolysis

5.2.1 The Warburg effect hypothesis

The Warburg effect is primarily used to describe a process of aerobic glycolysis in proliferating tumor and cancer cells where high concentrations of glucose are consumed at increased rates resulting in the production of lactate instead of CO_2 (very little) in the presence of oxygen (Feron 2009). In 1956, Otto Warburg explained that the origin of ascites cancer cells was when normal cells developed a state of low to none respiration and oxygen consumption with an increase in fermentation (Warburg 1956). The Warburg effect is dependent upon high influx of glucose and the availability of NAD during the conversion of pyruvate to lactate (Feron 2009). For example aerobic glycolysis is induced when activated T lymphocytes increase their glucose intake (Rodrı *et al*. 2007; Maciver *et al*. 2008). The Warburg effect does not only occur in cancerous or tumorigenic cells but in other cells as well; in one study Delgado (2010) suggested that in endothelial cells that were latently infected with the Kaposi's sarcoma herpesvirus (KSHV) the

61

Warburg effect was induced by the viral infection, and maintained the state of viral latency (Delgado *et al*. 2010). The authors proposed that the induction of the Warburg effect by KSHV promotes tumor formation, which relates to observations by Otto Warburg. In a pathogen infected cell, instead of glucose being primarily degraded for ATP production the process is directed towards lipid biosynthesis (Vander Heiden *et al.* 2009). Therefore it is possible that the infection by the virus promotes the state of Warburg effect within the infected cell and this could in turn explain how virus-dependent cancers are formed. In the current study there was a significant presence of glucose and also lactate in the latently infected cells, indicating aerobic glycolysis (because the cells were exposed to adequate O_2), suggesting that the Warburg effect was taking place.

5.2.2 Mitochondria disruption hypothesis

Macreadie and colleagues (1997) cloned an HIV-1 Vpr protein into a yeast vector and discovered mitochondrial dysfunction due to Vpr effects on five or more mitochondrial enzymes. The authors observed that respiratory deficiency didn't affect the fermentable carbon sources but it disrupted non-fermentable carbon sources where mitochondrial processes are required (Macreadie *et al*. 1997). Polo *et al* (2003) reported the possibility of mitochondrial disruption in HIV positive individuals on treatment and not on treatment. The disruption of mitochondrial function added with increased glucose and lipids have been associated with many HIV related metabolic disorders such as diabetes and lipodystrophy (Shikuma *et al*. 2005). The significant presence of glucose and lipids in latently infected cells (which are common indicators of these disorders) compared to the other experimental groups of this study suggests similar observations as other studies. Gene mutations of succinate dehydrogenase and fumarate hydratase involved in the tricarboxylic acid (TCA) cycle disrupt mitochondrial function and are associated with tumor syndromes (Feron 2009). In this study methylsuccinate and methylacetoacetate were detected in the latently infected cells, these are compounds metabolized in the mitochondria. The presence of these compounds suggests that there is some

62

mitochondrial respiration but most of the mitochondrial function is driven more to increase compounds for biomass than ATP production from oxidative phosphorylation, this is supported by the presence of methylacetoacetate which is a precursor for short chain acyl-CoA pathways that in turn form lipids (see point 5.3.1) (MacDonald *et al*. 2007).

For the reasons presented above it is hypothesized that mitochondrial disruption and the Warburg effect were caused by HIV infection and play a collaborative role in producing the glycolytic metabolite changes witnessed in this investigation. To confirm this, further investigations of actual metabolite concentrations could be conducted. Figure 5.1 is a hypothetical overview of the sequence of events of both processes, proposed from the current study findings.

Glucose metabolism within the latently infected U1 cell model
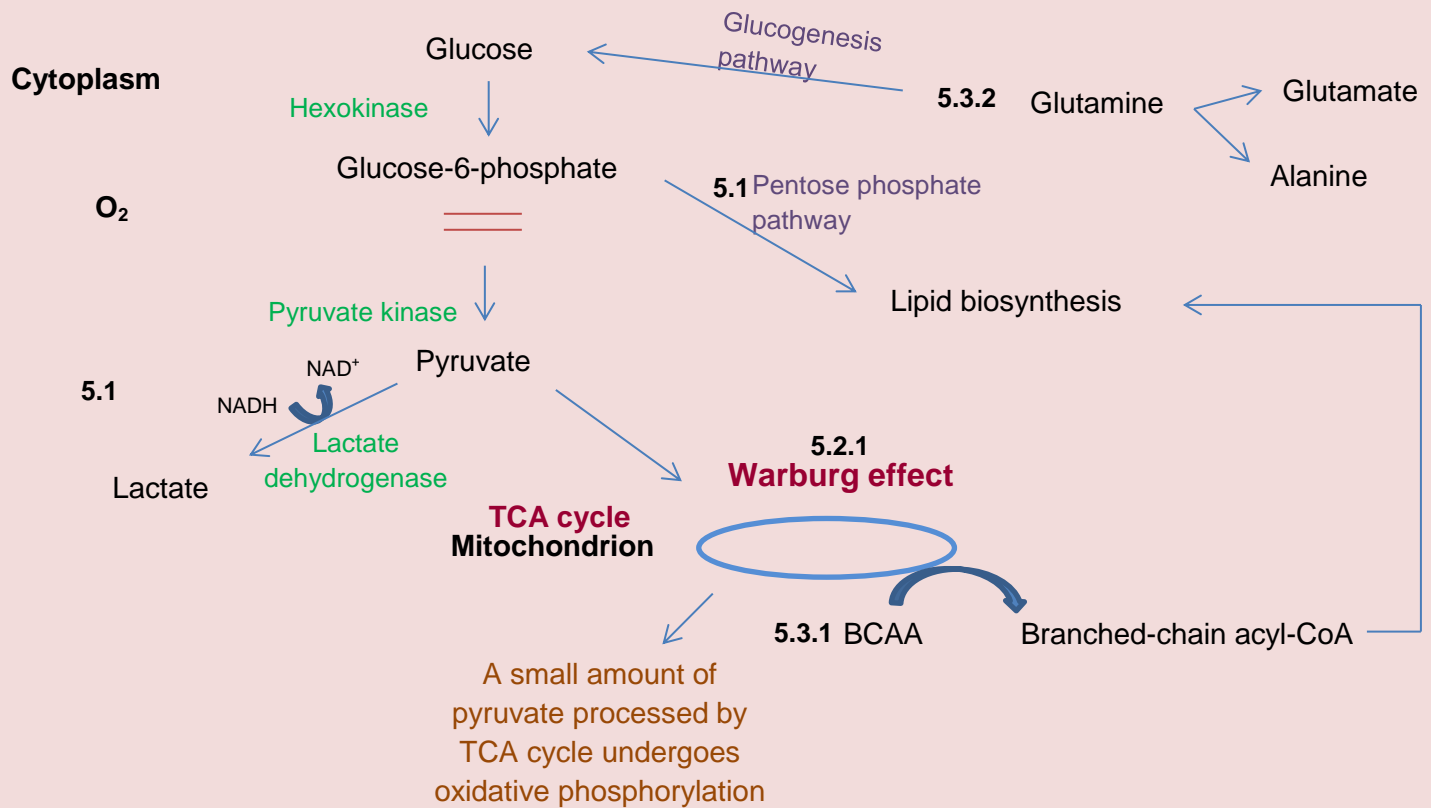
Figure 5.1: **Presented is a schematic diagram the latently infect U1 cell metabolism**, which is derived from the results of the study, the figure proposes the pathways and manner in which latent HIV infection influences the cell. Changes in these pathways may be the cause of the reported metabolic disorders in some HIV infected individuals.

5.3 Amino acid metabolites

Significantly altered amino acids were identified; some of these directly or indirectly contribute to what was suggested about the Warburg effect and mitochondrial dysfunction of the infected U1 cells, in which lipid biosynthesis was favoured more than oxidative phosphorylation. Also, these amino acids have been identified as key risk factors for metabolic disorders in HIV infected individuals. Therefore, the significant presence or absence of these metabolites in the latently or actively infected U1 cells could elucidate pathways the virus affects within the cells.

5.3.1 BCAA amino acids

Branched-chain amino acids (BCAA): leucine, isoleucine and valine are metabolized in the mitochondrion and degraded in two processes; one in which the amino acids are transaminated in the cytoplasm and are transported to the mitochondrion as 2-oxo-acids; while in the other process the BCAA travels into the mitochondrion via a transport protein and is converted into 2-oxo-acids (Wanders *et al.* 2012). The 2-oxo-acids undergo oxidative decarboxylation to form branched-chain acyl-CoA esters, thereafter lipids are synthesized (Wanders *et al.* 2012). In the current study multiple comparisons analysis showed that the significant alterations of lipids and leucine were attributed to the latently infected U1 cells compared to the other cell lines. Long chain acyl-CoA is a secretagogue of insulin, it is hypothesized that elevated levels of acyl-CoA as well as increased levels of glucose and lipids in various tissue influence changes associated with obesity and noninsulin-dependent diabetes (NIDDM), which result from the body's resistance to insulin (Prentki & Corkey 1996). Insulin resistance is reported as a metabolic anomaly observed in HIV infected individuals and is a precursor for diabetes and cardio-vascular disease (CVD) (Bonfanti *et al.* 2010; Taiwo 2005). Data presented here suggests that latent HIV infection may play a role in developing these risk factors.

Leucine is thought to stimulate protein synthesis in adipose cells independent of insulin through activation of a signal pathway involving the mammalian target of rapamycin (mTOR), a serine/threonine protein kinase (Mero 1999). The signal pathway is essential for protein synthesis, preadipocyte differentiation, adipose tissue morphology and leptin secretion. Excess levels of leucine and valine influence lipid concentration (Mero 1999). This is supported by the significant presence of lipids, leucine and valine found in the latently infected U1 cells. Lipodystrophy in HIV infected patients is characterized by the accumulation and changes in lipid distribution around the body, which causes body disfigurement in infected individuals (Carr *et al.* 2003).

The presence of these metabolites suggests that the virus influences cells to increase the production of lipids, *in vivo* the accumulation of these lipids promotes the development of metabolic risk factors and dysmorphic features.

5.3.2 Glutamate and glutamine amino acids

In HIV latently infected U1 cells compared to actively infected and uninfected cells, glutamine and glutamate were significantly altered. In the cell, glutamine is converted by glutaminase to malate (resulting in phosphoenolpyruvate or malate to pyruvate directly) and glucose (through the glucogenesis pathway) (Newsholme *et al.* 2003). The infected cells could have used this process to increase the supply of glucose which in turn could be used for production of energy and biosynthetic pathway intermediates. Glutamine promotes T-cell proliferation, macrophage phagocytosis, antigen presentation, B-lymphocyte differentiation, cytokine production and apoptosis (Newsholme *et al.* 2003). In lymphocytes, macrophages and neutrophils glutamine is converted to glutamate, aspartate and to alanine in the presence of pyruvate (Newsholme *et al.* 2003; McKnight *et al.* 2014; Yudkoff *et al.* 2005). Glutamate is used for cell survival in tissues such as the kidney, immune system cells, intestine, liver, specific neurons and β cells (Newsholme *et al.* 2003). In the current study glutamate/glutamine and alanine were significantly different

between experimental groups. Because glutamine is converted to glutamate and alanine, an increase in glutamate/alanine and a decrease in glutamine facilitate the survival of the virus within the infected cells by promoting cell survival and thus prolong viral latency.

5.3.3 Phosphocreatine

This amino acid is produced from the phosphorylation of creatine by creatine N-phosphotransferase (Hochachka & Mossey 1998). Phosphocreatine is important for regenerating ATP by reacting with ADP to form ATP and creatine (phosphocreatine + ADP + H^+ $\longleftrightarrow$ ATP + creatine) (Hochachka & Mossey 1998). Phosphocreatine was another amino acid found to be significantly different between the experimental groups. The significant presence of this amino acid suggests an alternate pathway which latently infected U1 cells use for energy production instead of oxidative phosphorylation.

5.3.4 Taurine

Taurine is found in high concentrations within the leukocyte (neutrophil) cytoplasm where it acts as an antioxidant for hypochlorous acid (HOCl), produced by myeloperoxidase-hydrogen peroxide-chloride system of neutrophils and monocytes (Raschke *et al.* 1995; Learn *et al.* 1990). The reaction produces a less reactive and non-toxic taurine-chloramine that protects leukocytes from chlorinated oxidants (Learn *et al.* 1990). It is possible that the latently infected U1 cells could use taurine as an antioxidant in this reaction to prevent cell degradation from the chlorinated oxidants, promoting cell survival and viral latency.

67

5.3.5 Choline

Actively infected cells were most responsible for the significant changes in choline between the experimental groups. Choline is required to produce phospholipid phosphatidylcholine, lysophosphatidylcholine, choline plasmalogen and sphingomyelin which are all components of the cell membrane (Zeisel & Blusztajn 1994; Spencer *et al*. 2011; Zeisel *et al*. 1991). Zeisel (1991) observed that subjects with choline deficiency report a decrease of 15% in normal serum cholesterol levels (Zeisel *et al*. 1991). Phosphatidylcholine derived from choline is required to form VLDL cholesterol (Zeisel & Blusztajn 1994). Increases in LDL, VLDL and triglycerides levels have been highly associated with an increase of HIV infection. This process could be used by the replicating virus to increase cholesterol, which is used to produce viral components and cell membrane components for viral release.

Platelet-activating factor (PAF, 1-O-alkyl-2-acetyl-sn-glycero-3-phosphocholine) is a choline phospholipid with a glycerol backbone attached to fatty alcohol and acetate residues (Zeisel & Blusztajn 1994). PAF activates platelet aggregation but most importantly it activates monocytes, macrophages and polymorphonuclear neutrophils (Zeisel & Blusztajn 1994). PAF related activation of monocytes may cause the reactivation of the latent virus, this could explain how the latent virus is activated *in vivo* in the absence of an external stimulus.

5.4 Lactate treated cells

After lactate treatment some metabolites that were initially detected were no longer detectable namely lipids, valine, leucine, choline, taurine and glycine (see Table 4.4). A new metabolite, cysteine, was detected and determined to be significantly different between the experimental groups. Karamichos and colleagues (2014) showed that an increase in lactate or the lactate/pyruvate ratio resulted in oxidative stress [which is a result of the accumulation of reactive oxygen species (ROS)] in human corneal keratocytes (HCKs) (Karamichos *et al.* 2014). ROS may cause cell death by damaging proteins, cell membranes, DNA and lipids (Karamichos *et al.* 2014). Cysteine is also considered an agent or indicator of oxidative stress (OS) (Stipanuk 2004). In this study, high concentrations of lactate resulted in an increase in cysteine; the significant presence of cysteine and the absence of significant lipids suggest the possibility of cell death from oxidative stress.

Chapter 6: Conclusion

Re-visiting the hypothesis: <u>Metabolic profiles of latently and actively infected U1 cell culture supernatants should be detectable by NMR spectroscopy</u>

NMR spectroscopy was successful in detecting metabolic profiles of HIV-1 latently and actively infected U1 cells. Compared to actively infected U1 and uninfected U937 cells, latently infected U1 cells contributed largely to the significant differences in metabolite profiles. Through statistical analysis, significantly different metabolites indicated that HIV infection induced aerobic glycolysis in infected cells and drove the glycolytic pathway for lipid biosynthesis and decreased oxidative phosphorylation producing a Warburg effect, this is clearly visible in the diagram presented in the discussion. In the current study, after lactate treatment the significant presence of cysteine, which is an indicator of OS, was detected in the actively infected U1 cell sample by NMR, suggesting that the increase in lactate concentration induces oxidative stress. The findings of this study show the possible mechanisms HIV uses to influence cell metabolism and provides an indication of the metabolic pathways which influence the occurrence of metabolic disorders identified in some HIV positive individuals.

70

Chapter 7: Future perspectives

- Quantitative NMR analysis of the infected cell supernatants would provide actual concentrations of metabolites in each sample, to show which metabolites are increased or decreased to produce the metabolic changes observed in the current study.

- A more sensitive instrument such as a mass spectrometer could be used to investigate if more metabolites can be detected in infected U1 cells, this could possibly indicate other metabolic pathways influenced by the virus.

- Studies have identified an association of the Warburg effect with prolonged KSHV and HIV co-infection resulted in cancer (Delgado *et al.* 2010). The Warburg effect in relation to HIV-1 latency alone should be further investigated to observe if cancer is induced, in the current study the infected cells exhibited the Warburg effect indicated by aerobic glycolysis.

References

Adams, M. L., *et al.* (1994). 'Cellular Latency in Human Immunodeficiency Virus-Infected Individuals with High CD4 Levels Can Be Detected by the Presence of Promoter-Proximal Transcripts.' *Proceedings of the National Academy of Sciences of the United States of America* 91 (9): 3862–66.

Agosto, L. M., *et al.* (2011). 'Patients on HAART Often Have an Excess of Unintegrated HIV DNA: Implications for Monitoring Reservoirs.' *Virology* 409 (1). Elsevier B.V.: 46–53. doi:10.1016/j.virol.2010.08.024.

Amet, T., *et al.* (2008). 'Statin-Induced Inhibition of HIV-1 Release from Latently Infected U1 Cells Reveals a Critical Role for Protein Prenylation in HIV-1 Replication.' *Microbes and Infection / Institut Pasteur* 10 (5): 471–80. doi:10.1016/j.micinf.2008.01.009.

Aoki, K., & Hideki, N. (1994). 'Sodium Benzylideneascorbate' 351: 105–8.

Avert. (2011). 'Worldwide HIV & AIDS Statistics Commentary.'

Barbaro, G. (2002). 'Cardiovascular Manifestations of HIV Infection.' *Circulation* 106 (11): 1420–25. doi:10.1161/01.CIR.0000031704.78200.59.

Basu, S. (2000). Necrotic but not apoptotic cell death releases heat shock proteins, which deliver a partial maturation signal to dendritic cells and activate the NF-kappaB pathway. *International Immunology*, 12(11), pp.1539–1546. Available at: https://academic.oup.com/intimm/article-lookup/doi/10.1093/intimm/12.11.1539.

Becker, S. (2007). *Inorganic Mass Spectrometry: Principles and Applications - Sabine Becker*. 1st ed. West Sussex, England: Wiley. http://0-eu.wiley.com.innopac.up.ac.za/WileyCDA/WileyTitle/productCd-0470517204.html.

Beckonert, O., *et al.* (2007). 'Metabolic Profiling , Metabolomic and Metabonomic Procedures for NMR Spectroscopy of Urine , Plasma , Serum and Tissue Extracts.' doi:10.1038/nprot.2007.376.

Beyoğlu, D., & Idle, J. R. (2013). 'Metabolomics and Its Potential in Drug Development.' *Biochemical Pharmacology* 85 (1): 12–20. doi:10.1016/j.bcp.2012.08.013.

Bhattacharya, S., & Husam, O. (2009). 'Novel Targets for Anti-Retroviral Therapy.'

The Journal of Infection 59 (6). Elsevier Ltd: 377–86. doi:10.1016/j.jinf.2009.09.014.

Blazkova, J., *et al.* (2009). 'CpG Methylation Controls Reactivation of HIV from Latency.' *PLoS Pathogens* 5 (8): e1000554. doi:10.1371/journal.ppat.1000554.

Bonfanti, P., *et al.* (2010). 'Is Metabolic Syndrome Associated to HIV Infection per Se? Results from the HERMES Study.' *Current HIV Research* 8 (2): 165–71. doi:10.2174/157016210790442731.

Brown, A., *et al.* (2006). 'In Vitro Modeling of the HIV-Macrophage Reservoir.' *Journal of Leukocyte Biology* 80 (5): 1127–35. doi:10.1189/jlb.0206126.

Brown, A. M. (2005). 'A New Software for Carrying out One-Way ANOVA Post Hoc Tests.' *Computer Methods and Programs in Biomedicine* 79 (1): 89–95. doi:10.1016/j.cmpb.2005.02.007.

Bugianesi, E., McCullough,A. J., & Marchesini, G. (2005). 'Insulin Resistance: A Metabolic Pathway to Chronic Liver Disease.' *Hepatology* 42 (5): 987–1000. doi:10.1002/hep.20920.

Carr, A., *et al.* (1998). 'A Syndrome of Peripheral Lipodystrophy, Hyperlipidaemia and Insulin Resistance in Patients Receiving HIV Protease Inhibitors.' *AIDS (London, England)* 12 (7): F51–58. doi:10.1097/00002030-199807000-00003.

Carr, A. (2010). 'HIV Lipodystrophy : Risk Factors , Pathogenesis , Diagnosis and Management.'

Carr, A., *et al.* (2003). 'An Objective Case Definition of Lipodystrophy in HIV-Infected Adults: A Case-Control Study.' *Lancet* 361 (9359): 726–35. doi:10.1016/S0140-6736(03)12656-6.

Cevallos-Cevallos, J. M., *et al.* (2009). 'Metabolomic Analysis in Food Science: A Review.' *Trends in Food Science & Technology* 20 (11-12). Elsevier Ltd: 557–66. doi:10.1016/j.tifs.2009.07.002.

Cevallos-Cevallos, J. M., & Reyes-De-Corcuera, J. I. (2012). 'Metabolomics in Food Science.' *Advances in Food and Nutrition Research* 67 (January): 1–24. doi:10.1016/B978-0-12-394598-3.00001-0.

Chavez, L., Calvanese, V., & Verdin, E. (2015). 'HIV Latency Is Established Directly and Early in Both Resting and Activated Primary CD4 T', 1–21. doi:10.1371/journal.ppat.1004955.

73

Chen, T., *et al*. (2014). Enhancement of auranofin-induced lung cancer cell apoptosis by selenocystine, a natural inhibitor of TrxR1 in vitro and in vivo. *Cell Death and Disease*, 5(4), p.e1191. Available at: http://www.nature.com/doifinder/10.1038/cddis.2014.132.

Chun, T. W., & Fauci, A. S. (1999). 'Latent Reservoirs of HIV: Obstacles to the Eradication of Virus.' *Proceedings of the National Academy of Sciences of the United States of America* 96 (20): 10958–61. doi:10.1073/pnas.96.20.10958.

Claudino, W. M., et al. (2012). 'Metabolomics in Cancer: A Bench-to-Bedside Intersection.' *Critical Reviews in Oncology/Hematology* 84 (1): 1–7. doi:10.1016/j.critrevonc.2012.02.009.

Clearinghouse, The NIDDK National Diabetes Information. (2014). 'Causes of Diabetes.' http://diabetes.niddk.nih.gov/dm/pubs/causes/index.aspx.

Coodley, G. O., Loveless, M. O., & Merrill, T. M. (1994). 'The HIV Wasting Syndrome: A Review.' *Journal of Acquired Immune Deficiency Syndromes* 7 (7): 681–94. http://europepmc.org/abstract/med/8207646.

Currie, P. F., *et al*. (1994). 'Heart Muscle Disease Related to HIV Infection: Prognostic Implications.' *BMJ (Clinical Research Ed.)* 309 (6969): 1605–7.

Dahl, V., Josefsson, L., & Palmer, S. (2010). 'HIV Reservoirs, Latency, and Reactivation: Prospects for Eradication.' *Antiviral Research* 85 (1): 286–94. doi:10.1016/j.antiviral.2009.09.016.

Daigneault, M., *et al*. (2012). 'Monocytes Regulate the Mechanism of T-Cell Death by Inducing Fas-Mediated Apoptosis during Bacterial Infection.' *PLoS Pathogens* 8 (7): 30. doi:10.1371/journal.ppat.1002814.

Delaney, M. (2006). 'History of HAART -- the True Story of How Effective Multi-Drug Therapy Was Developed for Treatment of HIV Disease.' *Retrovirology* 3 (1): 1. doi:10.1186/1742-4690-3-S1-S6.

Delgado, T., *et al*. (2010). 'Induction of the Warburg Effect by Kaposi's Sarcoma Herpesvirus Is Required for the Maintenance of Latently Infected Endothelial Cells.' *Proceedings of the National Academy of Sciences of the United States of America* 107 (23). National Academy of Sciences: 10696–701. doi:10.1073/pnas.1004882107.

Díaz, M., Herrero, M., García, L. A., & Quirós, C. (2010). 'Application of Flow

Cytometry to Industrial Microbial Bioprocesses.' *Biochemical Engineering Journal* 48 (3): 385–407. doi:10.1016/j.bej.2009.07.013.

Dobrowolski, R., *et al.* (2014). 'Chemometric Methods for Studying the Relationships Between Trace Elements in Laryngeal Cancer and Healthy Tissues.' *Biological Trace Element Research* 159 (1-3): 107–14. doi:10.1007/s12011-014-0013-9.

Drelichowska, J., Kwiatkowska, W., Knysz, B., & Witkiewicz, W. (2014). 'Metabolic Syndrome in HIV-Positive Patients.' *HIV & AIDS Review*. Polish AIDS Research Society. doi:10.1016/j.hivar.2014.09.002.

Eck, H., Frey, H., & Droge, W. (1989). 'Glutamate_Concentrations_in_Plasma.pdf.' *International Immunology* 1 (4).

Ellis, D. I., & Goodacre, R. (2006). 'Metabolic Fingerprinting in Disease Diagnosis: Biomedical Applications of Infrared and Raman Spectroscopy.' *The Analyst* 131 (8): 875–85. doi:10.1039/b602376m.

El-Sadr, W. M., *et al.* (2005). 'Effects of HIV Disease on Lipid, Glucose and Insulin Levels: Results from a Large Antiretroviral-Naive Cohort.' *HIV Medicine* 6 (2): 114–21. doi:10.1111/j.1468-1293.2005.00273.x.

Feron, O. (2009). 'Pyruvate into Lactate and Back: From the Warburg Effect to Symbiotic Energy Fuel Exchange in Cancer Cells.' *Radiotherapy and Oncology* 92 (3). Elsevier Ireland Ltd: 329–33. doi:10.1016/j.radonc.2009.06.025.

Finzi, D., *et al.* (2012). 'Identification of a Reservoir for HIV-1 in Patients on Highly Active Antiretroviral Therapy Identification of a Reservoir for HIV-1 in Patients on Highly Active Antiretroviral Therapy' 1295 (1997): 1295–1300. doi:10.1126/science.278.5341.1295.

Folks, T., *et al.* (1986). 'Induction of HTLV-III/LAV from a Nonvirus-Producing T-Cell Line: Implications for Latency.' *Science* 231 (4738). American Association for the Advancement of Science: 600–602. doi:10.1126/science.3003906.

Gambari, R., & Lampronti, L. (2006). 'Inhibition of Immunodeficiency Type-1 Virus (HIV-1) Life Cycle by Medicinal Plant Extracts and Plant-Derived Compounds.' *Lead Molecules from Natural Products*, 299–311.

Goldsmith, P., *et al.* (2010). 'Metabonomics: A Useful Tool for the Future Surgeon.' *Journal of Surgical Research* 160 (1). Elsevier Ltd: 122–32.

doi:10.1016/j.jss.2009.03.003.

Gyorkey, F., Melnick, J. L., & Gyorkey, P. (1987). 'Human Immunodeficiency Virus in Brain Biopsies of Patients with AIDS and Progressive Encephalopathy.' *The Journal of Infectious Diseases* 155 (5): 870–76. http://www.ncbi.nlm.nih.gov/pubmed/3644852.

Hewer, R., Vorster, J., Steffens, F. E., & Meyer, D. (2006). 'Applying Biofluid 1H NMR-Based Metabonomic Techniques to Distinguish between HIV-1 positive/AIDS Patients on Antiretroviral Treatment and HIV-1 Negative Individuals.' *Journal of Pharmaceutical and Biomedical Analysis* 41 (4): 1442–46. doi:10.1016/j.jpba.2006.03.006.

Hochachka, P. W., & Mossey, M. K. (1998). 'Does Muscle Creatine Phosphokinase Have Access to the Total Pool of Phosphocreatine plus Creatine?' *The American Journal of Physiology* 274 (3 Pt 2): R868–72.

Hollenbaugh, J. A., Munger, J., & Baek, K. (2011). 'Metabolite Profiles of Human Immunodeficiency Virus Infected CD4+ T Cells and Macrophages Using LC-MS/MS Analysis.' *Virology* 415 (2). Elsevier Inc.: 153–59. doi:10.1016/j.virol.2011.04.007.

Hortin, G. L., Landt, M., & Powderly, W. G. (1994). 'Changes in Plasma Amino Acid Concentrations in Response to HIV-1 Infection.' *Clinical Chemistry* 405 (405): 785–89.

Huang, J., *et al.* (2007). 'Cellular microRNAs Contribute to HIV-1 Latency in Resting Primary CD4+ T Lymphocytes.' *Nature Medicine* 13 (10): 1241–47. doi:10.1038/nm1639.

Huber, M. A. (2013). 'HIV: Infection Control/Exposure Control Issues for Oral Healthcare Workers.' http://www.dentalcare.com/en-US/dental-education/continuing-education/ce97/ce97.aspx?ModuleName=coursecontent&PartID=2&SectionID=-1.

Hunt, R. (2013). 'Virology - Human Immunodeficiency Virus and AIDS Life Cycle Of HIV.' http://www.microbiologybook.org/lecture/hiv7.htm.

Hutcheson, J. D., *et al.* (2010). Saving cells from ultrasound-induced apoptosis: Quantification of cell death and uptake following sonication and effects of

targeted calcium chelation. *Ultrasound in Medicine and Biology*, 36(6), pp.1008–1021.

Jankevics, A., *et al*. (2012). 'Separating the Wheat from the Chaff: A Prioritisation Pipeline for the Analysis of Metabolomics Datasets.' *Metabolomics : Official Journal of the Metabolomic Society* 8 (Suppl 1): 29–36. doi:10.1007/s11306-011-0341-0.

Johnson, V. A., *et al*. (2008). 'Update of the Drug Resistance Mutations in HIV-1: Spring 2008.' *Topics in HIV Medicine : A Publication of the International AIDS Society, USA* 16 (1): 62–68. http://www.ncbi.nlm.nih.gov/pubmed/18441382.

Jordan, A., Defechereux, P., & Verdin, E. (2001). 'The Site of HIV-1 Integration in the Human Genome Determines Basal Transcriptional Activity and Response to Tat Transactivation.' *The EMBO Journal* 20 (7): 1726–38. doi:10.1093/emboj/20.7.1726.

Jordan, A., Bisgrove, D., & Verdin, E. (2003). 'HIV Reproducibly Establishes a Latent Infection after Acute Infection of T Cells in Vitro.' *The EMBO Journal* 22 (8): 1868–77. doi:10.1093/emboj/cdg188.

Karamichos, D., *et al*. (2014). 'In Vitro Model Suggests Oxidative Stress Involved in Keratoconus Disease.' *Scientific Reports* 4 (January). Nature Publishing Group: 4608. doi:10.1038/srep04608.

Kauder, S. E. (2009). 'Epigenetic Regulation of HIV-1 Latency by Cytosine Methylation.' *PLoS Pathogens* 5 (6): e1000495. doi:10.1371/journal.ppat.1000495.

Khan, M. A., Collins, A. J., & Keane, W. F. (2000). 'Diabetes in the Elderly Population.' *Advances in Renal Replacement Therapy* 7 (1): 32–51. http://europepmc.org/abstract/med/10672916.

Kondo, M. (2010). 'Lymphoid and Myeloid Lineage Commitment in Multipotent Hematopoietic Progenitors.' *Immunological Reviews* 238 (1): 37–46. doi:10.1111/j.1600-065X.2010.00963.x.

Kulkosky, J., et al. (2001). 'Prostratin: Activation of Latent HIV-1 Expression Suggests a Potential Inductive Adjuvant Therapy for HAART.' *Journal of the American Society of Hematology* 98 (10): 3006–15. doi:10.1182/blood.V98.10.3006.

Kumar, A., Abbas, W., & Herbein, G. (2014). 'HIV-1 Latency in Monocytes/Macrophages.' *Viruses* 6 (4): 1837–60. doi:10.3390/v6041837.

Kumar, A., & Herbein, G. (2014). 'The Macrophage: A Therapeutic Target in HIV-1 Infection.' *Molecular and Cellular Therapies* 2 (1): 10. doi:10.1186/2052-8426-2-10.

Learn, D. B., Fried, V. A., & Thomas A J. (1990). 'Taurine and Hypotaurine Content of Human Leukocytes.' *Journal of Leukocyte Biology* 48 (2): 174–82.

Lindon, J. C., Nicholson, J. K., & Holmes, E. (2007). *The Handbook of Metabonomics and Metabolomics.* Edited by Elaine Lindon, John C. Nicholson, Jeremy K. Holmes. 1st ed. Amsterdam: Elservier. https://0-books.google.co.za.innopac.up.ac.za/books?hl=en&lr=&id=jXNr9UunNIYC&oi=fnd&pg=PP1&ots=6Msq1oCo_4&sig=iP8nQkCwe3LcZg_FiI7i30glLQ4#v=onepage&q&f=false.

Lindon, J. C., Nicholson, J.K., Holmes, E., & Everett, J. R. (2000). 'Metabonomics: Metabolic Processes Studied by NMR Spectroscopy of Biofluids.' doi:10.1002/1099-0534(2000)12:5<289::AID-CMR3>3.0.CO;2-W.

Lutz, N. W., Yahi, N., Fantini, J., & Cozzone. P. J. (1997). 'Perturbations of Glucose Metabolism Associated with HIV Infection in Human Intestinal Epithelial Cells: A Multinuclear Magnetic Resonance Spectroscopy Study.' *AIDS (London, England)* 11 (2): 147–55.

MacDonald, M. J., *et al.* (2007). Feasibility of pathways for transfer of acyl groups from mitochondria to the cytosol to form short chain acyl-CoAs in the pancreatic beta cell. *Journal of Biological Chemistry*, 282(42), pp.30596–30606.

Maciver, N. J., et al. (2008). 'Glucose Metabolism in Lymphocytes Is a Regulated Process with Significant Effects on Immune Cell Function and Survival' 84 (October): 1–9. doi:10.1189/jlb.0108024.

Mack, K. D., *et al.* (2003). 'HIV Insertions Within and Proximal to Host Cell Genes Are a Common Finding in Tissues Containing High Levels of HIV DNA and Macrophage-Associated p24 Antigen Expression.' *JAIDS Journal of Acquired Immune Deficiency Syndromes* 33 (3): 308–20. doi:10.1097/00126334-200307010-00004.

Macreadie, I. G., *et al.* (1997). 'HIV-1 Protein Vpr Causes Gross Mitochondrial Dysfunction in the Yeast Saccharomyces Cerevisiae.' *FEBS Letters* 410 (2-3). Federation of European Biochemical Societies: 145–49. doi:10.1016/S0014-5793(97)00542-5.

Maiuri, P., Knezevich, A., Bertrand, E., & Marcello A. (2011). 'Real-Time Imaging of the HIV-1 Transcription Cycle in Single Living Cells.' *Methods (San Diego, Calif.)* 53 (1): 62–67. doi:10.1016/j.ymeth.2010.06.015.

Mavel, S., *et al.* (2013). '1H-13C NMR-Based Urine Metabolic Profiling in Autism Spectrum Disorders.' *Talanta* 114. Elsevier: 95–102. doi:10.1016/j.talanta.2013.03.064.

McKnight, T. R., *et al.* (2014). 'A Combined Chemometric and Quantitative NMR Analysis of HIV/AIDS Serum Discloses Metabolic Alterations Associated with Disease Status.' *Mol. BioSyst.* 10 (11). Royal Society of Chemistry: 2889–97. doi:10.1039/C4MB00347K.

Mellerick, D. M., & Liu, H. (2004). Methanol exposure interferes with morphological cell movements in the Drosophila embryo and causes increased apoptosis in the CNS. *Journal of Neurobiology*, 60(3), pp.308–318.

Mero, A. (1999). 'Leucine Supplementation and Intensive Training.' *Sports Medicine* 27 (6): 347–58. doi:10.2165/00007256-199927060-00001.

Newsholme, P., *et al.* (2003). 'Glutamine and Glutamate--Their Central Role in Cell Metabolism and Function.' *Cell Biochemistry and Function* 21 (1): 1–9. doi:10.1002/cbf.1003.

Nicholson, J. K., Holmes, E., & Lindon, J. C. (2007). 'Metabonomics and Metabolomics Techniques and Their Applications in Mammalian Systems.'

Niki, E., *et al.* (2003). Cell death caused by selenium deficiency and protective effect of antioxidants. *Journal of Biological Chemistry*, 278(41), pp.39428–39434.

Orenstein, J. M. (2001). 'The Macrophage in HIV Infection.' *Immunobiology* 204 (5): 598–602. doi:10.1078/0171-2985-00098.

Pace, M. J., *et al.* (2011). 'HIV Reservoirs and Latency Models.' *Virology* 411 (2). Elsevier Inc.: 344–54. doi:10.1016/j.virol.2010.12.041.

Pépin, J. (2013). 'The Origins of AIDS: From Patient Zero to Ground Zero.' *Journal*

of Epidemiology and Community Health 67 (6): 473–75. doi:10.1136/jech-2012-201423.

Philippeos, C., Steffens, F.E., & Meyer. D. (2009). 'Comparative 1H NMR-Based Metabonomic Analysis of HIV-1 Sera.' *Journal of Biomolecular NMR* 44 (3): 127–37. doi:10.1007/s10858-009-9329-8.

Polo, R., Martinez, S., Madrigal, P., & Gonzalez-Muñoz. M. (2003). 'Factors Associated with Mitochondrial Dysfunction in Circulating Peripheral Blood Lymphocytes from HIV-Infected People.' *Journal of Acquired Immune Deficiency Syndromes (1999)* 34 (1): 32–36. doi:10.1097/00126334-200309010-00004.

Prentki, M., & Corkey, B. E. (1996). 'Are the -Cell Signaling Molecules Malonyl-CoA and Cystolic Long-Chain Acyl-CoA Implicated in Multiple Tissue Defects of Obesity and NIDDM?' *Diabetes* 45 (3): 273–83. doi:10.2337/diab.45.3.273.

Raghava, G. P. S. (2015). 'HIVbio: HIV Bioinformatics.' http://www.imtech.res.in/raghava/hivbio/cycle.html.

Rathbun, R. C. (2015). 'Antiretroviral Therapy for HIV Infection.' *Medscape. http://emedicine.medscape.com/article/1533218-overview.*

Raschke, P., Massoudy, P., & Becker, B. F. (1995). 'Taurine Protects the Heart from Neutrophil-Induced Reperfusion Injury.' *Free Radical Biology and Medicine* 19 (4): 461–71. doi:10.1016/0891-5849(95)00044-X.

Reape, T. J., & Groot, P. H. E. (1999). 'Chemokines and Atherosclerosis.' *Atherosclerosis* 147 (2): 213–25. doi:10.1016/S0021-9150(99)00346-9.

Reaven, G. M. (1997). 'Banting Lecture 1988. Role of Insulin Resistance in Human Disease. 1988.' *Nutrition (Burbank, Los Angeles County, Calif.)* 13 (1): 65; discussion 64, 66. doi:S0899900797806375 [pii].

Redel, L., *et al.* (2010). 'HIV-1 Regulation of Latency in the Monocyte-Macrophage Lineage and in CD4+ T Lymphocytes.' *Journal of Leukocyte Biology* 87 (4): 575–88. doi:10.1189/jlb.0409264.

Robertson, D. G., Nicholson, J., Holmes, E., & Lindon, J. (2005). 'Metabonomics in Toxicology : A Review' 85 (2): 809–22. doi:10.1093/toxsci/kfi102.

Robertson, D. G. (2005). 'Metabonomics in Toxicology: A Review.' *Toxicological Sciences* 85 (2): 809–22. doi:10.1093/toxsci/kfi102.

Rodrı, S., Saavedra, E., & Moreno-sa, R. (2007). 'Energy Metabolism in Tumor Cells' 274: 1393–1418. doi:10.1111/j.1742-4658.2007.05686.x.

Roux, A., Lison, D., Junot, C., & Heilier, J. (2011). 'Applications of Liquid Chromatography Coupled to Mass Spectrometry-Based Metabolomics in Clinical Chemistry and Toxicology: A Review.' *Clinical Biochemistry* 44 (1). The Canadian Society of Clinical Chemists: 119–35. doi:10.1016/j.clinbiochem.2010.08.016.

Saks, V. A., Kongas, O., Vendelin, M., & Kay, L. (2000). 'Role of the Creatine/phosphocreatine System in the Regulation of Mitochondrial Respiration.' *Acta Physiologica Scandinavica* 168 (4): 635–41. doi:10.1046/j.1365-201x.2000.00715.x.

Salek, R., Cheng, K., & Griffin, J. (2011). *The Study of Mammalian Metabolism through NMR-Based Metabolomics. Methods in Enzymology*. 1st ed. Vol. 500. Elsevier Inc. doi:10.1016/B978-0-12-385118-5.00017-7.

Saltiel, A. R., & Kahn, C. R. (2001). 'Glucose and Lipid Metabolism' 414 (December): 799–806.

Schillaci, G,. *et al.* (2005). 'Impact of Treatment with Protease Inhibitors on Aortic Stiffness in Adult Patients with Human Immunodeficiency Virus Infection.' *Arteriosclerosis, Thrombosis, and Vascular Biology* 25 (11). Lippincott Williams & Wilkins: 2381–85. doi:10.1161/01.ATV.0000183744.38509.de.

Shaw, R. J. (2006). 'Glucose Metabolism and Cancer.' *Current Opinion in Cell Biology* 18 (6): 598–608. doi:10.1016/j.ceb.2006.10.005.

Shikuma, C. M., Day, L. J., & Gerschenson, M. (2005). 'Insulin Resistance in the HIV-Infected Population : The Potential Role of Mitochondrial Dysfunction.' *Young* 2 (808): 255–62.

Siliciano, R. F., & Greene, W. C. (2011). 'HIV Latency.' *Cold Spring Harbor Perspectives in Medicine* 1 (1). doi:10.1101/cshperspect.a007096.

Sitole, L. J., Williams, A. A., & Meyer, D. (2013). 'Metabonomic Analysis of HIV-Infected Biofluids.' *Molecular bioSystems* 9 (1): 18–28. doi:10.1039/c2mb25318f.

Sitole, L., Steffens, F., & Meyer, D. (2015). 'Raman Spectroscopy-Based Metabonomics of HIV-Infected Sera Detects Amino Acid and Glutathione

Changes.' *Current Metabolomics* 3 (1): 65–75.

Slama, L., Le Camus, C., Serfaty, L., Pialoux, G., Capeau, J., & Gharakhanian, S. (2009). 'Metabolic Disorders and Chronic Viral Disease: The Case of HIV and HCV.' *Diabetes & Metabolism* 35 (1): 1–11. doi:10.1016/j.diabet.2008.08.003.

Sleasman, J. W., & Goodenow, M. M. (2003). '13. HIV-1 Infection.' *Journal of Allergy and Clinical Immunology* 111 (2): S582–92. doi:10.1067/mai.2003.91.

Smith, L. (2015). 'Immuno-Oncology Promises to Be the Next "Big Thing" In Biotechnology'. http://smithonstocks.com/immuno-oncology-promises-to-be-the-next-big-thing-in-biotechnology/.

Spencer, M. D., *et al.* (2011). 'Association between Composition of the Human Gastrointestinal Microbiome and Development of Fatty Liver with Choline Deficiency.' *Gastroenterology* 140 (3). Elsevier Inc.: 976–86. doi:10.1053/j.gastro.2010.11.049.

Stipanuk, M. H. (2004). 'Sulfur Amino Acid Metabolism: Pathways for Production and Removal of Homocysteine and Cysteine.' *Annual Review of Nutrition* 24 (January). Annual Reviews: 539–77. doi:10.1146/annurev.nutr.24.012003.132418.

Stuart, B. (2005). *Infrared Spectroscopy*. Hoboken, NJ, USA: John Wiley & Sons, Inc.

Szefer, P. (2003). 'Chapter 18 - Application of Chemometric Techniques in Analytical Evaluation of Biological and Environmental Samples', 355–88.

Taiwo, B. O. (2005). 'Insulin Resistance, HIV Infection, and Anti-HIV Therapies.' *The AIDS Reader* 15 (4): 171–76, 179–80. http://europepmc.org/abstract/med/15844237.

Tebit, D. M., *et al.* (2010). 'Divergent Evolution in Reverse Transcriptase (RT) of HIV-1 Group O and M Lineages: Impact on Structure, Fitness, and Sensitivity to Nonnucleoside RT Inhibitors.' *Journal of Virology* 84 (19): 9817–30. doi:10.1128/JVI.00991-10.

Tiemessen, C. T., Kilroe, B., & Martin, D. J.(1998). 'Interleukin-4 Regulation of Cytokine-Induced HIV1 and Interleukin-8 Expression in Promonocytic U1 Cells Is Concentration- and Cytokine-Dependent.' *Research in Virology* 149 (1): 21–27.

Trygg, J., Holmes, E., &Lundstedt, T. (2007). 'Chemometrics in Metabonomics.' *Journal of Proteome Research* 6 (2): 469–79. doi:10.1021/pr060594q.

Tyagi, M., Pearson, R. J., & Karn, J. (2010). 'Establishment of HIV Latency in Primary CD4 2 Cells Is due to Epigenetic Transcriptional Silencing and P-TEFb Restriction □' 84 (13): 6425–37. doi:10.1128/JVI.01519-09.

UNAIDS. (2014). 'Statistics: Worldwide.' http://www.unaids.org/en/resources/campaigns/2014/2014gapreport/factsheet.

Van Der Valk, M., *et al.* (2001). 'Lipodystrophy in HIV-1-Positive Patients Is Associated with Insulin Resistance in Multiple Metabolic Pathways.' *AIDS (London, England)* 15 (16): 2093–2100.

Van Der Werf, M.J., Jellema, H.J., & Hankemeier, T. (2005). 'Microbial Metabolomics: Replacing Trial-and-Error by the Unbiased Selection and Ranking of Targets.' *Journal of Industrial Microbiology and Biotechnology* 32 (6): 234–52. doi:10.1007/s10295-005-0231-4.

Van Lint, C., Emiliani, S., Ott, M., & Verdin, E. (1996). 'Transcriptional Activation and Chromatin Remodeling of the HIV-1 Promoter in Response to Histone Acetylation.' *The EMBO Journal* 15 (5). European Molecular Biology Organization: 1112–20. /pmc/articles/PMC450009/?report=abstract.

Vander Heiden, M. G., Cantley, L. C., & Thompson, C. B. (2009). 'Understanding the Warburg Effect: The Metabolic Requirements of Cell Proliferation.' *Science (New York, N.Y.)* 324 (5930): 1029–33. doi:10.1126/science.1160809.

Wanders, R. J., Duran, M., & Loupatty, F. J. (2012). Enzymology of the branched-chain amino acid oxidation disorders: The valine pathway. *Journal of Inherited Metabolic Disease*, 35(1), pp.5–12.

Warburg, O. (1956). On the Origin of Cancer Cells. *Science*, 123(3191), pp.309–314. Available at: http://www.sciencemag.org/cgi/doi/10.1126/science.123.3191.309 [Accessed November 4, 2014].

Williams, A. *et al.* (2012). Qualitative serum organic acid profiles of HIV-infected individuals not on antiretroviral treatment. *Metabolomics*, 8(5), pp.804–818.

Williams, R. J. (1951). 'Individual Metabolic Patterns and Human Disease: An Exploratory Study Utilizing Predominantly Paper Chromatographic Methods.'

Williams, S. A. *et al*. (2006). 'NF-kappaB p50 Promotes HIV Latency through HDAC Recruitment and Repression of Transcriptional Initiation.' *The EMBO Journal* 25 (1): 139–49. doi:10.1038/sj.emboj.7600900.

Wishart, D. S. (2011). 'Advances in Metabolite Identification.' *Bioanalysis* 3 (15). Future Science Ltd London, UK: 1769–82. doi:10.4155/bio.11.155.

Worm, S.W., *et al*. (2010). High prevalence of the metabolic syndrome in HIV-infected patients: impact of different definitions of the metabolic syndrome. *AIDS (London, England)*, 24(3), pp.427–35.

Worm, S. W., & Lundgren, J. D. (2011). The metabolic syndrome in HIV. *Best Practice and Research: Clinical Endocrinology and Metabolism*, 25(3), pp.479–486. Available at: http://dx.doi.org/10.1016/j.beem.2010.10.018.

Yudkoff, M., *et al*. (2005). Brain amino acid requirements and toxicity: the example of leucine. *The Journal of nutrition*, 135(6 Suppl), p.1531S–8S.

Zeisel, S. H., & Blusztajn, J. K., (1994). Choline and human nutrition. *Annual review of nutrition*, 14, pp.269–296.

Zeisel, S. H. *et al*. (1991). Choline, an essential nutrient for humans. *The FASEB Journal*, 5(7), pp.2093–2098. Available at: http://0-www.fasebj.org.innopac.up.ac.za/content/5/7/2093.abstract.

Zhao, Y. *et al*. (2008). Mechanisms and methods in glucose metabolism and cell death. *Methods in enzymology*, 442, pp.439–57. Available at: http://www.sciencedirect.com/science/article/pii/S0076687908014225 [Accessed April 28, 2015].

Zolopa, A. R. (2010). 'The Evolution of HIV Treatment Guidelines: Current State-of-the-Art of ART.' *Antiviral Research* 85 (1): 241–44. doi:10.1016/j.antiviral.2009.10.018.

Appendix

In this chapter the supplementary data is provided and explained.

Cell lysis by sonication

The experiments were conducted on different days, hence the different compensation gates. The first plot fig A1, 36 % of cells had undergone cell death after 5 min of sonication using a tip sonicator most of the cells were still viable. In figure A2 after 10 min waterbath sonication only 20 % of cells had lysed. More time was required to achieve the same extent cell lysis seen with freeze-thaw method therefore sonication method was abandoned.
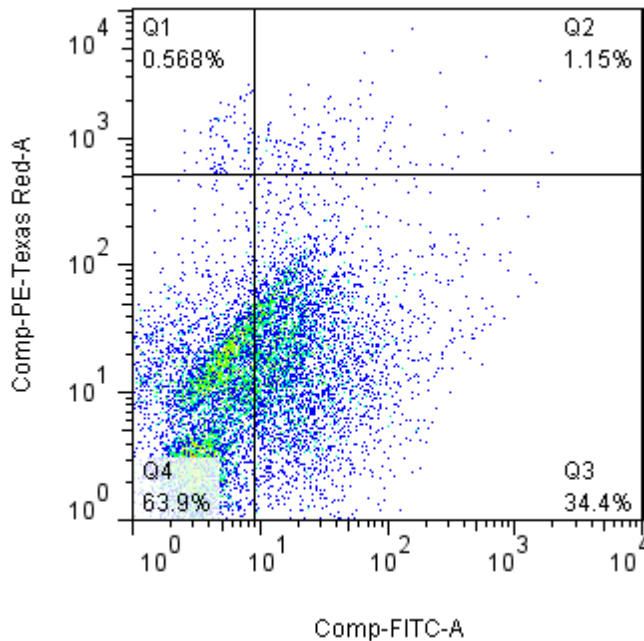
Figure A1: **Tip sonication**. The cells (2 x 10^6 cells/ml) were lysed for 5 min with a tip sonicator only 36 % Q1-3 had lysed, 64 % were still detected as viable Q4.
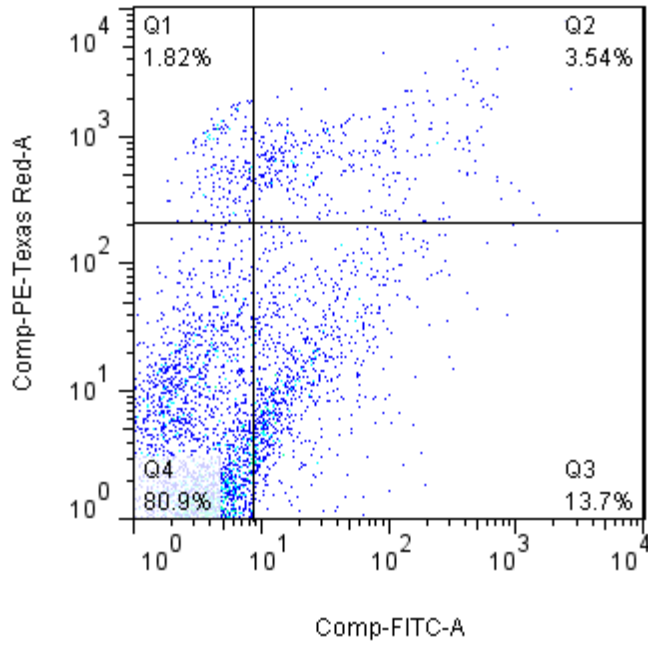
Figure A2: **Waterbath sonication**. Cells (2 x 10^6 cells/ml) were placed in a waterbath at 37 ºC for 10 min, 20% Q1-3 had lysed, 80 % remained viable Q4.

Table A1: Multiple statistical comparison analysis of the samples using P-values

Multiple Comparisons

LSD

Dependent Variable			Mean Difference (I-J)	Std. Error	Sig.	95% Confidence Interval Lower Bound	95% Confidence Interval Upper Bound
Z001X8.675	Unstimulated U1 Cells	Stimulated U1 Cells	,14871	,13432	,311	-,1799	,4774
		U937 cells	-,05422	,13432	,700	-,3829	,2744
	Stimulated U1 Cells	Unstimulated U1 Cells	-,14871	,13432	,311	-,4774	,1799
		U937 cells	-,20293	,13432	,182	-,5316	,1257
	U937 cells	Unstimulated U1 Cells	,05422	,13432	,700	-,2744	,3829
		Stimulated U1 Cells	,20293	,13432	,182	-,1257	,5316
Z002X8.635	Unstimulated U1 Cells	Stimulated U1 Cells	,22851	,12594	,120	-,0797	,5367
		U937 cells	-,02567	,12594	,845	-,3338	,2825
	Stimulated U1 Cells	Unstimulated U1 Cells	-,22851	,12594	,120	-,5367	,0797
		U937 cells	-,25418	,12594	,090	-,5623	,0540
	U937 cells	Unstimulated U1 Cells	,02567	,12594	,845	-,2825	,3338
		Stimulated U1 Cells	,25418	,12594	,090	-,0540	,5623
Z003X8.595	Unstimulated U1 Cells	Stimulated U1 Cells	,23132	,13306	,133	-,0943	,5569
		U937 cells	-,02717	,13306	,845	-,3528	,2984
	Stimulated U1 Cells	Unstimulated U1 Cells	-,23132	,13306	,133	-,5569	,0943
		U937 cells	-,25849	,13306	,100	-,5841	,0671
	U937 cells	Unstimulated U1 Cells	,02717	,13306	,845	-,2984	,3528
		Stimulated U1 Cells	,25849	,13306	,100	-,0671	,5841
Z004X8.555	Unstimulated U1 Cells	Stimulated U1 Cells	,18822	,13287	,206	-,1369	,5133
		U937 cells	-,06167	,13287	,659	-,3868	,2634
	Stimulated U1 Cells	Unstimulated U1 Cells	-,18822	,13287	,206	-,5133	,1369
		U937 cells	-,24989	,13287	,109	-,5750	,0752
	U937 cells	Unstimulated U1 Cells	,06167	,13287	,659	-,2634	,3868
		Stimulated U1 Cells	,24989	,13287	,109	-,0752	,5750
Z005X8.515	Unstimulated	Stimulated U1	,18056	,12897	,211	-,1350	,4961

	U1 Cells	Cells					
		U937 cells	-,14736	,12897	,297	-,4629	,1682
	Stimulated U1 Cells	Unstimulated U1 Cells	-,18056	,12897	,211	-,4961	,1350
		U937 cells	-.32792*	,12897	,044	-,6435	-,0123
	U937 cells	Unstimulated U1 Cells	,14736	,12897	,297	-,1682	,4629
		Stimulated U1 Cells	.32792*	,12897	,044	,0123	,6435
Z006X8.475	Unstimulated U1 Cells	Stimulated U1 Cells	,19580	,12124	,157	-,1009	,4925
		U937 cells	-,07832	,12124	,542	-,3750	,2183
	Stimulated U1 Cells	Unstimulated U1 Cells	-,19580	,12124	,157	-,4925	,1009
		U937 cells	-,27412	,12124	,064	-,5708	,0225
	U937 cells	Unstimulated U1 Cells	,07832	,12124	,542	-,2183	,3750
		Stimulated U1 Cells	,27412	,12124	,064	-,0225	,5708
Z007X8.435	Unstimulated U1 Cells	Stimulated U1 Cells	,17304	,13142	,236	-,1485	,4946
		U937 cells	-,03341	,13142	,808	-,3550	,2882
	Stimulated U1 Cells	Unstimulated U1 Cells	-,17304	,13142	,236	-,4946	,1485
		U937 cells	-,20645	,13142	,167	-,5280	,1151
	U937 cells	Unstimulated U1 Cells	,03341	,13142	,808	-,2882	,3550
		Stimulated U1 Cells	,20645	,13142	,167	-,1151	,5280
Z008X8.395	Unstimulated U1 Cells	Stimulated U1 Cells	,15804	,12972	,269	-,1594	,4754
		U937 cells	-,05849	,12972	,668	-,3759	,2589
	Stimulated U1 Cells	Unstimulated U1 Cells	-,15804	,12972	,269	-,4754	,1594
		U937 cells	-,21653	,12972	,146	-,5339	,1009
	U937 cells	Unstimulated U1 Cells	,05849	,12972	,668	-,2589	,3759
		Stimulated U1 Cells	,21653	,12972	,146	-,1009	,5339
Z009X8.355	Unstimulated U1 Cells	Stimulated U1 Cells	,20256	,13044	,171	-,1166	,5217
		U937 cells	-,05366	,13044	,695	-,3728	,2655
	Stimulated U1 Cells	Unstimulated U1 Cells	-,20256	,13044	,171	-,5217	,1166
		U937 cells	-,25622	,13044	,097	-,5754	,0630
	U937 cells	Unstimulated U1 Cells	,05366	,13044	,695	-,2655	,3728
		Stimulated U1 Cells	,25622	,13044	,097	-,0630	,5754
Z010X8.315	Unstimulated U1 Cells	Stimulated U1 Cells	,22517	,12848	,130	-,0892	,5396

		U937 cells	-,03261	,12848	,808	-,3470	,2818
	Stimulated U1 Cells	Unstimulated U1 Cells	-,22517	,12848	,130	-,5396	,0892
		U937 cells	-,25778	,12848	,092	-,5722	,0566
	U937 cells	Unstimulated U1 Cells	,03261	,12848	,808	-,2818	,3470
		Stimulated U1 Cells	,25778	,12848	,092	-,0566	,5722
Z011X8.275	Unstimulated U1 Cells	Stimulated U1 Cells	,24359	,12319	,095	-,0579	,5450
		U937 cells	-,01263	,12319	,922	-,3141	,2888
	Stimulated U1 Cells	Unstimulated U1 Cells	-,24359	,12319	,095	-,5450	,0579
		U937 cells	-,25622	,12319	,083	-,5577	,0452
	U937 cells	Unstimulated U1 Cells	,01263	,12319	,922	-,2888	,3141
		Stimulated U1 Cells	,25622	,12319	,083	-,0452	,5577
Z012X8.235	Unstimulated U1 Cells	Stimulated U1 Cells	,21643	,12651	,138	-,0931	,5260
		U937 cells	-,06035	,12651	,650	-,3699	,2492
	Stimulated U1 Cells	Unstimulated U1 Cells	-,21643	,12651	,138	-,5260	,0931
		U937 cells	-,27677	,12651	,071	-,5863	,0328
	U937 cells	Unstimulated U1 Cells	,06035	,12651	,650	-,2492	,3699
		Stimulated U1 Cells	,27677	,12651	,071	-,0328	,5863
Z013X4.397	Unstimulated U1 Cells	Stimulated U1 Cells	.31795[*]	,10481	,023	,0615	,5744
		U937 cells	,11582	,10481	,311	-,1406	,3723
	Stimulated U1 Cells	Unstimulated U1 Cells	-.31795[*]	,10481	,023	-,5744	-,0615
		U937 cells	-,20212	,10481	,102	-,4586	,0543
	U937 cells	Unstimulated U1 Cells	-,11582	,10481	,311	-,3723	,1406
		Stimulated U1 Cells	,20212	,10481	,102	-,0543	,4586
Z014X4.357	Unstimulated U1 Cells	Stimulated U1 Cells	.52123[*]	,15464	,015	,1428	,8996
		U937 cells	,12567	,15464	,447	-,2527	,5041
	Stimulated U1 Cells	Unstimulated U1 Cells	-.52123[*]	,15464	,015	-,8996	-,1428
		U937 cells	-.39556[*]	,15464	,043	-,7740	-,0172
	U937 cells	Unstimulated U1 Cells	-,12567	,15464	,447	-,5041	,2527
		Stimulated U1 Cells	.39556[*]	,15464	,043	,0172	,7740
Z015X4.317	Unstimulated U1 Cells	Stimulated U1 Cells	,28945	,29507	,365	-,4326	1,0115
		U937 cells	,13592	,29507	,661	-,5861	,8579

	Stimulated U1 Cells	Unstimulated U1 Cells	-,28945	,29507	,365	-1,0115	,4326
		U937 cells	-,15353	,29507	,621	-,8755	,5685
	U937 cells	Unstimulated U1 Cells	-,13592	,29507	,661	-,8579	,5861
		Stimulated U1 Cells	,15353	,29507	,621	-,5685	,8755
Z016X4.277	Unstimulated U1 Cells	Stimulated U1 Cells	-,06687	,43025	,882	-1,1197	,9859
		U937 cells	,13279	,43025	,768	-,9200	1,1856
	Stimulated U1 Cells	Unstimulated U1 Cells	,06687	,43025	,882	-,9859	1,1197
		U937 cells	,19966	,43025	,659	-,8531	1,2524
	U937 cells	Unstimulated U1 Cells	-,13279	,43025	,768	-1,1856	,9200
		Stimulated U1 Cells	-,19966	,43025	,659	-1,2524	,8531
Z017X4.237	Unstimulated U1 Cells	Stimulated U1 Cells	,05873	,25988	,829	-,5772	,6946
		U937 cells	,19958	,25988	,472	-,4363	,8355
	Stimulated U1 Cells	Unstimulated U1 Cells	-,05873	,25988	,829	-,6946	,5772
		U937 cells	,14085	,25988	,607	-,4950	,7768
	U937 cells	Unstimulated U1 Cells	-,19958	,25988	,472	-,8355	,4363
		Stimulated U1 Cells	-,14085	,25988	,607	-,7768	,4950
Z018X4.197	Unstimulated U1 Cells	Stimulated U1 Cells	.41662[*]	,07149	,001	,2417	,5915
		U937 cells	.19595[*]	,07149	,034	,0210	,3709
	Stimulated U1 Cells	Unstimulated U1 Cells	-.41662[*]	,07149	,001	-,5915	-,2417
		U937 cells	-.22066[*]	,07149	,021	-,3956	-,0457
	U937 cells	Unstimulated U1 Cells	-.19595[*]	,07149	,034	-,3709	-,0210
		Stimulated U1 Cells	.22066[*]	,07149	,021	,0457	,3956
Z019X4.157	Unstimulated U1 Cells	Stimulated U1 Cells	.52757[*]	,08250	,001	,3257	,7294
		U937 cells	.29401[*]	,08250	,012	,0922	,4959
	Stimulated U1 Cells	Unstimulated U1 Cells	-.52757[*]	,08250	,001	-,7294	-,3257
		U937 cells	-.23356[*]	,08250	,030	-,4354	-,0317
	U937 cells	Unstimulated U1 Cells	-.29401[*]	,08250	,012	-,4959	-,0922
		Stimulated U1 Cells	.23356[*]	,08250	,030	,0317	,4354
Z020X4.117	Unstimulated U1 Cells	Stimulated U1 Cells	.48149[*]	,07581	,001	,2960	,6670
		U937 cells	.19912[*]	,07581	,039	,0136	,3846
	Stimulated U1 Cells	Unstimulated U1 Cells	-.48149[*]	,07581	,001	-,6670	-,2960

			Mean Diff	Std. Error	Sig.	Lower	Upper
		U937 cells	-.28237[*]	,07581	,010	-,4679	-,0969
	U937 cells	Unstimulated U1 Cells	-.19912[*]	,07581	,039	-,3846	-,0136
		Stimulated U1 Cells	.28237[*]	,07581	,010	,0969	,4679
Z021X4.077	Unstimulated U1 Cells	Stimulated U1 Cells	.51402[*]	,12995	,007	,1961	,8320
		U937 cells	,12122	,12995	,387	-,1968	,4392
	Stimulated U1 Cells	Unstimulated U1 Cells	-.51402[*]	,12995	,007	-,8320	-,1961
		U937 cells	-.39280[*]	,12995	,023	-,7108	-,0748
	U937 cells	Unstimulated U1 Cells	-,12122	,12995	,387	-,4392	,1968
		Stimulated U1 Cells	.39280[*]	,12995	,023	,0748	,7108
Z022X4.037	Unstimulated U1 Cells	Stimulated U1 Cells	,06488	,26250	,813	-,5774	,7072
		U937 cells	-,01852	,26250	,946	-,6608	,6238
	Stimulated U1 Cells	Unstimulated U1 Cells	-,06488	,26250	,813	-,7072	,5774
		U937 cells	-,08340	,26250	,761	-,7257	,5589
	U937 cells	Unstimulated U1 Cells	,01852	,26250	,946	-,6238	,6608
		Stimulated U1 Cells	,08340	,26250	,761	-,5589	,7257
Z023X3.997	Unstimulated U1 Cells	Stimulated U1 Cells	,13780	,29200	,654	-,5767	,8523
		U937 cells	,19410	,29200	,531	-,5204	,9086
	Stimulated U1 Cells	Unstimulated U1 Cells	-,13780	,29200	,654	-,8523	,5767
		U937 cells	,05630	,29200	,853	-,6582	,7708
	U937 cells	Unstimulated U1 Cells	-,19410	,29200	,531	-,9086	,5204
		Stimulated U1 Cells	-,05630	,29200	,853	-,7708	,6582
Z024X3.957	Unstimulated U1 Cells	Stimulated U1 Cells	,34247	,18814	,119	-,1179	,8028
		U937 cells	,37406	,18814	,094	-,0863	,8344
	Stimulated U1 Cells	Unstimulated U1 Cells	-,34247	,18814	,119	-,8028	,1179
		U937 cells	,03159	,18814	,872	-,4288	,4919
	U937 cells	Unstimulated U1 Cells	-,37406	,18814	,094	-,8344	,0863
		Stimulated U1 Cells	-,03159	,18814	,872	-,4919	,4288
Z025X3.917	Unstimulated U1 Cells	Stimulated U1 Cells	,36775	,19339	,106	-,1055	,8410
		U937 cells	,16659	,19339	,422	-,3066	,6398
	Stimulated U1 Cells	Unstimulated U1 Cells	-,36775	,19339	,106	-,8410	,1055
		U937 cells	-,20116	,19339	,338	-,6744	,2721

	U937 cells	Unstimulated U1 Cells	-,16659	,19339	,422	-,6398	,3066
		Stimulated U1 Cells	,20116	,19339	,338	-,2721	,6744
Z026X3.877	Unstimulated U1 Cells	Stimulated U1 Cells	.73180*	,23787	,022	,1497	1,3139
		U937 cells	,46440	,23787	,099	-,1177	1,0465
	Stimulated U1 Cells	Unstimulated U1 Cells	-.73180*	,23787	,022	-1,3139	-,1497
		U937 cells	-,26740	,23787	,304	-,8495	,3147
	U937 cells	Unstimulated U1 Cells	-,46440	,23787	,099	-1,0465	,1177
		Stimulated U1 Cells	,26740	,23787	,304	-,3147	,8495
Z027X3.837	Unstimulated U1 Cells	Stimulated U1 Cells	.48706*	,11765	,006	,1992	,7749
		U937 cells	,15256	,11765	,242	-,1353	,4404
	Stimulated U1 Cells	Unstimulated U1 Cells	-.48706*	,11765	,006	-,7749	-,1992
		U937 cells	-.33450*	,11765	,029	-,6224	-,0466
	U937 cells	Unstimulated U1 Cells	-,15256	,11765	,242	-,4404	,1353
		Stimulated U1 Cells	.33450*	,11765	,029	,0466	,6224
Z028X3.797	Unstimulated U1 Cells	Stimulated U1 Cells	,28195	,13231	,077	-,0418	,6057
		U937 cells	,02177	,13231	,875	-,3020	,3455
	Stimulated U1 Cells	Unstimulated U1 Cells	-,28195	,13231	,077	-,6057	,0418
		U937 cells	-,26018	,13231	,097	-,5839	,0636
	U937 cells	Unstimulated U1 Cells	-,02177	,13231	,875	-,3455	,3020
		Stimulated U1 Cells	,26018	,13231	,097	-,0636	,5839
Z029X3.757	Unstimulated U1 Cells	Stimulated U1 Cells	,23271	,19156	,270	-,2360	,7014
		U937 cells	,01444	,19156	,942	-,4543	,4832
	Stimulated U1 Cells	Unstimulated U1 Cells	-,23271	,19156	,270	-,7014	,2360
		U937 cells	-,21827	,19156	,298	-,6870	,2505
	U937 cells	Unstimulated U1 Cells	-,01444	,19156	,942	-,4832	,4543
		Stimulated U1 Cells	,21827	,19156	,298	-,2505	,6870
Z030X3.717	Unstimulated U1 Cells	Stimulated U1 Cells	-3.16935*	,26107	,000	-3,8082	-2,5305
		U937 cells	-3.90058*	,26107	,000	-4,5394	-3,2618
	Stimulated U1 Cells	Unstimulated U1 Cells	3.16935*	,26107	,000	2,5305	3,8082
		U937 cells	-.73123*	,26107	,031	-1,3700	-,0924
	U937 cells	Unstimulated U1 Cells	3.90058*	,26107	,000	3,2618	4,5394

92

		Stimulated U1 Cells	.73123*	,26107	,031	,0924	1,3700
Z031X3.677	Unstimulated U1 Cells	Stimulated U1 Cells	1.49261*	,37375	,007	,5781	2,4072
		U937 cells	1.29981*	,37375	,013	,3853	2,2143
	Stimulated U1 Cells	Unstimulated U1 Cells	-1.49261*	,37375	,007	-2,4072	-,5781
		U937 cells	-,19281	,37375	,624	-1,1074	,7217
	U937 cells	Unstimulated U1 Cells	-1.29981*	,37375	,013	-2,2143	-,3853
		Stimulated U1 Cells	,19281	,37375	,624	-,7217	1,1074
Z032X3.638	Unstimulated U1 Cells	Stimulated U1 Cells	3.12843*	,60352	,002	1,6517	4,6052
		U937 cells	3.10160*	,60352	,002	1,6248	4,5784
	Stimulated U1 Cells	Unstimulated U1 Cells	-3.12843*	,60352	,002	-4,6052	-1,6517
		U937 cells	-,02683	,60352	,966	-1,5036	1,4499
	U937 cells	Unstimulated U1 Cells	-3.10160*	,60352	,002	-4,5784	-1,6248
		Stimulated U1 Cells	,02683	,60352	,966	-1,4499	1,5036
Z033X3.598	Unstimulated U1 Cells	Stimulated U1 Cells	.64620*	,18657	,013	,1897	1,1027
		U937 cells	.48542*	,18657	,041	,0289	,9419
	Stimulated U1 Cells	Unstimulated U1 Cells	-.64620*	,18657	,013	-1,1027	-,1897
		U937 cells	-,16078	,18657	,422	-,6173	,2957
	U937 cells	Unstimulated U1 Cells	-.48542*	,18657	,041	-,9419	-,0289
		Stimulated U1 Cells	,16078	,18657	,422	-,2957	,6173
Z034X3.558	Unstimulated U1 Cells	Stimulated U1 Cells	.59530*	,16221	,010	,1984	,9922
		U937 cells	,29694	,16221	,117	-,1000	,6939
	Stimulated U1 Cells	Unstimulated U1 Cells	-.59530*	,16221	,010	-,9922	-,1984
		U937 cells	-,29836	,16221	,115	-,6953	,0986
	U937 cells	Unstimulated U1 Cells	-,29694	,16221	,117	-,6939	,1000
		Stimulated U1 Cells	,29836	,16221	,115	-,0986	,6953
Z035X3.518	Unstimulated U1 Cells	Stimulated U1 Cells	.24821*	,08359	,025	,0437	,4527
		U937 cells	-,06076	,08359	,495	-,2653	,1438
	Stimulated U1 Cells	Unstimulated U1 Cells	-.24821*	,08359	,025	-,4527	-,0437
		U937 cells	-.30897*	,08359	,010	-,5135	-,1044
	U937 cells	Unstimulated U1 Cells	,06076	,08359	,495	-,1438	,2653
		Stimulated U1 Cells	.30897*	,08359	,010	,1044	,5135

Z036X3.478	Unstimulated U1 Cells	Stimulated U1 Cells	-,08757	,19148	,664	-,5561	,3810
		U937 cells	-,12124	,19148	,550	-,5898	,3473
	Stimulated U1 Cells	Unstimulated U1 Cells	,08757	,19148	,664	-,3810	,5561
		U937 cells	-,03367	,19148	,866	-,5022	,4349
	U937 cells	Unstimulated U1 Cells	,12124	,19148	,550	-,3473	,5898
		Stimulated U1 Cells	,03367	,19148	,866	-,4349	,5022
Z037X3.438	Unstimulated U1 Cells	Stimulated U1 Cells	.34542*	,14055	,049	,0015	,6893
		U937 cells	,24851	,14055	,127	-,0954	,5924
	Stimulated U1 Cells	Unstimulated U1 Cells	-.34542*	,14055	,049	-,6893	-,0015
		U937 cells	-,09691	,14055	,516	-,4408	,2470
	U937 cells	Unstimulated U1 Cells	-,24851	,14055	,127	-,5924	,0954
		Stimulated U1 Cells	,09691	,14055	,516	-,2470	,4408
Z038X3.398	Unstimulated U1 Cells	Stimulated U1 Cells	-,18671	,10755	,133	-,4499	,0764
		U937 cells	-,19766	,10755	,116	-,4608	,0655
	Stimulated U1 Cells	Unstimulated U1 Cells	,18671	,10755	,133	-,0764	,4499
		U937 cells	-,01095	,10755	,922	-,2741	,2522
	U937 cells	Unstimulated U1 Cells	,19766	,10755	,116	-,0655	,4608
		Stimulated U1 Cells	,01095	,10755	,922	-,2522	,2741
Z039X3.358	Unstimulated U1 Cells	Stimulated U1 Cells	.40192*	,06595	,001	,2405	,5633
		U937 cells	,15464	,06595	,057	-,0067	,3160
	Stimulated U1 Cells	Unstimulated U1 Cells	-.40192*	,06595	,001	-,5633	-,2405
		U937 cells	-.24728*	,06595	,010	-,4087	-,0859
	U937 cells	Unstimulated U1 Cells	-,15464	,06595	,057	-,3160	,0067
		Stimulated U1 Cells	.24728*	,06595	,010	,0859	,4087
Z040X3.318	Unstimulated U1 Cells	Stimulated U1 Cells	,15102	,12837	,284	-,1631	,4651
		U937 cells	-,02055	,12837	,878	-,3347	,2936
	Stimulated U1 Cells	Unstimulated U1 Cells	-,15102	,12837	,284	-,4651	,1631
		U937 cells	-,17157	,12837	,230	-,4857	,1426
	U937 cells	Unstimulated U1 Cells	,02055	,12837	,878	-,2936	,3347
		Stimulated U1 Cells	,17157	,12837	,230	-,1426	,4857
Z041X3.278	Unstimulated U1 Cells	Stimulated U1 Cells	-1.33824*	,32825	,007	-2,1414	-,5350

			Mean Difference	Std. Error	Sig.	Lower Bound	Upper Bound
		U937 cells	,12397	,32825	,719	-,6792	,9272
	Stimulated U1 Cells	Unstimulated U1 Cells	1.33824*	,32825	,007	,5350	2,1414
		U937 cells	1.46220*	,32825	,004	,6590	2,2654
	U937 cells	Unstimulated U1 Cells	-,12397	,32825	,719	-,9272	,6792
		Stimulated U1 Cells	-1.46220*	,32825	,004	-2,2654	-,6590
Z042X3.238	Unstimulated U1 Cells	Stimulated U1 Cells	2,39046	1,13919	,081	-,3970	5,1780
		U937 cells	2,32206	1,13919	,088	-,4654	5,1096
	Stimulated U1 Cells	Unstimulated U1 Cells	-2,39046	1,13919	,081	-5,1780	,3970
		U937 cells	-,06841	1,13919	,954	-2,8559	2,7191
	U937 cells	Unstimulated U1 Cells	-2,32206	1,13919	,088	-5,1096	,4654
		Stimulated U1 Cells	,06841	1,13919	,954	-2,7191	2,8559
Z043X3.198	Unstimulated U1 Cells	Stimulated U1 Cells	-,36180	,16513	,071	-,7659	,0423
		U937 cells	-,19634	,16513	,279	-,6004	,2077
	Stimulated U1 Cells	Unstimulated U1 Cells	,36180	,16513	,071	-,0423	,7659
		U937 cells	,16547	,16513	,355	-,2386	,5695
	U937 cells	Unstimulated U1 Cells	,19634	,16513	,279	-,2077	,6004
		Stimulated U1 Cells	-,16547	,16513	,355	-,5695	,2386
Z044X3.158	Unstimulated U1 Cells	Stimulated U1 Cells	.25680*	,10489	,050	,0001	,5135
		U937 cells	.28712*	,10489	,034	,0305	,5438
	Stimulated U1 Cells	Unstimulated U1 Cells	-.25680*	,10489	,050	-,5135	-,0001
		U937 cells	,03033	,10489	,782	-,2263	,2870
	U937 cells	Unstimulated U1 Cells	-.28712*	,10489	,034	-,5438	-,0305
		Stimulated U1 Cells	-,03033	,10489	,782	-,2870	,2263
Z045X3.118	Unstimulated U1 Cells	Stimulated U1 Cells	,10954	,07396	,189	-,0714	,2905
		U937 cells	-,02549	,07396	,742	-,2065	,1555
	Stimulated U1 Cells	Unstimulated U1 Cells	-,10954	,07396	,189	-,2905	,0714
		U937 cells	-,13504	,07396	,118	-,3160	,0459
	U937 cells	Unstimulated U1 Cells	,02549	,07396	,742	-,1555	,2065
		Stimulated U1 Cells	,13504	,07396	,118	-,0459	,3160
Z046X3.078	Unstimulated U1 Cells	Stimulated U1 Cells	-,09004	,16112	,597	-,4843	,3042
		U937 cells	-,14967	,16112	,389	-,5439	,2446

	Stimulated U1 Cells	Unstimulated U1 Cells	,09004	,16112	,597	-,3042	,4843
		U937 cells	-,05963	,16112	,724	-,4539	,3346
	U937 cells	Unstimulated U1 Cells	,14967	,16112	,389	-,2446	,5439
		Stimulated U1 Cells	,05963	,16112	,724	-,3346	,4539
Z047X3.038	Unstimulated U1 Cells	Stimulated U1 Cells	.56870*	,14337	,007	,2179	,9195
		U937 cells	,33837	,14337	,056	-,0125	,6892
	Stimulated U1 Cells	Unstimulated U1 Cells	-.56870*	,14337	,007	-,9195	-,2179
		U937 cells	-,23033	,14337	,159	-,5811	,1205
	U937 cells	Unstimulated U1 Cells	-,33837	,14337	,056	-,6892	,0125
		Stimulated U1 Cells	,23033	,14337	,159	-,1205	,5811
Z048X2.998	Unstimulated U1 Cells	Stimulated U1 Cells	-,00587	,08401	,947	-,2114	,1997
		U937 cells	-,14402	,08401	,137	-,3496	,0616
	Stimulated U1 Cells	Unstimulated U1 Cells	,00587	,08401	,947	-,1997	,2114
		U937 cells	-,13815	,08401	,151	-,3437	,0674
	U937 cells	Unstimulated U1 Cells	,14402	,08401	,137	-,0616	,3496
		Stimulated U1 Cells	,13815	,08401	,151	-,0674	,3437
Z049X2.958	Unstimulated U1 Cells	Stimulated U1 Cells	,22155	,17356	,249	-,2031	,6462
		U937 cells	,18717	,17356	,322	-,2375	,6119
	Stimulated U1 Cells	Unstimulated U1 Cells	-,22155	,17356	,249	-,6462	,2031
		U937 cells	-,03437	,17356	,850	-,4591	,3903
	U937 cells	Unstimulated U1 Cells	-,18717	,17356	,322	-,6119	,2375
		Stimulated U1 Cells	,03437	,17356	,850	-,3903	,4591
Z050X2.918	Unstimulated U1 Cells	Stimulated U1 Cells	,01384	,12648	,916	-,2957	,3233
		U937 cells	-,02170	,12648	,869	-,3312	,2878
	Stimulated U1 Cells	Unstimulated U1 Cells	-,01384	,12648	,916	-,3233	,2957
		U937 cells	-,03553	,12648	,788	-,3450	,2740
	U937 cells	Unstimulated U1 Cells	,02170	,12648	,869	-,2878	,3312
		Stimulated U1 Cells	,03553	,12648	,788	-,2740	,3450
Z051X2.878	Unstimulated U1 Cells	Stimulated U1 Cells	-,10625	,09477	,305	-,3382	,1257
		U937 cells	-,14437	,09477	,179	-,3763	,0875
	Stimulated U1 Cells	Unstimulated U1 Cells	,10625	,09477	,305	-,1257	,3382

		U937 cells	-,03812	,09477	,701	-,2700	,1938
	U937 cells	Unstimulated U1 Cells	,14437	,09477	,179	-,0875	,3763
		Stimulated U1 Cells	,03812	,09477	,701	-,1938	,2700
Z052X2.838	Unstimulated U1 Cells	Stimulated U1 Cells	.31871*	,10704	,025	,0568	,5806
		U937 cells	,12452	,10704	,289	-,1374	,3864
	Stimulated U1 Cells	Unstimulated U1 Cells	-.31871*	,10704	,025	-,5806	-,0568
		U937 cells	-,19419	,10704	,120	-,4561	,0677
	U937 cells	Unstimulated U1 Cells	-,12452	,10704	,289	-,3864	,1374
		Stimulated U1 Cells	,19419	,10704	,120	-,0677	,4561
Z053X2.798	Unstimulated U1 Cells	Stimulated U1 Cells	,24227	,10719	,065	-,0200	,5046
		U937 cells	,03319	,10719	,767	-,2291	,2955
	Stimulated U1 Cells	Unstimulated U1 Cells	-,24227	,10719	,065	-,5046	,0200
		U937 cells	-,20908	,10719	,099	-,4714	,0532
	U937 cells	Unstimulated U1 Cells	-,03319	,10719	,767	-,2955	,2291
		Stimulated U1 Cells	,20908	,10719	,099	-,0532	,4714
Z054X2.758	Unstimulated U1 Cells	Stimulated U1 Cells	-,28880	,12725	,064	-,6002	,0226
		U937 cells	-,03299	,12725	,804	-,3444	,2784
	Stimulated U1 Cells	Unstimulated U1 Cells	,28880	,12725	,064	-,0226	,6002
		U937 cells	,25581	,12725	,091	-,0556	,5672
	U937 cells	Unstimulated U1 Cells	,03299	,12725	,804	-,2784	,3444
		Stimulated U1 Cells	-,25581	,12725	,091	-,5672	,0556
Z055X2.718	Unstimulated U1 Cells	Stimulated U1 Cells	.19886*	,07753	,043	,0092	,3886
		U937 cells	,00069	,07753	,993	-,1890	,1904
	Stimulated U1 Cells	Unstimulated U1 Cells	-.19886*	,07753	,043	-,3886	-,0092
		U937 cells	-.19817*	,07753	,043	-,3879	-,0085
	U937 cells	Unstimulated U1 Cells	-,00069	,07753	,993	-,1904	,1890
		Stimulated U1 Cells	.19817*	,07753	,043	,0085	,3879
Z056X2.678	Unstimulated U1 Cells	Stimulated U1 Cells	,10277	,10904	,382	-,1640	,3696
		U937 cells	-,01849	,10904	,871	-,2853	,2483
	Stimulated U1 Cells	Unstimulated U1 Cells	-,10277	,10904	,382	-,3696	,1640
		U937 cells	-,12125	,10904	,309	-,3881	,1456

			Mean Diff	Std. Error	Sig.	Lower	Upper
	U937 cells	Unstimulated U1 Cells	,01849	,10904	,871	-,2483	,2853
		Stimulated U1 Cells	,12125	,10904	,309	-,1456	,3881
Z057X2.638	Unstimulated U1 Cells	Stimulated U1 Cells	,12175	,09212	,234	-,1037	,3472
		U937 cells	,01421	,09212	,882	-,2112	,2396
	Stimulated U1 Cells	Unstimulated U1 Cells	-,12175	,09212	,234	-,3472	,1037
		U937 cells	-,10754	,09212	,287	-,3330	,1179
	U937 cells	Unstimulated U1 Cells	-,01421	,09212	,882	-,2396	,2112
		Stimulated U1 Cells	,10754	,09212	,287	-,1179	,3330
Z058X2.598	Unstimulated U1 Cells	Stimulated U1 Cells	,16218	,07927	,087	-,0318	,3561
		U937 cells	-,01153	,07927	,889	-,2055	,1824
	Stimulated U1 Cells	Unstimulated U1 Cells	-,16218	,07927	,087	-,3561	,0318
		U937 cells	-,17370	,07927	,071	-,3677	,0203
	U937 cells	Unstimulated U1 Cells	,01153	,07927	,889	-,1824	,2055
		Stimulated U1 Cells	,17370	,07927	,071	-,0203	,3677
Z059X2.558	Unstimulated U1 Cells	Stimulated U1 Cells	.29642[*]	,08248	,011	,0946	,4982
		U937 cells	,04360	,08248	,616	-,1582	,2454
	Stimulated U1 Cells	Unstimulated U1 Cells	-.29642[*]	,08248	,011	-,4982	-,0946
		U937 cells	-.25282[*]	,08248	,022	-,4546	-,0510
	U937 cells	Unstimulated U1 Cells	-,04360	,08248	,616	-,2454	,1582
		Stimulated U1 Cells	.25282[*]	,08248	,022	,0510	,4546
Z060X2.518	Unstimulated U1 Cells	Stimulated U1 Cells	,20076	,10991	,118	-,0682	,4697
		U937 cells	-,11781	,10991	,325	-,3868	,1511
	Stimulated U1 Cells	Unstimulated U1 Cells	-,20076	,10991	,118	-,4697	,0682
		U937 cells	-.31857[*]	,10991	,027	-,5875	-,0496
	U937 cells	Unstimulated U1 Cells	,11781	,10991	,325	-,1511	,3868
		Stimulated U1 Cells	.31857[*]	,10991	,027	,0496	,5875
Z061X2.478	Unstimulated U1 Cells	Stimulated U1 Cells	,12322	,10580	,288	-,1357	,3821
		U937 cells	-,12109	,10580	,296	-,3800	,1378
	Stimulated U1 Cells	Unstimulated U1 Cells	-,12322	,10580	,288	-,3821	,1357
		U937 cells	-,24431	,10580	,060	-,5032	,0146
	U937 cells	Unstimulated U1 Cells	,12109	,10580	,296	-,1378	,3800

		Stimulated U1 Cells	,24431	,10580	,060	-,0146	,5032
Z062X2.438	Unstimulated U1 Cells	Stimulated U1 Cells	,01224	,08570	,891	-,1975	,2219
		U937 cells	-,12584	,08570	,192	-,3355	,0839
	Stimulated U1 Cells	Unstimulated U1 Cells	-,01224	,08570	,891	-,2219	,1975
		U937 cells	-,13808	,08570	,158	-,3478	,0716
	U937 cells	Unstimulated U1 Cells	,12584	,08570	,192	-,0839	,3355
		Stimulated U1 Cells	,13808	,08570	,158	-,0716	,3478
Z063X2.398	Unstimulated U1 Cells	Stimulated U1 Cells	-,21531	,09739	,069	-,4536	,0230
		U937 cells	-,11797	,09739	,271	-,3563	,1203
	Stimulated U1 Cells	Unstimulated U1 Cells	,21531	,09739	,069	-,0230	,4536
		U937 cells	,09734	,09739	,356	-,1410	,3356
	U937 cells	Unstimulated U1 Cells	,11797	,09739	,271	-,1203	,3563
		Stimulated U1 Cells	-,09734	,09739	,356	-,3356	,1410
Z064X2.358	Unstimulated U1 Cells	Stimulated U1 Cells	,21391	,08772	,051	-,0007	,4285
		U937 cells	.27624[*]	,08772	,020	,0616	,4909
	Stimulated U1 Cells	Unstimulated U1 Cells	-,21391	,08772	,051	-,4285	,0007
		U937 cells	,06233	,08772	,504	-,1523	,2770
	U937 cells	Unstimulated U1 Cells	-.27624[*]	,08772	,020	-,4909	-,0616
		Stimulated U1 Cells	-,06233	,08772	,504	-,2770	,1523
Z065X2.318	Unstimulated U1 Cells	Stimulated U1 Cells	.12586[*]	,04174	,024	,0237	,2280
		U937 cells	.15624[*]	,04174	,010	,0541	,2584
	Stimulated U1 Cells	Unstimulated U1 Cells	-.12586[*]	,04174	,024	-,2280	-,0237
		U937 cells	,03038	,04174	,494	-,0717	,1325
	U937 cells	Unstimulated U1 Cells	-.15624[*]	,04174	,010	-,2584	-,0541
		Stimulated U1 Cells	-,03038	,04174	,494	-,1325	,0717
Z066X2.278	Unstimulated U1 Cells	Stimulated U1 Cells	,06766	,12428	,606	-,2364	,3718
		U937 cells	,06051	,12428	,644	-,2436	,3646
	Stimulated U1 Cells	Unstimulated U1 Cells	-,06766	,12428	,606	-,3718	,2364
		U937 cells	-,00715	,12428	,956	-,3112	,2969
	U937 cells	Unstimulated U1 Cells	-,06051	,12428	,644	-,3646	,2436
		Stimulated U1 Cells	,00715	,12428	,956	-,2969	,3112

Z067X2.238	Unstimulated U1 Cells	Stimulated U1 Cells	,12168	,11933	,347	-,1703	,4137
		U937 cells	,04278	,11933	,732	-,2492	,3348
	Stimulated U1 Cells	Unstimulated U1 Cells	-,12168	,11933	,347	-,4137	,1703
		U937 cells	-,07890	,11933	,533	-,3709	,2131
	U937 cells	Unstimulated U1 Cells	-,04278	,11933	,732	-,3348	,2492
		Stimulated U1 Cells	,07890	,11933	,533	-,2131	,3709
Z068X2.198	Unstimulated U1 Cells	Stimulated U1 Cells	-.23437*	,06806	,014	-,4009	-,0678
		U937 cells	-.25004*	,06806	,010	-,4166	-,0835
	Stimulated U1 Cells	Unstimulated U1 Cells	.23437*	,06806	,014	,0678	,4009
		U937 cells	-,01566	,06806	,826	-,1822	,1509
	U937 cells	Unstimulated U1 Cells	.25004*	,06806	,010	,0835	,4166
		Stimulated U1 Cells	,01566	,06806	,826	-,1509	,1822
Z069X2.158	Unstimulated U1 Cells	Stimulated U1 Cells	-.34335*	,09644	,012	-,5793	-,1074
		U937 cells	-,10903	,09644	,301	-,3450	,1269
	Stimulated U1 Cells	Unstimulated U1 Cells	.34335*	,09644	,012	,1074	,5793
		U937 cells	,23432	,09644	,051	-,0017	,4703
	U937 cells	Unstimulated U1 Cells	,10903	,09644	,301	-,1269	,3450
		Stimulated U1 Cells	-,23432	,09644	,051	-,4703	,0017
Z070X2.118	Unstimulated U1 Cells	Stimulated U1 Cells	-,32473	,16819	,102	-,7363	,0868
		U937 cells	,02084	,16819	,905	-,3907	,4324
	Stimulated U1 Cells	Unstimulated U1 Cells	,32473	,16819	,102	-,0868	,7363
		U937 cells	,34557	,16819	,086	-,0660	,7571
	U937 cells	Unstimulated U1 Cells	-,02084	,16819	,905	-,4324	,3907
		Stimulated U1 Cells	-,34557	,16819	,086	-,7571	,0660
Z071X2.078	Unstimulated U1 Cells	Stimulated U1 Cells	-,13429	,16205	,439	-,5308	,2622
		U937 cells	,16185	,16205	,356	-,2347	,5584
	Stimulated U1 Cells	Unstimulated U1 Cells	,13429	,16205	,439	-,2622	,5308
		U937 cells	,29615	,16205	,117	-,1004	,6927
	U937 cells	Unstimulated U1 Cells	-,16185	,16205	,356	-,5584	,2347
		Stimulated U1 Cells	-,29615	,16205	,117	-,6927	,1004
Z072X2.038	Unstimulated U1 Cells	Stimulated U1 Cells	,00344	,16072	,984	-,3898	,3967

		U937 cells	,26215	,16072	,154	-,1311	,6554
	Stimulated U1 Cells	Unstimulated U1 Cells	-,00344	,16072	,984	-,3967	,3898
		U937 cells	,25871	,16072	,159	-,1346	,6520
	U937 cells	Unstimulated U1 Cells	-,26215	,16072	,154	-,6554	,1311
		Stimulated U1 Cells	-,25871	,16072	,159	-,6520	,1346
Z073X1.998	Unstimulated U1 Cells	Stimulated U1 Cells	-,13844	,14110	,364	-,4837	,2068
		U937 cells	-,00412	,14110	,978	-,3494	,3411
	Stimulated U1 Cells	Unstimulated U1 Cells	,13844	,14110	,364	-,2068	,4837
		U937 cells	,13432	,14110	,378	-,2109	,4796
	U937 cells	Unstimulated U1 Cells	,00412	,14110	,978	-,3411	,3494
		Stimulated U1 Cells	-,13432	,14110	,378	-,4796	,2109
Z074X1.958	Unstimulated U1 Cells	Stimulated U1 Cells	-.77835[*]	,16008	,003	-1,1700	-,3866
		U937 cells	-.64380[*]	,16008	,007	-1,0355	-,2521
	Stimulated U1 Cells	Unstimulated U1 Cells	.77835[*]	,16008	,003	,3866	1,1700
		U937 cells	,13455	,16008	,433	-,2571	,5262
	U937 cells	Unstimulated U1 Cells	.64380[*]	,16008	,007	,2521	1,0355
		Stimulated U1 Cells	-,13455	,16008	,433	-,5262	,2571
Z075X1.919	Unstimulated U1 Cells	Stimulated U1 Cells	-,06618	,15473	,684	-,4448	,3124
		U937 cells	,25079	,15473	,156	-,1278	,6294
	Stimulated U1 Cells	Unstimulated U1 Cells	,06618	,15473	,684	-,3124	,4448
		U937 cells	,31696	,15473	,086	-,0616	,6956
	U937 cells	Unstimulated U1 Cells	-,25079	,15473	,156	-,6294	,1278
		Stimulated U1 Cells	-,31696	,15473	,086	-,6956	,0616
Z076X1.879	Unstimulated U1 Cells	Stimulated U1 Cells	-.56310[*]	,06320	,000	-,7177	-,4085
		U937 cells	-.22565[*]	,06320	,012	-,3803	-,0710
	Stimulated U1 Cells	Unstimulated U1 Cells	.56310[*]	,06320	,000	,4085	,7177
		U937 cells	.33745[*]	,06320	,002	,1828	,4921
	U937 cells	Unstimulated U1 Cells	.22565[*]	,06320	,012	,0710	,3803
		Stimulated U1 Cells	-.33745[*]	,06320	,002	-,4921	-,1828
Z077X1.839	Unstimulated U1 Cells	Stimulated U1 Cells	-.70388[*]	,02884	,000	-,7745	-,6333
		U937 cells	-.27150[*]	,02884	,000	-,3421	-,2009

	Stimulated U1 Cells	Unstimulated U1 Cells	.70388*	,02884	,000	,6333	,7745
		U937 cells	.43239*	,02884	,000	,3618	,5030
	U937 cells	Unstimulated U1 Cells	.27150*	,02884	,000	,2009	,3421
		Stimulated U1 Cells	-.43239*	,02884	,000	-,5030	-,3618
Z078X1.799	Unstimulated U1 Cells	Stimulated U1 Cells	-.68921*	,03381	,000	-,7719	-,6065
		U937 cells	-.30337*	,03381	,000	-,3861	-,2206
	Stimulated U1 Cells	Unstimulated U1 Cells	.68921*	,03381	,000	,6065	,7719
		U937 cells	.38583*	,03381	,000	,3031	,4686
	U937 cells	Unstimulated U1 Cells	.30337*	,03381	,000	,2206	,3861
		Stimulated U1 Cells	-.38583*	,03381	,000	-,4686	-,3031
Z079X1.759	Unstimulated U1 Cells	Stimulated U1 Cells	-.80326*	,11160	,000	-1,0763	-,5302
		U937 cells	-.31443*	,11160	,030	-,5875	-,0414
	Stimulated U1 Cells	Unstimulated U1 Cells	.80326*	,11160	,000	,5302	1,0763
		U937 cells	.48883*	,11160	,005	,2158	,7619
	U937 cells	Unstimulated U1 Cells	.31443*	,11160	,030	,0414	,5875
		Stimulated U1 Cells	-.48883*	,11160	,005	-,7619	-,2158
Z080X1.719	Unstimulated U1 Cells	Stimulated U1 Cells	-.70820*	,13631	,002	-1,0417	-,3747
		U937 cells	-,22058	,13631	,157	-,5541	,1130
	Stimulated U1 Cells	Unstimulated U1 Cells	.70820*	,13631	,002	,3747	1,0417
		U937 cells	.48762*	,13631	,012	,1541	,8212
	U937 cells	Unstimulated U1 Cells	,22058	,13631	,157	-,1130	,5541
		Stimulated U1 Cells	-.48762*	,13631	,012	-,8212	-,1541
Z081X1.679	Unstimulated U1 Cells	Stimulated U1 Cells	-.89987*	,11010	,000	-1,1693	-,6305
		U937 cells	-.37939*	,11010	,014	-,6488	-,1100
	Stimulated U1 Cells	Unstimulated U1 Cells	.89987*	,11010	,000	,6305	1,1693
		U937 cells	.52048*	,11010	,003	,2511	,7899
	U937 cells	Unstimulated U1 Cells	.37939*	,11010	,014	,1100	,6488
		Stimulated U1 Cells	-.52048*	,11010	,003	-,7899	-,2511
Z082X1.639	Unstimulated U1 Cells	Stimulated U1 Cells	-1.01388*	,04087	,000	-1,1139	-,9139
		U937 cells	-.51174*	,04087	,000	-,6117	-,4117
	Stimulated U1 Cells	Unstimulated U1 Cells	1.01388*	,04087	,000	,9139	1,1139

					Sig.	Lower	Upper
		U937 cells	.50214*	,04087	,000	,4021	,6021
	U937 cells	Unstimulated U1 Cells	.51174*	,04087	,000	,4117	,6117
		Stimulated U1 Cells	-.50214*	,04087	,000	-,6021	-,4021
Z083X1.599	Unstimulated U1 Cells	Stimulated U1 Cells	-1.09558*	,02530	,000	-1,1575	-1,0337
		U937 cells	-.48328*	,02530	,000	-,5452	-,4214
	Stimulated U1 Cells	Unstimulated U1 Cells	1.09558*	,02530	,000	1,0337	1,1575
		U937 cells	.61230*	,02530	,000	,5504	,6742
	U937 cells	Unstimulated U1 Cells	.48328*	,02530	,000	,4214	,5452
		Stimulated U1 Cells	-.61230*	,02530	,000	-,6742	-,5504
Z084X1.559	Unstimulated U1 Cells	Stimulated U1 Cells	-1.07959*	,02869	,000	-1,1498	-1,0094
		U937 cells	-.51491*	,02869	,000	-,5851	-,4447
	Stimulated U1 Cells	Unstimulated U1 Cells	1.07959*	,02869	,000	1,0094	1,1498
		U937 cells	.56468*	,02869	,000	,4945	,6349
	U937 cells	Unstimulated U1 Cells	.51491*	,02869	,000	,4447	,5851
		Stimulated U1 Cells	-.56468*	,02869	,000	-,6349	-,4945
Z085X1.519	Unstimulated U1 Cells	Stimulated U1 Cells	-.89551*	,07875	,000	-1,0882	-,7028
		U937 cells	-.34690*	,07875	,005	-,5396	-,1542
	Stimulated U1 Cells	Unstimulated U1 Cells	.89551*	,07875	,000	,7028	1,0882
		U937 cells	.54861*	,07875	,000	,3559	,7413
	U937 cells	Unstimulated U1 Cells	.34690*	,07875	,005	,1542	,5396
		Stimulated U1 Cells	-.54861*	,07875	,000	-,7413	-,3559
Z086X1.479	Unstimulated U1 Cells	Stimulated U1 Cells	-.44795*	,15280	,026	-,8218	-,0741
		U937 cells	-,03889	,15280	,808	-,4128	,3350
	Stimulated U1 Cells	Unstimulated U1 Cells	.44795*	,15280	,026	,0741	,8218
		U937 cells	.40906*	,15280	,037	,0352	,7829
	U937 cells	Unstimulated U1 Cells	,03889	,15280	,808	-,3350	,4128
		Stimulated U1 Cells	-.40906*	,15280	,037	-,7829	-,0352
Z087X1.439	Unstimulated U1 Cells	Stimulated U1 Cells	-.54378*	,11792	,004	-,8323	-,2552
		U937 cells	-,17724	,11792	,184	-,4658	,1113
	Stimulated U1 Cells	Unstimulated U1 Cells	.54378*	,11792	,004	,2552	,8323
		U937 cells	.36654*	,11792	,021	,0780	,6551

	(I) Group	(J) Group	Mean Difference	Std. Error	Sig.	Lower Bound	Upper Bound
	U937 cells	Unstimulated U1 Cells	,17724	,11792	,184	-,1113	,4658
		Stimulated U1 Cells	-.36654*	,11792	,021	-,6551	-,0780
Z088X1.399	Unstimulated U1 Cells	Stimulated U1 Cells	-.69449*	,11520	,001	-,9764	-,4126
		U937 cells	-.39975*	,11520	,013	-,6816	-,1179
	Stimulated U1 Cells	Unstimulated U1 Cells	.69449*	,11520	,001	,4126	,9764
		U937 cells	.29474*	,11520	,043	,0129	,5766
	U937 cells	Unstimulated U1 Cells	.39975*	,11520	,013	,1179	,6816
		Stimulated U1 Cells	-.29474*	,11520	,043	-,5766	-,0129
Z089X1.359	Unstimulated U1 Cells	Stimulated U1 Cells	-1.08197*	,21238	,002	-1,6016	-,5623
		U937 cells	-,21163	,21238	,358	-,7313	,3081
	Stimulated U1 Cells	Unstimulated U1 Cells	1.08197*	,21238	,002	,5623	1,6016
		U937 cells	.87034*	,21238	,006	,3507	1,3900
	U937 cells	Unstimulated U1 Cells	,21163	,21238	,358	-,3081	,7313
		Stimulated U1 Cells	-.87034*	,21238	,006	-1,3900	-,3507
Z090X1.319	Unstimulated U1 Cells	Stimulated U1 Cells	-.24814*	,07763	,019	-,4381	-,0582
		U937 cells	-,01192	,07763	,883	-,2019	,1780
	Stimulated U1 Cells	Unstimulated U1 Cells	.24814*	,07763	,019	,0582	,4381
		U937 cells	.23622*	,07763	,023	,0463	,4262
	U937 cells	Unstimulated U1 Cells	,01192	,07763	,883	-,1780	,2019
		Stimulated U1 Cells	-.23622*	,07763	,023	-,4262	-,0463
Z091X1.279	Unstimulated U1 Cells	Stimulated U1 Cells	-.86372*	,12679	,000	-1,1740	-,5535
		U937 cells	-,27077	,12679	,077	-,5810	,0395
	Stimulated U1 Cells	Unstimulated U1 Cells	.86372*	,12679	,000	,5535	1,1740
		U937 cells	.59295*	,12679	,003	,2827	,9032
	U937 cells	Unstimulated U1 Cells	,27077	,12679	,077	-,0395	,5810
		Stimulated U1 Cells	-.59295*	,12679	,003	-,9032	-,2827
Z092X1.239	Unstimulated U1 Cells	Stimulated U1 Cells	-7.49178*	,11794	,000	-7,7804	-7,2032
		U937 cells	-8.42497*	,11794	,000	-8,7136	-8,1364
	Stimulated U1 Cells	Unstimulated U1 Cells	7.49178*	,11794	,000	7,2032	7,7804
		U937 cells	-.93319*	,11794	,000	-1,2218	-,6446
	U937 cells	Unstimulated U1 Cells	8.42497*	,11794	,000	8,1364	8,7136

		Stimulated U1 Cells	.93319*	,11794	,000	,6446	1,2218
Z093X1.199	Unstimulated U1 Cells	Stimulated U1 Cells	5.51116*	,53397	,000	4,2046	6,8177
		U937 cells	5.02266*	,53397	,000	3,7161	6,3292
	Stimulated U1 Cells	Unstimulated U1 Cells	-5.51116*	,53397	,000	-6,8177	-4,2046
		U937 cells	-,48850	,53397	,396	-1,7951	,8181
	U937 cells	Unstimulated U1 Cells	-5.02266*	,53397	,000	-6,3292	-3,7161
		Stimulated U1 Cells	,48850	,53397	,396	-,8181	1,7951
Z094X1.159	Unstimulated U1 Cells	Stimulated U1 Cells	1,60062	,70057	,062	-,1136	3,3148
		U937 cells	1.82625*	,70057	,040	,1120	3,5405
	Stimulated U1 Cells	Unstimulated U1 Cells	-1,60062	,70057	,062	-3,3148	,1136
		U937 cells	,22564	,70057	,758	-1,4886	1,9399
	U937 cells	Unstimulated U1 Cells	-1.82625*	,70057	,040	-3,5405	-,1120
		Stimulated U1 Cells	-,22564	,70057	,758	-1,9399	1,4886
Z095X1.119	Unstimulated U1 Cells	Stimulated U1 Cells	-.52551*	,13528	,008	-,8565	-,1945
		U937 cells	-,32848	,13528	,051	-,6595	,0025
	Stimulated U1 Cells	Unstimulated U1 Cells	.52551*	,13528	,008	,1945	,8565
		U937 cells	,19704	,13528	,196	-,1340	,5281
	U937 cells	Unstimulated U1 Cells	,32848	,13528	,051	-,0025	,6595
		Stimulated U1 Cells	-,19704	,13528	,196	-,5281	,1340
Z096X1.079	Unstimulated U1 Cells	Stimulated U1 Cells	-.52032*	,11287	,004	-,7965	-,2441
		U937 cells	-.33363*	,11287	,025	-,6098	-,0574
	Stimulated U1 Cells	Unstimulated U1 Cells	.52032*	,11287	,004	,2441	,7965
		U937 cells	,18669	,11287	,149	-,0895	,4629
	U937 cells	Unstimulated U1 Cells	.33363*	,11287	,025	,0574	,6098
		Stimulated U1 Cells	-,18669	,11287	,149	-,4629	,0895
Z097X1.039	Unstimulated U1 Cells	Stimulated U1 Cells	-.31676*	,11116	,029	-,5888	-,0448
		U937 cells	-,13461	,11116	,271	-,4066	,1374
	Stimulated U1 Cells	Unstimulated U1 Cells	.31676*	,11116	,029	,0448	,5888
		U937 cells	,18215	,11116	,152	-,0899	,4542
	U937 cells	Unstimulated U1 Cells	,13461	,11116	,271	-,1374	,4066
		Stimulated U1 Cells	-,18215	,11116	,152	-,4542	,0899

Z098X0.999	Unstimulated U1 Cells	Stimulated U1 Cells	-,24148	,10649	,064	-,5021	,0191
		U937 cells	-,00077	,10649	,994	-,2613	,2598
	Stimulated U1 Cells	Unstimulated U1 Cells	,24148	,10649	,064	-,0191	,5021
		U937 cells	,24071	,10649	,065	-,0199	,5013
	U937 cells	Unstimulated U1 Cells	,00077	,10649	,994	-,2598	,2613
		Stimulated U1 Cells	-,24071	,10649	,065	-,5013	,0199
Z099X0.959	Unstimulated U1 Cells	Stimulated U1 Cells	,17807	,23451	,476	-,3958	,7519
		U937 cells	,46588	,23451	,094	-,1079	1,0397
	Stimulated U1 Cells	Unstimulated U1 Cells	-,17807	,23451	,476	-,7519	,3958
		U937 cells	,28781	,23451	,266	-,2860	,8616
	U937 cells	Unstimulated U1 Cells	-,46588	,23451	,094	-1,0397	,1079
		Stimulated U1 Cells	-,28781	,23451	,266	-,8616	,2860
Z100X0.919	Unstimulated U1 Cells	Stimulated U1 Cells	,09035	,16053	,594	-,3025	,4832
		U937 cells	,30388	,16053	,107	-,0889	,6967
	Stimulated U1 Cells	Unstimulated U1 Cells	-,09035	,16053	,594	-,4832	,3025
		U937 cells	,21353	,16053	,232	-,1793	,6063
	U937 cells	Unstimulated U1 Cells	-,30388	,16053	,107	-,6967	,0889
		Stimulated U1 Cells	-,21353	,16053	,232	-,6063	,1793

Lipids are found at chemical shift 1.119, 1.199 and 1.239;

Glucose 3.558, 3.598, 3.638, 3.677 and 3.717

Lactate 1.319, 1.359, 1.399, 1.439, 4.117, 4.157, 4.197

106